

Award Number: W81XWH-04-1-0250

TITLE: Early Detection of Prostate Cancer

PRINCIPAL INVESTIGATOR: Massood Atashbar, Ph.D.
Dr. Bruce Evan Bejcek

CONTRACTING ORGANIZATION: Western Michigan University
Kalamazoo, Michigan 49008-5425

REPORT DATE: January 2007

TYPE OF REPORT: Final Addendum

PREPARED FOR: U.S. Army Medical Research and Materiel Command
Fort Detrick, Maryland 21702-5012

DISTRIBUTION STATEMENT: Approved for Public Release;
Distribution Unlimited

The views, opinions and/or findings contained in this report are those of the author(s) and should not be construed as an official Department of the Army position, policy or decision unless so designated by other documentation.

REPORT DOCUMENTATION PAGE

Form Approved
OMB No. 0704-0188

Public reporting burden for this collection of information is estimated to average 1 hour per response, including the time for reviewing instructions, searching existing data sources, gathering and maintaining the data needed, and completing and reviewing this collection of information. Send comments regarding this burden estimate or any other aspect of this collection of information, including suggestions for reducing this burden to Department of Defense, Washington Headquarters Services, Directorate for Information Operations and Reports (0704-0188), 1215 Jefferson Davis Highway, Suite 1204, Arlington, VA 22202-4302. Respondents should be aware that notwithstanding any other provision of law, no person shall be subject to any penalty for failing to comply with a collection of information if it does not display a currently valid OMB control number. **PLEASE DO NOT RETURN YOUR FORM TO THE ABOVE ADDRESS.**

1. REPORT DATE (<i>DD-MM-YYYY</i>) 01-01-2007			2. REPORT TYPE Final Addendum			3. DATES COVERED (<i>From - To</i>) 1 May 2006 – 31 Dec 2006			
4. TITLE AND SUBTITLE Early Detection of Prostate Cancer						5a. CONTRACT NUMBER			
						5b. GRANT NUMBER W81XWH-04-1-0250			
						5c. PROGRAM ELEMENT NUMBER			
6. AUTHOR(S) Massood Atashbar, Ph.D. and Dr. Bruce Evan Bejcek E-Mail: massood.atashbar@wmich.edu						5d. PROJECT NUMBER			
						5e. TASK NUMBER			
						5f. WORK UNIT NUMBER			
7. PERFORMING ORGANIZATION NAME(S) AND ADDRESS(ES) Western Michigan University Kalamazoo, Michigan 49008-5425						8. PERFORMING ORGANIZATION REPORT NUMBER			
9. SPONSORING / MONITORING AGENCY NAME(S) AND ADDRESS(ES) U.S. Army Medical Research and Materiel Command Fort Detrick, Maryland 21702-5012						10. SPONSOR/MONITOR'S ACRONYM(S)			
						11. SPONSOR/MONITOR'S REPORT NUMBER(S)			
12. DISTRIBUTION / AVAILABILITY STATEMENT Approved for Public Release; Distribution Unlimited									
13. SUPPLEMENTARY NOTES									
14. ABSTRACT Acoustic wave sensors have been widely used for detection of various chemical and biological species in liquid media. An improved binding of Protein A and IgG molecules on QCM biosensors by modifying the gold surface of the quartz crystal with a 35nm polystyrene film followed by an acidic treatment was accomplished. Also, the increase in the sensitivity of the QCM biosensor with CNT as the chemical interface was studied. Immobilization of the PSA at different concentrations on gold surface was achieved and corresponding sensor responses were registered. Using ELISA technique it was verified that PSA was bound to both the crystals and the 96 well plates. Following this, SH-SAW devices have been designed in a differential configuration to be used as biosensors with high selectivity. These SH-SAW devices were fabricated at the Microfabrication facility at University of Michigan, Ann Arbor. The frequency response of these SH-SAW devices and their performance when used in the oscillator configuration has also been recorded. A complete physical structure which can house the sensor along with the associated analog circuitry has been designed and developed. This structure provides electromagnetic shielding as well as reducing the effects of vibration and motion to the entire sensing system.									
15. SUBJECT TERMS No subject terms provided									
16. SECURITY CLASSIFICATION OF:						17. LIMITATION OF ABSTRACT	18. NUMBER OF PAGES	19a. NAME OF RESPONSIBLE PERSON	
a. REPORT		b. ABSTRACT		c. THIS PAGE				19b. TELEPHONE NUMBER (<i>include area code</i>)	
U		U		U		UU	95		

TABLE OF CONTENTS

PAGE No.

Abstract.....	4
Introduction.....	5
SH-SAW sensor and the associated electronic circuitry.....	10
SH-SAW device fabrication and testing.....	11
Physical Structure	13
Experimental Details.....	14
Protein and Antibody	14
Materials	14
Experimental Procedures	14
Characterization tools and methods	15
Results and Discussions.....	16
CNT based QCM sensor	20
ELISA	22
Key research accomplishments.....	24
Reportable outcomes.....	25
Manuscripts, abstracts, presentations, patent applied	25
Degrees obtained that are supported by this award	26
List of personnel	27
Conclusions.....	27
References.....	28
Collected Figure Captions.....	32
Appendices.....	68

Abstract

Acoustic wave sensors have been widely used for detection of various chemical and biological species in liquid media. An improved binding of Protein A and IgG molecules on QCM biosensors by modifying the gold surface of the quartz crystal with a 35nm polystyrene film followed by an acidic treatment was accomplished. Also, the increase in the sensitivity of the QCM biosensor with CNT as the chemical interface was studied. Immobilization of the PSA at different concentrations on gold surface was achieved and corresponding sensor responses were registered. Using ELISA technique it was verified that PSA was bound to both the crystals and the 96 well plates. Following this, SH-SAW devices have been designed in a differential configuration to be used as biosensors with high selectivity. These SH-SAW devices were fabricated at the Microfabrication facility at University of Michigan, Ann Arbor. The frequency response of these SH-SAW devices and their performance when used in the oscillator configuration has also been recorded. A complete physical structure which can house the sensor along with the associated analog circuitry has been designed and developed. This structure provides electromagnetic shielding as well as reducing the effects of vibration and motion to the entire sensing system.

Introduction

According to the American Cancer Society Facts and Figures, there would be an estimated 230,110 new cases of prostate cancer in the year 2004 with around 29,900 deaths. Prostate cancer, therefore, is a considerable burden to not only those individuals that contract the disease but also to society as a whole. Being able to successfully treat prostate cancer would therefore have a significant impact on morbidity and mortality for a large group of individuals. Prostate specific antigen (PSA), a protein with a molecular weight of 33-34 KDa, has been found to be the most effective marker for diagnosis and detection of prostate cancer. Low concentrations of PSA would be detected using acoustic wave sensors because of their high sensitivity and ability to operate in a liquid environment.

Biosensors with rapid and highly sensitive detection capabilities of various biomolecules including PSA are of great demand in the field of life sciences. Existing immunoassay techniques such as enzyme linked immunoassay (ELISA), fluoroimmunoassay (FIA) and radioimmunoassay (RIA) require specific labels for detection purposes thus making them more complex and time consuming [1, 2, 3]. Further these techniques are cumbersome, laborious, expensive, and hazardous. Developing biosensors for detecting the concentration and activities of the various biological species therefore becomes very important. Recently acoustic wave sensors have been developed for the specific detection of various chemical and biological molecules in liquid media. The chemical interface

selectively adsorbs materials in the solvent to the surface of the sensing area. Changes in the physical parameters of an acoustic device may perturb the mechanical properties of the wave and/or its associated electrical field. For biological sensors, binding of a substance onto the resonating membrane surface causes a decrease in the acoustic wave velocity, which is related to the resonant frequency of the device. The changes in the acoustic and electromagnetic properties of the chip can be directly proportional to the changes in mass.

In this project in order to detect biomolecules, we have followed the following steps which are the achievements of the work to date:

- Preparation of protein chips for immobilization of various antibodies including Prostate Specific Antibodies.
- Studying the protein chips integrity in terms of uniformity and denaturation using the Atomic Force Microscopy technique.
- Exploration of various chemical interfaces like ultrathin polymer films and novel nanostructured materials to improve the sensitivity of gravimetric devices.
- Immobilization of Prostate Specific Antibodies on gold surfaces to construct the calibration curves for various concentrations of antibodies.
- Verification of PSA immobilization with ELISA technique.
- Design and development of Shear Horizontal Surface Acoustic Wave devices for biomolecular sensing.

Since the required PSA detection limit is in the range of 4ng/ml to 20 ng/ml, we planned to develop a versatile technique(s) which can be employed for devices intended for our research. To this end we have chosen two methods for improvement of the sensitivity of the gravimetric devices. 1) Employing an ultrathin polymer film (35 nm thickness) and exploring the chemical modification required for biomolecule immobilization 2) utilizing carbon nanotubes as chemical interface by exploitation of hydrophobic interactions between the surface of CNT and biomolecules.

Quartz Crystal Microbalances (QCM) which is a Thickness Shear Mode (TSM) acoustic wave device was used to quantify and qualify the methodology described above. QCMs are based on these principles wherein a shift in the resonant frequency of the QCM can be attributed to the mass bound on the sensor membrane as per the Sauerbrey equation [4]

$$\Delta f = \frac{-2f_0^2 \Delta m}{A \sqrt{\rho_q \mu_q}} \quad (1)$$

where f_0 is the fundamental resonant frequency, A is the piezoelectrically active area defined by the two gold electrodes, ρ_q is the density of quartz (2.648 g cm^{-3}) and μ_q is the shear modulus ($2.947 \times 10^{11} \text{ dyn cm}^{-2}$). Equation (1) is based on an assumption that the mass has been rigidly attached to the crystal and has negligible thickness as compared to the crystal as a whole [4]. Under such conditions the thin film acts as an extension of the quartz thickness and experiences no shear force during the crystal oscillation [4].

Quartz Crystal Microbalances have been used extensively for protein sensing [5, 6] and gravimetric immunoassays [1, 2, 7, 8, 9]. The simple relationship between the change in frequency (Δf) and the change in mass (Δm) enables QCM to be widely used in sensing

applications. Modification of QCM surface with various polymers like polyurethane [10, 11], polyethylene amine [12, 13, 14], and polystyrene [8, 15, 16] have been previously reported. Polystyrene (PS) is a very common polymer with a high processing ability due to its solubility in most of the organic solvents. The Young's modulus of PS is $\sim 3\text{GPa}$ as compared to $\sim 3\text{MPa}$ of polyurethane. Due to this high mechanical strength no significant viscoelastic coupling effects are observed between PS and the quartz crystal [17]. This particular property of PS makes it an ideal choice as an interfacial layer to improve the biomolecular binding. Previous reports on PS modified QCM surfaces involved immobilization of biomolecules directly onto the polymer surface [8, 15, 16]. In this research work we have developed the silanization technique which improves the hydrophilicity of the PS surface by providing the terminal amine groups which in turn increase the number active sites of the surface for biomolecule immobilization.

Carbon nanotube is an interesting material at the intersection of bio- and nano-technologies. Although carbon nanotubes have many applications, one of the most important and promising applications which might find a significant place in the technologies related to these buckytubes is its biosensing ability [18, 19]. The unique electronic properties of CNT in conjunction with the specific recognition properties of the incubated biomolecules would make CNTs as ideal nanoscale biosensors. A careful observation reveals that carbon nanotubes have the large surface area with all the carbon atoms on the surface. Hence, by a careful alteration of the surface chemistry of the carbon nanotube, they can be exploited for biosensing applications [20] which is motivation behind using CNTs as a chemical interface on the mass sensitive devices. It has been

recently demonstrated that individual semiconducting single wall carbon nanotubes can be used for the detection of glucose oxidase [21]. Controlled attachment of the glucose oxidase enzyme (GOx) to the SWNT sidewall was achieved through a linking molecule which resulted in a clear change of the conductance of the sensing device. We employed QCM to quantify the mass of the biomolecules bound on the surface of the nanotubes.

Historically antibodies have served as important diagnostic tools for the detection of diverse conditions and diseases including those that affect the thyroid, HIV, diabetes, pregnancy, and several types of cancer. In clinical settings, antibodies have been used in several different assays including radioimmunoassays (RIAs), enzyme linked immunoassays (ELISAs) and Western blots. The utility of these assays relies on their ease of use, reproducibility, accuracy and relatively low cost. To expand the technology that is available for the use of antibody based assays we are developing an acoustic wave sensor for the detection of antibody-antigen complexes from complex mixtures. The advantages to this system will be that it is highly reproducible, inexpensive, relatively easy to use and highly portable and more sensitive than the assays in which antibodies are typically used. Although the structure of antibodies are obviously highly variable, they also contain regions of high similarity and the methods that we develop will rely on the interaction of the detection system with those regions of similarity for the detection of the antibody-antigen complexes. The technology that is created will therefore be readily transferable to the detection of other antibody-antigen complexes of clinical interest. Due to the prevalence and clinical relevance we chose to develop this technology for the detection of prostate specific antigen (PSA), a biomarker that has been used for the

detection of prostate cancer in men. Increased concentration of this antigen has been correlated with the staging of prostate cancer and it has a long history of use in a clinical setting as a biomarker. We have immobilized various concentrations of Prostate Specific Antibodies on gold surfaces to construct the calibration curves of antibody.

SH-SAW sensor and the associated electronic circuitry

Following successful improvement of the sensitivity of the QCM biosensor using polystyrene and CNT modified surfaces, focus was shifted to the fabrication and testing of biosensors based on Shear Horizontal Surface Acoustic Wave (SH-SAW) sensors. Each chip consists of two SH-SAW devices as shown in the schematic of Figure 1 (one device to the left and the other to the right). SH-SAW devices were designed to operate in a differential mode with one of them being the reference device and the other operating as the sensor.

Each of these devices will operate as oscillator and the difference in frequency of these devices will be obtained using a mixer. The frequency of oscillation of the sensor alone will be perturbed by the biomolecule whereas the frequency of oscillation of both the reference device and the sensor will be affected by unwanted interferences. Therefore, the difference frequency is the change caused due to biomolecule interaction alone and this can be used to quantify the concentration of biomolecules. Figure 2 shows the block diagram of the overall electronic circuitry. Figure 3 shows the diecast aluminum enclosure that is currently housing the two amplifiers and the mixer for testing purposes.

SH-SAW device fabrication and testing

Differential SH-SAW devices were designed and .gds files were prepared the layout of which is shown in Figure 4. The devices were fabricated on 64° rotated Y-cut Lithium Niobate substrates at the University of Michigan's Microfabrication facility in Ann Arbor, Michigan. Figure 5 shows the alignment of the devices on the wafer with respect to the major flat and for fabrication of the devices the following step sequence was followed:

Step1:

The first step of fabrication starts with the cleaning of the substrate by immersing it in a solution of soapy water with a pH between 7.0 and 8.5 or low concentration ammonia in water, followed by hand-wiping in a mixture of four parts alcohol and one part acetone. The hand wiping is in a continuous motion from one edge to the other to avoid leading- or trailing edge stains. Throughout the cleaning process, it is critical to avoid letting the wafer dry during intermediary steps or prior to the final drying step. Premature drying can leave stains or residue from the baths or cleaning solutions that can be difficult to remove.

Step 2:

Subsequently chromium and gold are evaporated (Enerjet e beam evaporator) (Figure 6). This is obtained by sequential sputtering of chromium and gold with thickness of 40nm and 60nm respectively.

Step 3:

The photoresist is spun on the front side of the wafer (Figure 7).

Step 4:

Photo resist is exposed to UV light using the mask and developed (Figure 8).

Step 5:

Photolithography to remove exposed chromium and gold (Figure 9).

Step 6:

Photoresist is stripped to produce final device (Figure 10 is the top view and Figure 11 is a 3-dimensional view).

Step 7:

The wafer is final diced using blue tape on one side to produce individual devices. Figure 12 shows the fabricated devices cut on blue tape.

Following this, the individual devices were tested. For this purpose, silver paste was used to glue the connecting wires to the contact pads and the external traces. Figure 13 shows the copper board with SMA connectors which were used to test the SH-SAW devices.

The frequency response of the devices was then measured using Network Analyzer. Figure 14 shows the frequency response of the SH-SAW device over a frequency span of 40 MHz centered at 110 MHz. It can be seen that the device loss at center frequency is around 6.5 dB.

The SH-SAW device was then placed in a feedback loop with an amplifier forming an oscillator. Figure 15 shows the output from the oscillator measured using a Spectrum

Analyzer over a frequency span of 40 MHz. The oscillation frequency is 109.4 MHz and the output power is -3.3369 dBm.

Physical Structure

The SAW sensor is sensitive to vibration and motion. To reduce these factors, a new physical structure is being developed which can house the sensors and the associated electronics and can seal the sensor from the rest of the structure. It consists of a base made from half-inch solid steel plate is used to mount the rest of the structure on. This steel plate is five inches by nine inches and weighs approximately 9 lbs.

A small aluminum box (Figure 16) will be manufactured to house some of the electronics as well as support the analog printed circuit board and Kynar board. This box will be welded from 3/8" aluminum sheet.

Two posts will then be mounted to the top of the aluminum housing that fit through 1/2 inch holes in the Kynar board (Figure 17). Springs on these posts provide constant pressure down on the Kynar board to keep electrical contacts and a good seal around the SAW sensor. This design also allows for simple removal of the Kynar board for cleaning, access to the SAW sensor, and access to the analog printed circuit board.

A larger aluminum box will also be used for shielding against electromagnetic interference. This box slides over the aluminum housing and rests on the steel base (Figure 18).

Experimental Details

Protein and Antibody

fPSA (BioDesign International Inc), Protein A (Sigma-Aldrich) and mouse monoclonal IgG antibody (BioDesign International Inc) were used throughout these studies. Protein A, fPSA and monoclonal IgG were resuspended in phosphate buffered saline (PBS; Sigma-Aldrich) at desired concentrations and stored at -20°C in $50\mu\text{l}$ aliquots before use.

Materials

Polystyrene, 3-Aminopropyl triethoxysilane (3-APTES), glutaraldehyde, acetone, glycine and sodium chloride were purchased from Sigma-Aldrich Chemical Company. Polystyrene dissolved in chloroform (7% w/v) was used to coat the QCM chips. Solutions of 5% 3-APTES in acetone, 5% glutaraldehyde in milli-Q water, PBS buffer with pH 7.0 in milli-Q water were prepared. 0.1M Glycine solution in milli-Q water, 0.1M glycine-HCl buffer with pH 2.4 and 0.5M NaCl solution was prepared. CNTs were purchased from Carbolex Inc.

Experimental Procedures

For promoting the immobilization of Protein A and to provide the necessary amine groups on the gold surface the protocol of Muramatsu et al. (1987) was followed [1]. To remove any organic contamination from the surface of the crystal and improve the hydrophilic nature of the chip, it was cleaned with Piranha solution (3 parts of H_2SO_4 in 1 part of 30 % H_2O_2). Enough Piranha solution was employed to cover the gold surface of the chip and allowed to incubate at room temperature for two minutes before rinsing with milli-Q water. This procedure was repeated twice. Subsequently the chip was blown dried

in a stream of nitrogen gas. A 5% solution of 3-APTES in acetone was added to create a self-assembled monolayer (SAM). After 1 hour the sample was rinsed with milli-Q water after the APTES treatment to remove the physisorbed molecules. The chip was placed in a 5% glutaraldehyde solution for 3 hours to allow for the cross linking between the chip and the Protein A. The crystal was then covered with 20 μ l solution of Protein A (0.5 mg/ml). After 1 hour the solution was removed and the crystal was subjected to several wash-dry cycles with milli-Q water until the QCM crystal reached its steady resonant frequency. The chip was then covered with 0.1 M glycine dissolved in PBS for 1 hour to block any sites not bound to Protein A on the glutaraldehyde modified chip. The chip was then rinsed with 0.1M glycine-HCl buffer (pH 2.4) to wash off any excess proteins or glycine before being thoroughly rinsed with milli-Q water. 20 μ l of the mouse monoclonal IgG solution was then incubated on the chip for 1 hour followed by rinsing with 0.5M NaCl to remove any non-specifically adsorbed antibody. For the experiments in which binding was measured with the polymer film, polystyrene was spin coated onto the chip at a speed of 1000 rpm and then treated with 50 % (v/v) HNO₃ in concentrated H₂SO₄ for 1 hour [22]. The substrate was then modified with 3-APTES followed by glutaraldehyde as described above.

Characterization tools and methods

A Quartz Crystal Microbalance (Stanford Research Systems QCM100) with 5MHz AT-cut quartz crystals (gold coated) was used to quantitatively study the ability to bind Protein A and mouse monoclonal IgG to the chip. The gold surface, which forms the active area for immobilization was 1.37cm² and the mass sensitivity of the crystal was

0.057 Hz/ng/cm². Frequency was monitored using a Stanford Research System Universal Time Interval Counter (Model No. SR620).

Qualitative studies were made using AFM (Themomicroscopes Inc.; Autoprobe CP Research machine) in non-contact mode. For AFM studies silicon substrates were used with the same modification techniques as those described above for the QCM chips. The AFM tips used for imaging were silicon with an approximate radius of curvature of 20nm. Biomolecular imaging was performed in non-contact mode. The AFM images were analyzed using image-processing software (IP 2.1) to calculate the RMS roughness value.

Results and Discussions

Protein A, which has a particularly high affinity for the F_c fragment of IgG, was immobilized first on the chips to prevent the random immobilization of the antibodies, maximizing the ability of the chip immobilized antibodies to bind to antigens [1, 2]. Figure 19 shows the QCM frequency response to Protein A immobilization without the polystyrene film. Point 1 refers to the point of addition of the Protein A containing solution to the chip. Point 2 indicates when the crystal was subjected to several wash-dry cycles and point 3 represents the frequency of crystal when Protein A was specifically bound on the surface. The frequency shift due to this direct binding was 220 Hz. From the Sauerbrey equation, this frequency shift corresponds to a 2.8 µg mass uptake.

To determine if antibodies could bind to the Protein A that had been immobilized, antibody containing solutions were incubated with the chips. In Figure 20 point 1 indicates the time at which the antibody containing solution was added to the crystal. The binding of the antibody to the immobilized Protein A caused a decrease in the resonant frequency and stabilization occurred after 15 minutes. Point 2 represents the time when the crystal was rinsed with 0.5M NaCl to remove any non-specifically adsorbed IgG and point 3 corresponds to the final resonant frequency after the NaCl rinsing. The frequency shift for IgG immobilization was found to be 282 Hz which corresponds to a calculated mass change of 3.61 μg .

To determine if covering the chips with a thin polymer film could also increase the efficiency of Protein A binding and hence improvement in antibody immobilization, we coated the surface of several chips with ultra thin film of polystyrene. However, polystyrene films are hydrophobic in nature causing the biomolecules to denature and hence lose their activity [23]. To avoid denaturation of the biomolecules, the polymer film functional groups such as amino, hydroxyl groups can be chemically added. This helps the biomolecules retain their activity as immobilization now takes place through the hydrophilic arms of the polymer film [24, 25]. To increase the hydrophilicity of the surface which would increase the ability to add the functional groups, the chips were subjected to an acidic treatment followed by aqueous silanization [22]. Figure 21 shows the schematic representation of the acidic treatment and the APTES modification of polystyrene. The acid treatment provides NO_2 groups and the APTES modification creates a polymer film with an amine group that can react with the glutaraldehyde used to covalently attach the biomolecules to the surface.

This improvement in the hydrophilicity was confirmed by monitoring the water distribution on polystyrene and APTES modified polystyrene surfaces. Figure 22.a and Figure 22.b show the water distribution images (recorded using a Digital Blue Computer microscope) on polystyrene and modified polystyrene surfaces. As is evident from the images there is a decrease in the contact angle of about 34° for APTES modified polystyrene surfaces compared to the unmodified surface indicating improvement in hydrophilicity.

Figure 23 shows the AFM image of IgG immobilized on polystyrene coated surface. It can be seen that there is a uniform coverage of the antibody molecules of approximately 10 nm in size on the substrate. The AFM imaging performed two hours after the biomolecules immobilization revealed that the molecules still retain their characteristic “heart shape” proving that they still are not denatured.

The biomolecule immobilization on polystyrene coated surfaces was then quantitatively studied with QCM and compared to the immobilization performed without polystyrene film. Figure 24 shows the QCM response to Protein A immobilization. Point 1 indicates the time when Protein A was added and as can be seen the signal became stable only after 20 minutes. Point 2 represents when several wash-dry cycles were performed and point 3 is the time at which the frequency stabilized once all non-specifically adsorbed molecules were rinsed away. The registered frequency shift was 364 Hz which corresponds to a mass change of 4.66 μg . This represented a 65% increase when compared to the QCM

chips that were not coated with the polymer film. Similar results were obtained for the binding of IgG. The QCM response (Figure 25) for IgG immobilization on the polystyrene surface showed a frequency shift of 391 Hz corresponding to a mass uptake of 5.01 μ g. This represented a 40% increase when compared to chips that had not been modified with polystyrene.

AFM images of the bare gold crystal and polystyrene coated crystal along with the height profile of the surface along a line are shown in Figure 26 and Figure 27 respectively. The AFM studies (as is evident from Figure 26) revealed that the gold coated quartz crystals had a RMS surface roughness of 98.4nm. An appreciable decrease in the surface roughness to 1.75nm was observed when the crystal was coated with an ultra thin layer of polystyrene. Gold and polystyrene are both hydrophobic in nature. APTES modification of the gold surface although improves the hydrophilicity of the surface, it doesn't result in much decrease in the roughness of the surface. On the other hand APTES modification of the polystyrene coated surface not only improves the hydrophilicity of the surface but there is a marked improvement in the surface roughness because of the polymer film. The improved biomolecular binding and hence the increased frequency shifts may be attributed to this improvement in the surface smoothness.

We speculate that with a gold surface roughness of 98.4nm, the orientation of the protein A molecules is not uniform and hence there are chances that the active sites on one protein molecule would sterically hinder the active sites on the other resulting in a non uniform binding of biomolecules and hence loss of active sites. On the other hand a polymer coated surface although decreases the available surface area, provides the

biomolecules with a much more plane and uniform surface resulting in less steric hindrance. Hence more active sites for antibody immobilization are available resulting in improved binding and hence higher sensitivity.

CNT based QCM sensor

CNT experiments were performed using 5 MHz AT-cut Quartz crystals coated with carbon nanotubes casted on the gold surface of the chip. Then the chip was baked at 50°C for one hour. The presence of the CNT on the gold surface was confirmed by Raman spectroscopy. Figure 28 shows the Raman spectrum of CNT on the gold surface. The characteristic G-band and D-band peaks of the carbon nanotube can be observed. Figure 29 is an AFM micrograph of the CNT and protein molecules. From this Figure, it can be seen that protein molecules were bound on the sidewalls of the tube and bundles of CNT were decorated with Streptavidin molecules.

The quantitative study of mass uptake of CNT network due to biomolecules immobilization was performed using QCM. In this part, the chemical interface is the CNT matrix on the gold surface coated on the QCM crystal. Measurements of CNT coated QCM crystals were performed by covering the chips with PBS before addition of the protein solutions. Figure 30 depicts the QCM response using streptavidin. For a concentration of 1 μ M of streptavidin, a change of 120 Hz in resonant frequency was recorded. From the Sauerbrey equation the mass bound was calculated to be 1.538 μ g. when the concentration on the chip was increased to 2 μ M, the change in the frequency was found to be 26Hz. This corresponds to a mass uptake of 0.33 μ g. The lower frequency shift can be attributed to fewer active sites available for the protein molecules

as described in the conductance based sensors.

Similar experiments were performed with IgG and the frequency change was 248Hz using a 2 μ M concentration. Figure 31 shows the QCM response for the IgG incubation. When the crystal was resonating at its natural frequency, the carbon nanotube solution was introduced on to the chip. After the chloroform evaporated, the frequency stabilized and the CNT formed a uniform matrix on the surface. Then PBS was introduced on to the chip and due to change in the viscosity a frequency shift was recorded. After the frequency stabilized, finally the IgG antibody was introduced and the frequency change of 248 Hz was recorded for a concentration of 2 μ M. This frequency corresponds to mass of 3.17 μ g. The frequency shift was found to be approximately 50Hz for same concentration of IgG immobilized directly on the gold surface which suggests that there is a five fold increase in the number of biomolecules bound when CNT was used as chemical interface.

PSA at different concentrations (550ng/ml, 275 ng/ml, 68.5 ng/ml) were incubated on the surface of QCM chips to construct the calibration curve of antibody. Figure 32 depicts the QCM measurement for antibody at a concentration of 550ng/ml. The frequency shift exhibited by the crystal at this concentration was around 262Hz. The procedure for the PSA detection was as follow:

- A – cover chip with 5% 3-Aminopropyl triethoxysilane in acetone for 1 hour
- B – remove 3-APTES
- C – cover chip with 5% gluteraldehyde solution for 3 hours

D – remove gluteraldehyde; add 20 μ l of protein A (conc. of 500 μ l/ml) plus 1 ml PBS for 2 hours

E - Remove protein A; Add 1 ml of 0.1M glycine dissolved in PBS for 1 hour

F - Remove glycine; rinse with 0.1M Glycine-HCL buffer (pH 2.4) and rinse with milli-Q water; Add 20 μ l of IgG (conc. of 160 μ l/ml) plus 1 ml PBS for 1 hour

G - Remove IgG; add 1 ml PSA (conc. 550 ng/ml)

H – Remove PSA

Figures 33 and 34 depict measurements for 275 ng/ml and 68.5 ng/ml PSA concentrations and the measured frequency shifts were 139Hz and 94 Hz respectively.

ELISA

To ensure that PSA is bounding on the crystals a comparative study using Elisa kit was used. The procedure for this comparative study was as follow:

1. Attach PSA to QCM crystal and to 96 well plate in the normal procedure. (500 μ g/ml)
2. Wash crystals and plate wells with wash buffer (PBS with 0.05% Tween-20) 2X
3. Block crystals and wells with PBS containing 5% Sucrose and 1% Bovine Serum Albumin. (200 μ l)
4. Incubate in humidified chamber for 1 hour at room temperature.
5. Wash crystals and wells 3X with wash buffer.

6. Add monoclonal antibody to PSA to the wells and the crystal. (concentration – 2 $\mu\text{g/ml}$, amount – 100 μl)
7. Incubate in humidified chamber for 2 hours at room temperature.
8. Wash crystals and wells 3X with wash buffer.
9. Add Peroxidase-conjugated AffiniPure Goat Anti-Mouse IgG to crystals and wells. (1:5000 dilution according to manufacturer instructions)
10. Incubate in humidified chamber for 2 hours at room temperature.
11. Wash crystals and wells 2X with wash buffer.
12. Add color reagent (TMB tablet in phosphate/citrate buffer (1 tablet in 10 ml of buffer). Cover with foil as TMB is light sensitive. Add 4 μl of 30% H_2O_2 to TMB solution one minute before adding to wells and crystal. Add 100 μl and cover with foil. Allow to develop for 20 minutes.
13. Add 100 μl of 0.1 M phosphic acid to stop the reaction.
14. Read on spectrophotometer, PowerWave 200, with the wave length of 450nm.
The solution from the crystals was transferred to wells on the 96 well plate for reading.

The Elisa was run in a 96 well plate to serve as a control that the reaction was in fact occurring on the crystals due to this being an unconventional way to run Elisa. The other control was a negative control of not adding the Streptavidin HRP. The assay was run twice but upon the second run the color reagent got contaminated and no results were obtained.

Results:

96 well plate: 2.336

2.402

96 well plate without HRP: 0.067

Crystal: average of 3 wells – 1.397

Crystal without HRP: average of 3 wells – 0.046

It is clear from these results that PSA was in fact bound to both the crystals and the 96 well plate.

Key research accomplishments

Key research accomplishments of this work includes:

- 1) Ultrathin polystyrene polymer films can be used to enhance the sensitivity and these films can be chemically treated to provide necessary terminal groups to tether biomolecules to the surface.
- 2) A 40% to 60% improvement in sensor sensitivity was demonstrated with aqueous silanization was achieved.
- 3) Novel nanostructure materials like carbon nanotubes have been integrated with existing technologies to push the detection limit of acoustic wave based sensors.
- 4) CNT based interfacial layer showed five fold improvement of the sensor response.
- 5) PSA antibody at different concentrations was immobilized on the gold surface.
- 6) Using Elisa technique it was shown that PSA was in fact bound to both the crystals and the 96 well plates.

- 7) Shear Horizontal Surface Acoustic Wave (SH-SAW) devices have been designed and fabricated to operate a differential mode as biosensors with high sensitivity.
- 8) SH-SAW devices have tested and characterized for both time domain and frequency domain.
- 9) The response of these SH-SAW devices and their performance when used in the oscillator configuration has also been tested.
- 10) A complete physical structure which can house the sensor along with the associated analog circuitry has been designed and developed to provide electromagnetic shielding as well as reduce the effects of vibration and motion to the entire sensing system.

Reportable outcomes

Manuscripts, abstracts, presentations, patent applied

1. M.Z. Atashbar, B. Bejcek, A. Vijh, and S. Singamaneni “QCM Biosensor with ultra thin polymer film”, *Sensor and Actuators B*, Vol. 107, Issue 2: Jun 2005, pp. 945–951.
2. M.Z. Atashbar, B.E. Bejcek, S. Singamaneni “Carbon nanotube network-based biomolecule detection” *Sensors Journal*, IEEE, Volume 6, Issue 3, Jun 2006 pp. 524 – 528.
3. M.Z. Atashbar, B. Bejcek, and S. Singamaneni “SWNT Network for biomolecule detection” in *Functional Carbon Nanotubes*, edited by D.L. Carroll, B. Weisman,

- S. Roth, and A. Rubio (Mater. Res. Soc. Symp. Proc. 858E, Warrendale, PA , 2005), pp. HH14.8.1- HH14.8.6 (2005)
4. M.Z. Atashbar, B. Bejcek, S. Singamaneni “Carbon nanotube based biosensors”, IEEE Sensor conference, Vienna, Austria, Oct. 24th-27th, 2004, pp. 1048 - 1051 (2004).
 5. M.Z. Atashbar, B. Bejcek, A. Vijn, S. Singamaneni “Sensitivity enhancement of QCM biosenor with polymer treatment”, 2004 IEEE International Ultrasonics, Ferroelectrics, and Frequency Control, 23-27th August 2004 pp. 329-332, Monntreal, Canada (2004).
 6. M.Z. Atashbar, B. Bejcek, A. Vijn, and S. Singamaneni “Piezoelectric biosensor for prostate cancer detection”, 4th Annual Symposium of Michigan Prostate Research Colloquium, Van Andel Research Institute, Grand Rapids, MI, May 1, (2004).
 7. M.Z. Atashbar and B. Bejcek, “Integrated sensor microsystem and method for detection bimolecular in liquid”, WMU IP Case #73 on 10/12/2005, and PCT application was filed on 10/23/2006

Degrees obtained that are supported by this award

1. Mr. Srikant Signamanieni, MSc. in Electrical Engineering, December 2004
2. Mr. Aditya Vijn, MSc. in Electrical Engineering, December 2004

List of personnel

1. Dr. Massood Atashbar
2. Dr. Bruce Evan Bejcek
3. Mr. Srikant Signamanieni
4. Mr. Aditya Vijn
5. Mrs. Krystal Anderson

Conclusions

Owing to the increasing demands in consumer, medical and military field's development of the highly sensitive biosensors has gained utmost importance. It was demonstrated that the treatment of the QCM quartz chips with polystyrene exhibited a significant decrease in the RMS roughness of the gold crystal, resulting in a surface that was more uniform. The disadvantage of this technique, however, is that the hydrophobicity of the surface remains high. To counteract this undesirable trait, chips were treated by a simple aqueous silanization technique, which resulted in a significant improvement in the hydrophilicity of the surface. Chips that had an improved hydrophilicity were successfully utilized for biomolecular immobilization. Protein A resulted in a shift of 364 Hz on the polystyrene modified surface as opposed to the 220 Hz shift of frequency for direct immobilization. Subsequent IgG immobilizations also showed similar trend with the frequency shifts being 391Hz and 282 Hz for immobilizations with and without the polymer film respectively. AFM imaging revealed uniform biomolecule coverage on polymer coated surfaces. This improved binding of biomolecules when coated with

polystyrene is hypothesized to be due to the marked improvement in the roughness of the surface over which the biomolecules were immobilized.

The biomolecules were adsorbed on the sidewalls of carbon nanotube. The mass of the biomolecule bound was quantitatively analyzed using QCM and CNT coated crystals exhibited a five fold increase in biomolecule adsorption. In summary one can conclude that carbon nanotube can find significant applications in the new generation of biosensors. Functionalization of carbon nanotube might significantly improve the chemical compatibility and selectivity of the sensors. Immobilization of PSA on gold surfaces was accomplished. Using Elisa technique it was shown that PSA was in fact bound to both the crystals and the 96 well plates. SH-SAW devices were designed in a differential configuration to be used as biosensors with high selectivity. These SH-SAW devices fabricated at the Microfabrication facility at University of Michigan, Ann Arbor. The frequency response of these SH-SAW devices and their performance when used in the oscillator configuration has also been recorded. A complete physical structure which can house the sensor along with the associated analog circuitry has been designed and developed. This structure provides electromagnetic shielding as well as reducing the effects of vibration and motion to the entire sensing system.

References

1. H. Muramatsu, J. M. Dicks, E. Tamiya, I. Karube, Piezoelectric Crystal Biosensor Modified with Protein A for Determination of Immunoglobulins, *Analytical Chemistry* 59 (1987) 2760-2763.

2. F. Caruso, E. Rodda, D. N. Furlong, Orientational Aspects of Antibody Immobilization and Immunological Activity on Quartz Crystal Microbalance Electrodes, *Journal of Colloid and Interface Science* 178 (1996) 104–115.
3. Y. Y. Wong, S. P. Ng, M. H. Ng, S. H. Si, S. Z. Yao, Y. S. Fung, Immunosensor for the Differentiation and Detection of Salmonella Species Based on a Quartz Crystal Microbalance, *Biosensors & Bioelectronics* 17 (2002) 676-684.
4. G. Sauerbrey, *Zeitschrift Fur Physik* 155 (1959) 206-222.
5. C. Barnes, C. D'Silva, J. P. Jones, T. J. Lewis, Lectin coated piezoelectric crystal biosensors, *Sensors and Actuators B: Chemical* 7 (1992) 347-350.
6. S. Imai, H. Mizuno, M. Suzuki, T. Takeuchi, E. Tamiya, F. Mashige, A. Ohkubo, I. Karube, Total urinary protein sensor based on a piezoelectric quartz crystal, *Analytica Chimica Acta* 292 (1994) pp 65-70,.
7. B. Guo, J. Anzai, T. Osa, Adsorption Behavior of Serum Albumin on Electrode Surfaces and the Effects of Electrode Potential, *Chemical & Pharmaceutical Bulletin* 44 (1996) 800-803.
8. S. P.Sakti, P. Hauptmann, B. Zimmermann, F. Buhling, S. Ansorge, Disposable HSA QCM-immunosensor for practical measurement in liquid, *Sensors & Actuators B* 78 (2001) 257-262.
9. D. M. Gryte, M. D. Ward, W. S. Hu, Real-Time Measurement of Anchorage-Dependent Cell Adhesion using a Quartz Crystal Microbalance, *Biotechnology Progress* 9 (1993) 105-108.

10. O. Hayden, R. Bindeus, F. L. Dickert, Combining atomic force microscope and quartz crystal microbalance studies for cell detection, *Measurement Science and Technology* 14 (2003) 1876–1881.
11. O. Hayden and F. L. Dickert, Selective Microorganism Detection with Cell Surface Imprinted Polymers, *Advanced Materials* 13 (2001) 1480-1483.
12. B. König and M. Grätzel, Development of a piezoelectric immunosensor for the detection of human erythrocytes, *Analytica Chimica Acta* 276 (1993) 329-333.
13. B. König and M. Grätzel, Detection of human T-lymphocytes with a piezoelectric immunosensor, *Analytica Chimica Acta* 281 (1993) 13-18.
14. E. P. Sochaczewski and J. H. T. Luong, Development of a piezoelectric immunosensor for the detection of *Salmonella typhimurium*, *Enzyme and Microbial Technology* 12 (1993) 173-177.
15. S. P. Sakti, S. Rosler, R. Lucklum, P. Hauptmann, F. Buhling, S. Ansorge, Thick polystyrene-coated quartz crystal microbalance as a basis of a cost effective immunosensor, *Sensors & Actuators A* 76 (1999) 98-102.
16. C. Fredriksson, S. Khilman, B. Kasemo, D. M. Steel, In vitro real-time characterization of cell attachment and spreading, *Journal Of Materials Science: Materials In Medicine* 9 (1998) 785- 788.
17. R. Lucklum, C. Behling, P. Hauptmann, Gravimetric and non-gravimetric chemical quartz crystal resonators, *Sensors And Actuators B* 65 (2000) 277-283.
18. R. J. Chen, S. Bangsaruntip, K. A. Drouvalakis, N. W. ShiKam, M. Shim, Y. Li, W. Kim, E. J. Utz, and H. Dai, *PNAS*, vol. 100, p. 4984, (2003).
19. Y. Lin, F. Lu, Y. Tu, and Z. Ren, *Nanoletters*, vol. 4, p. 191, (2004).

20. R. J. Chen, H. C. Choi, S. Bangsaruntip, E. Yenilmez, X. Tang, Q. Wang, Y. L. Chang, and H. Dai, *Journal of American Chemical Society*, vol. 126, p. 1563, (2004).
21. K. Besteman, J. O. Lee, F. G. N. Wiertz, H. A. Heering, and C. Dekker, *Nanoletters*, vol. 3, p. 727, (2003).
22. J. Kaur, K. V. Singh, M. Raje, G. C. Varshney, C. R. Suri, Strategies for direct attachment of hapten to a polystyrene support for applications in enzyme-linked immunosorbent assay (ELISA), *Analytica Chimica Acta* 506 (2004) 133–135.
23. J.E. Butler, L. Ni, W.R. Brown, K.S. Joshi, J. Chang, B. Rosenberg, E.W. Voss, Jr, The immunochemistry of sandwich elisas—VI. Greater than 90% of monoclonal and 75% of polyclonal anti-fluorescyl capture antibodies (CAbs) are denatured by passive adsorption, *Molecular Immunology* 30 (1993) 1165-1175.
24. J. Buijs, J. W. T. Lichtenbelt, W. Norde, J. Lyklema, Adsorption of monoclonal IgGs and their F(ab')₂ fragments onto polymeric surfaces, *Colloids and Surfaces B: Biointerfaces* 5 (1995) 11-23.
25. N. Zammateo, C. Girardeaux, D. Delforge, J. J. Pireaux, J. Remacle, Amination of Polystyrene Microwells: Application to the Covalent Grafting of DNA Probes for Hybridization Assays, *Analytical Biochemistry* 236 (1996) 85-94.

Collected Figure Captions

Figure 1. Shear Horizontal Surface Acoustic Wave (SH-SAW) Sensor Chip.

Figure 2. Block diagram of the electronic circuitry.

Figure 3. Aluminum enclosure containing the two amplifiers and the mixer.

Figure 4. SH-SAW Device layout.

Figure 5. Alignment of SAW devices on wafer with respect to the major flat.

Figure 6. Substrate with Chromium and Gold.

Figure 7. Substrate with chromium, gold and photoresist

Figure 8. Substrate with chromium, gold and developed photoresist.

Figure 9. Substrate with exposed chromium and gold removed.

Figure 10. Final device.

Figure 11. 3-dimensional view of the final device.

Figure 12. Fabricated SH-SAW devices cut on blue tape.

Figure 13. SH-SAW devices on copper board with SMA connectors.

Figure 14. Frequency Response of the SH-SAW device.

Figure 15. SH-SAW Oscillator output.

Figure 16. Aluminum Housing for Analog and Digital Circuitry.

Figure 17. Kynar Board residing on Aluminum Box along with the sliding lid.

Figure 18. Aluminum Lid Covering the Base and providing Electromagnetic Shielding.

Figure 19. QCM frequency response for Protein A immobilization without polystyrene.

Figure 20. QCM frequency response for IgG immobilization without polystyrene.

Figure 21. Polystyrene film when treated with acid and 3-APTES; (a) Polystyrene film (b) Formation of the NO₂ groups by acidic treatment (c) Formation of the amine groups by silanization.

Figure 22. Image of water distribution on polystyrene (a) and APTES modified polystyrene (b) surfaces.

Figure 23. AFM image of IgG immobilized on polystyrene coated surface (b) height profile of the surface along a line.

Figure 24. QCM frequency response for Protein A immobilization on polystyrene

Figure 25. QCM frequency response for IgG immobilization on polystyrene.

Figure 26. (a) AFM image of the gold surface and the (b) height profile of the surface along a line.

Figure 27. (a) AFM image of polystyrene coated gold surface and (b) the height profile of the polystyrene surface along a line.

Figure 28. Raman spectrum of gold surface of QCM casted with SWNT.

Figure 29. Streptavidin molecules decorating the SWNT side walls.

Figure 30. QCM response for various concentrations streptavidin.

Figure 31. QCM response for various concentrations of IgG.

Figure 32. Frequency shift for PSA antibody (550ng/ml) immobilization.

Figure 33. Frequency shift for fPSA antibody (275ng/ml) immobilization.

Figure 34. Frequency shift for PSA antibody (68.5ng/ml) immobilization.

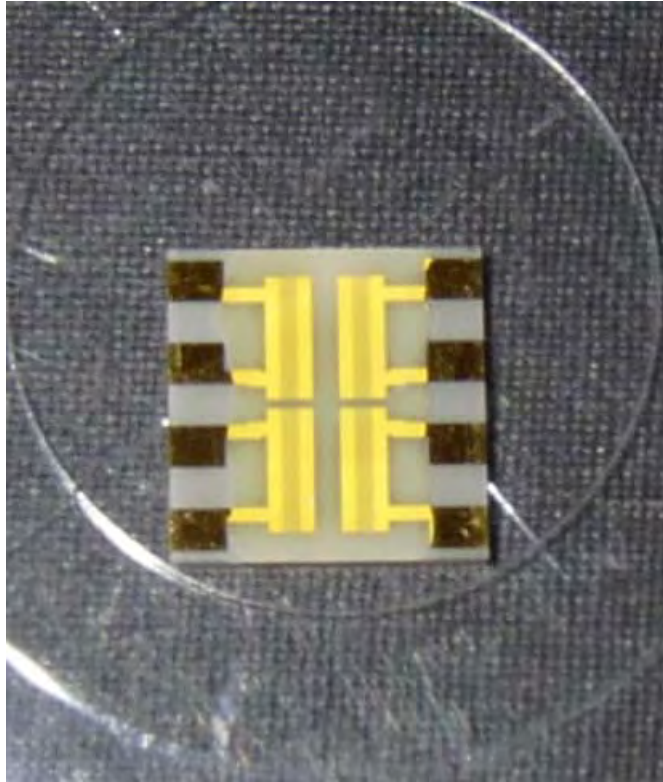


Figure 1. Shear Horizontal Surface Acoustic Wave (SH-SAW) Sensor Chip.

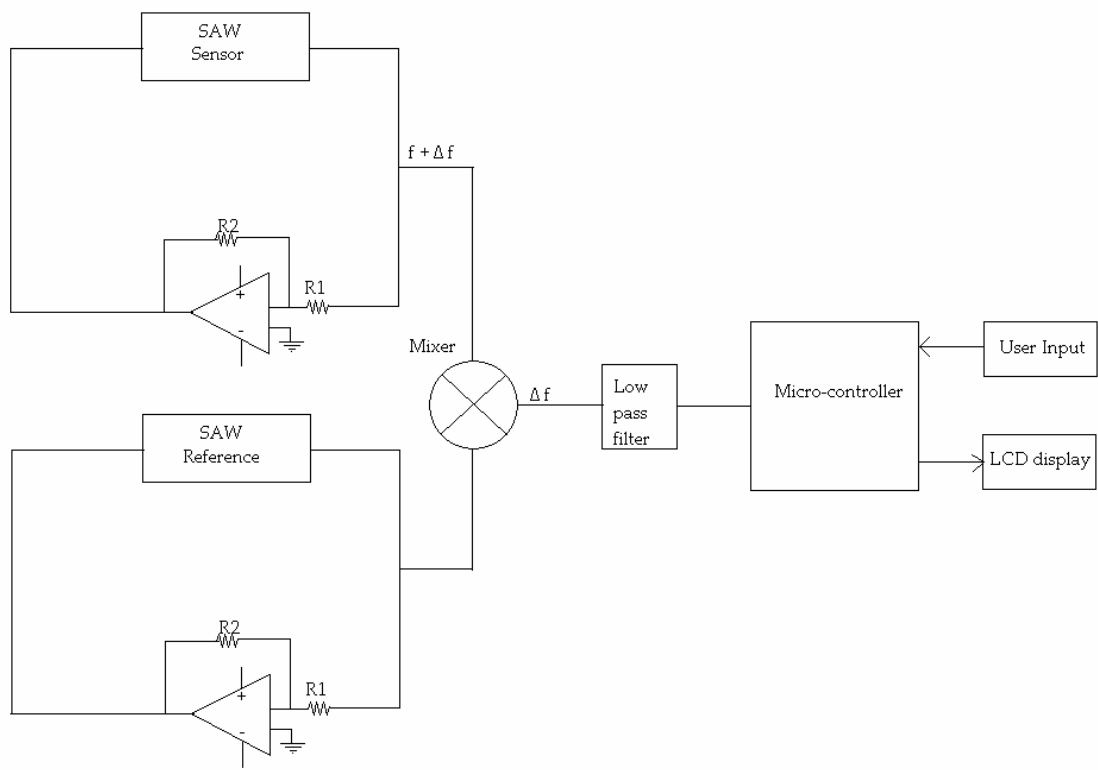


Figure 2. Block diagram of the electronic circuitry.

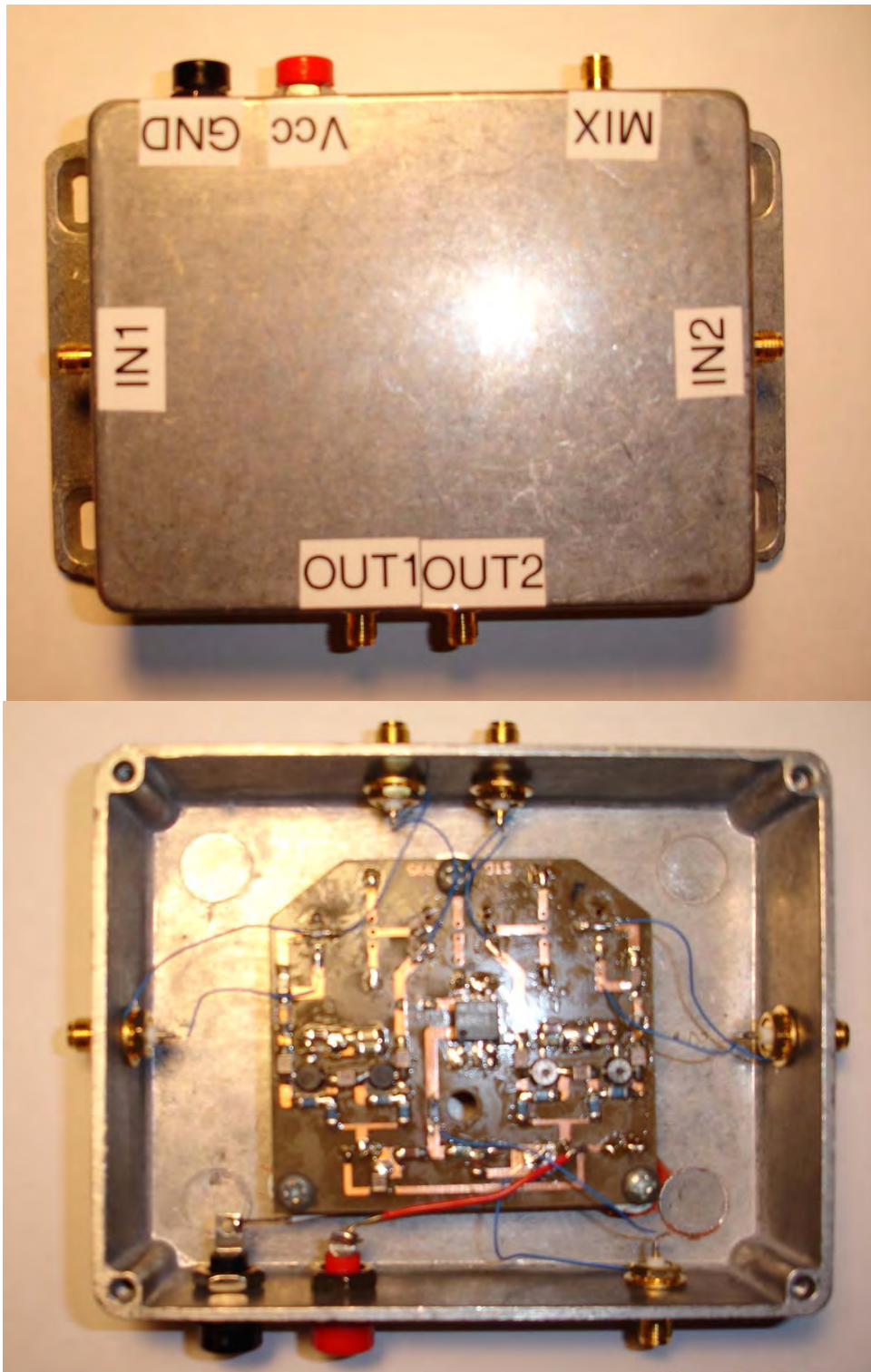


Figure 3. Aluminum enclosure containing the two amplifiers and the mixer.

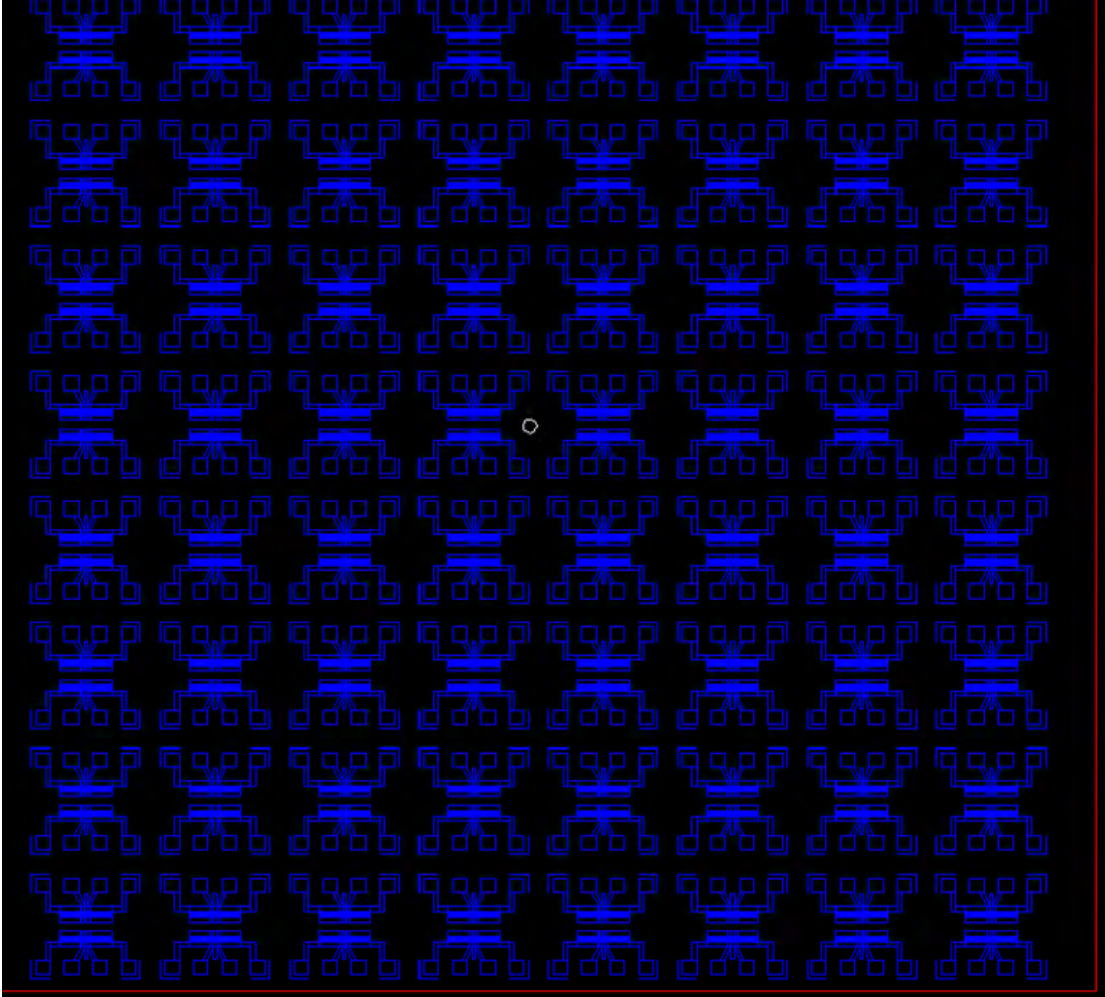


Figure 4. SH-SAW Device layout.

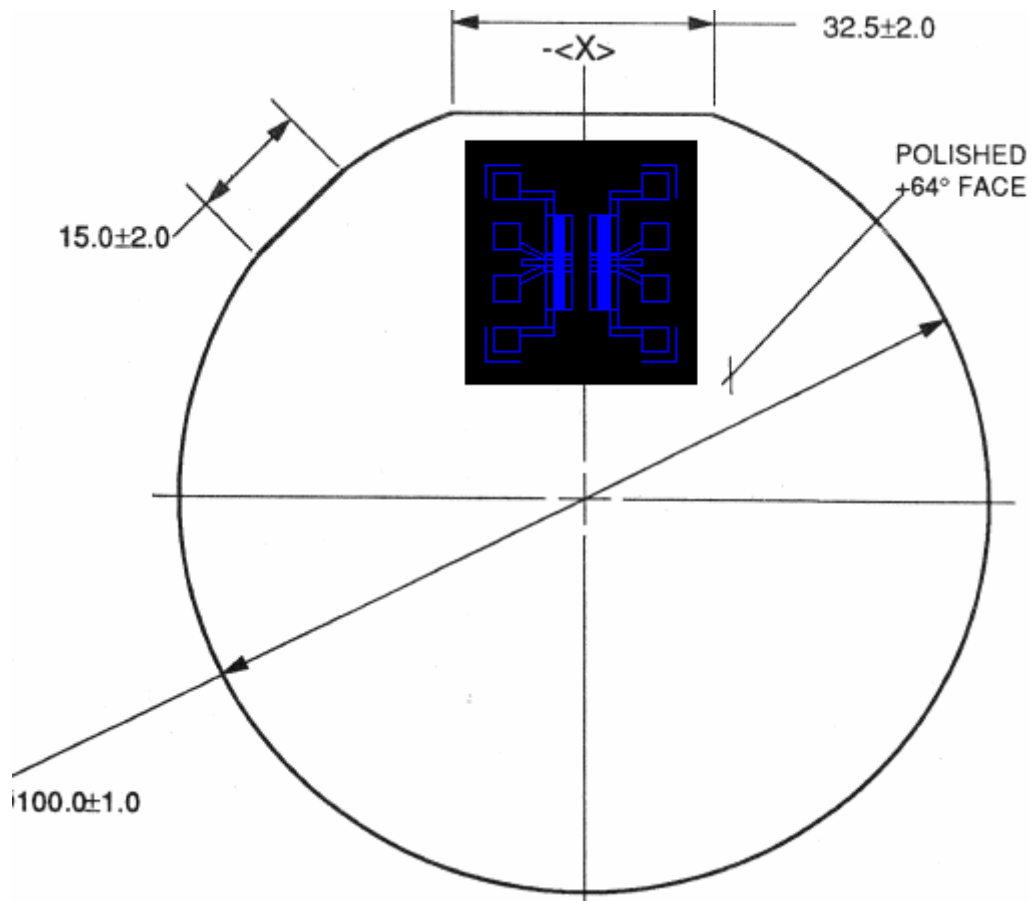


Figure 5. Alignment of SAW devices on wafer with respect to the major flat.

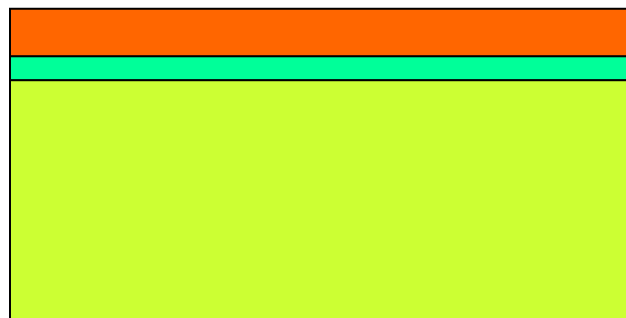


Figure 6. Substrate with Chromium and Gold.

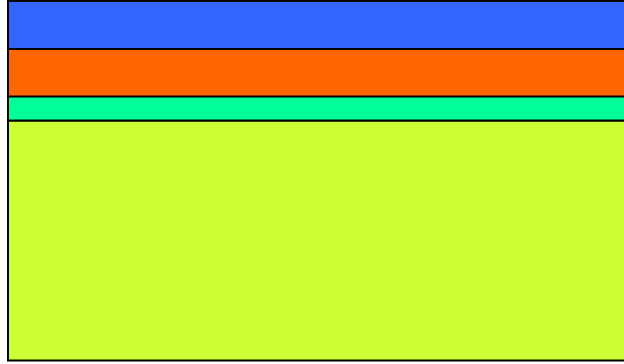


Figure 7. Substrate with chromium, gold and photoresist.

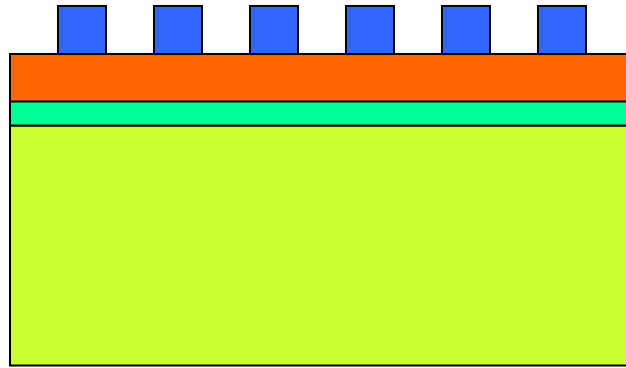


Figure 8. Substrate with chromium, gold and developed photoresist.

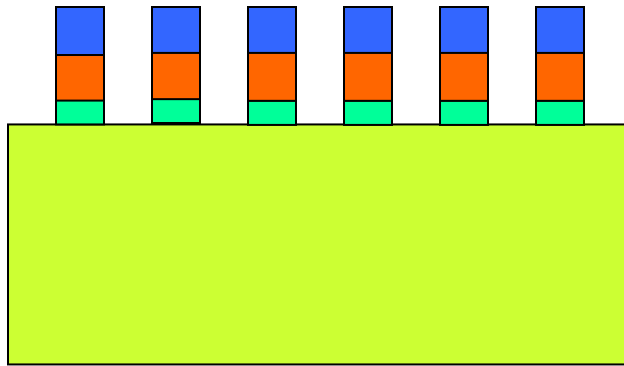


Figure 9. Substrate with exposed chromium and gold removed.

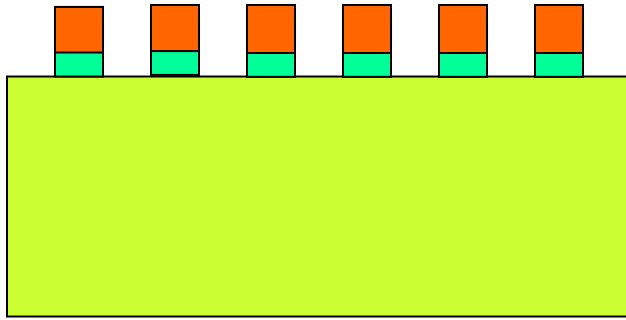


Figure 10. Final device.

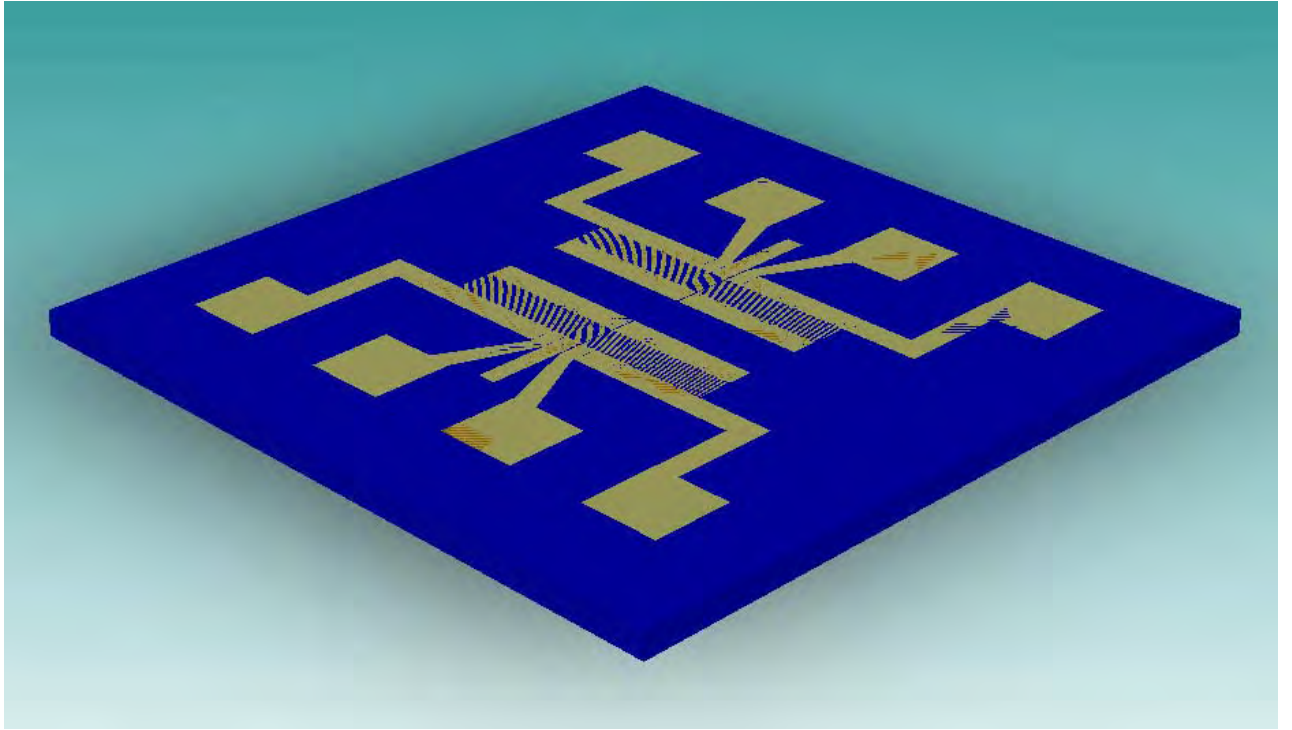


Figure 11. 3-dimensional view of the final device.

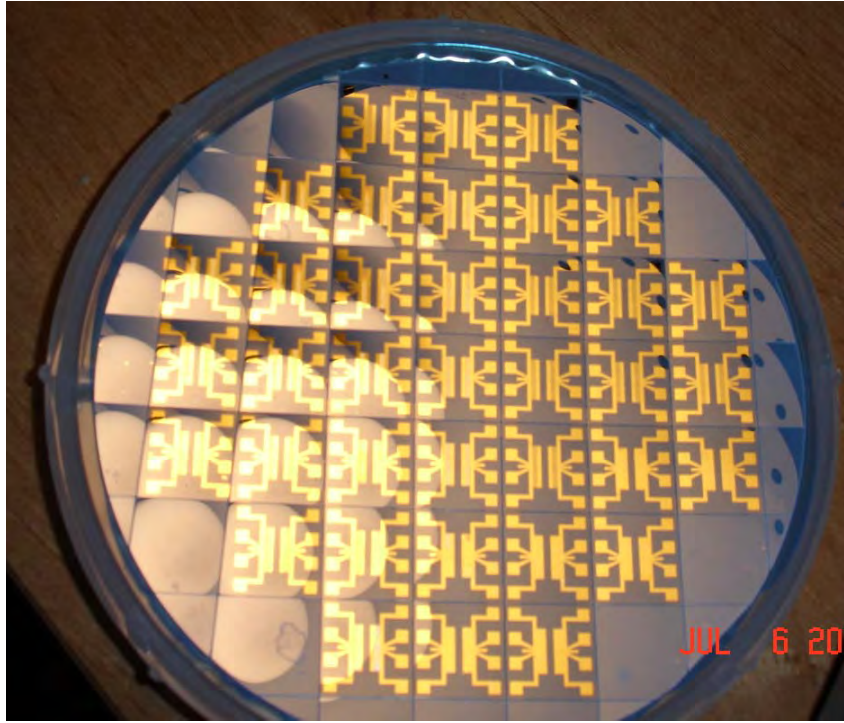


Figure 12. Fabricated SH-SAW devices cut on blue tape.

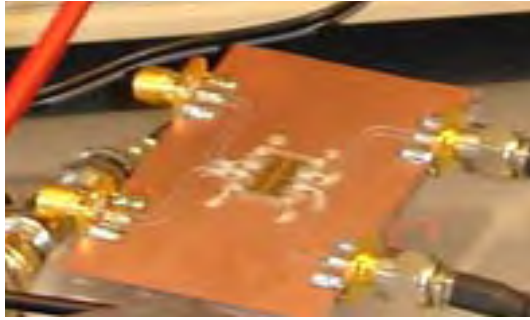


Figure 13. SH-SAW devices on copper board with SMA connectors.

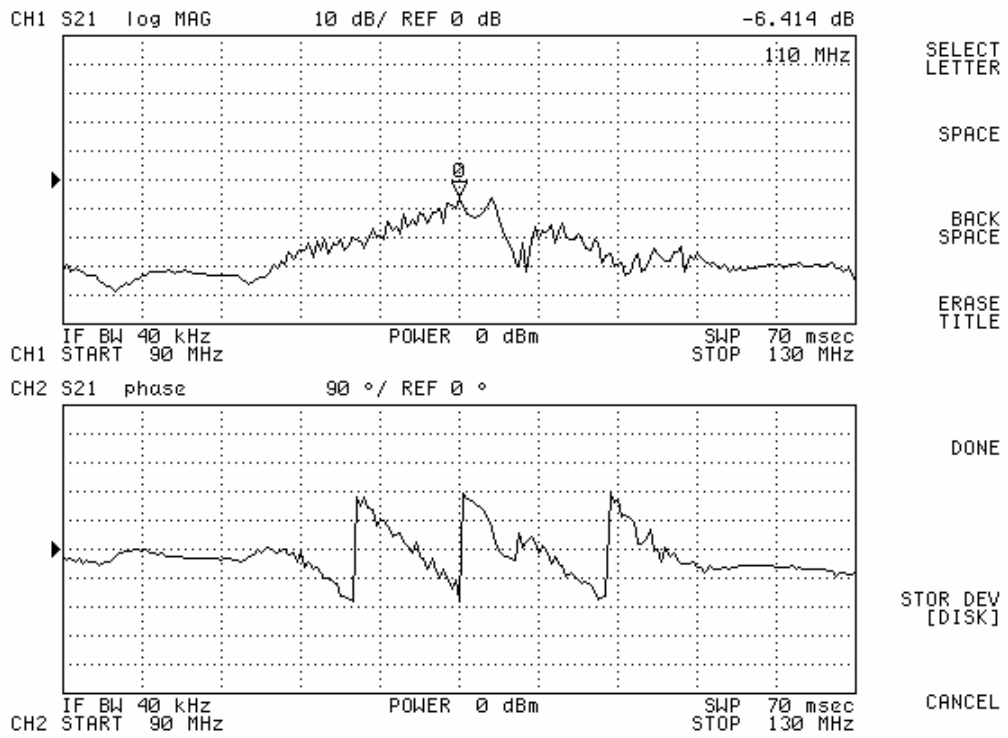


Figure 14. Frequency Response of the SH-SAW device.

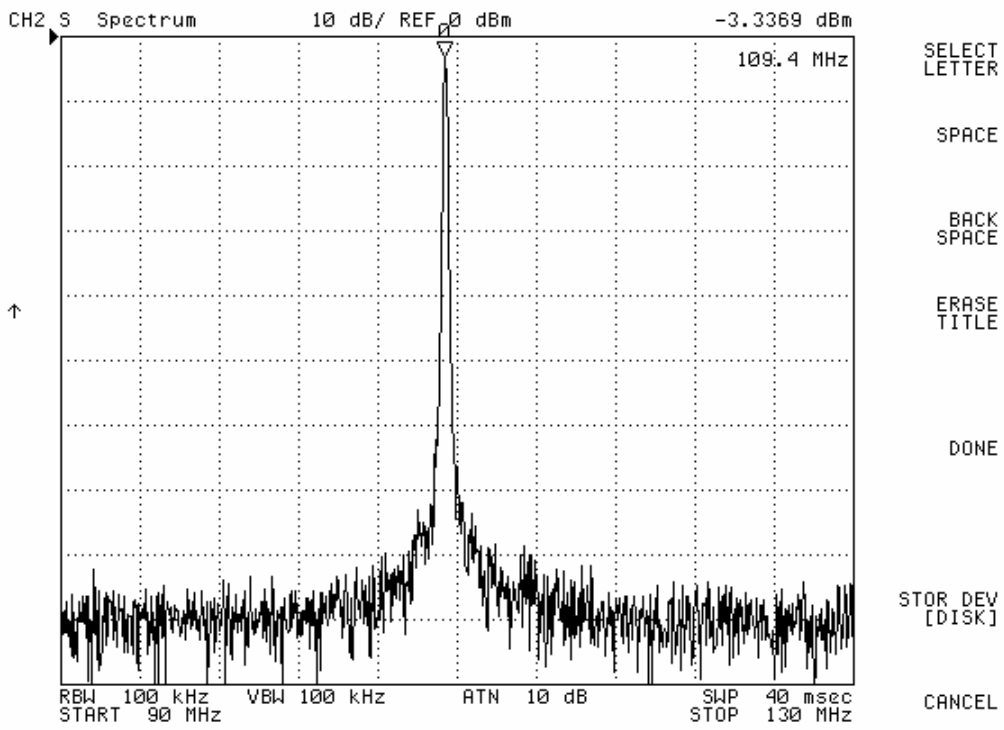


Figure 15. SH-SAW Oscillator output.

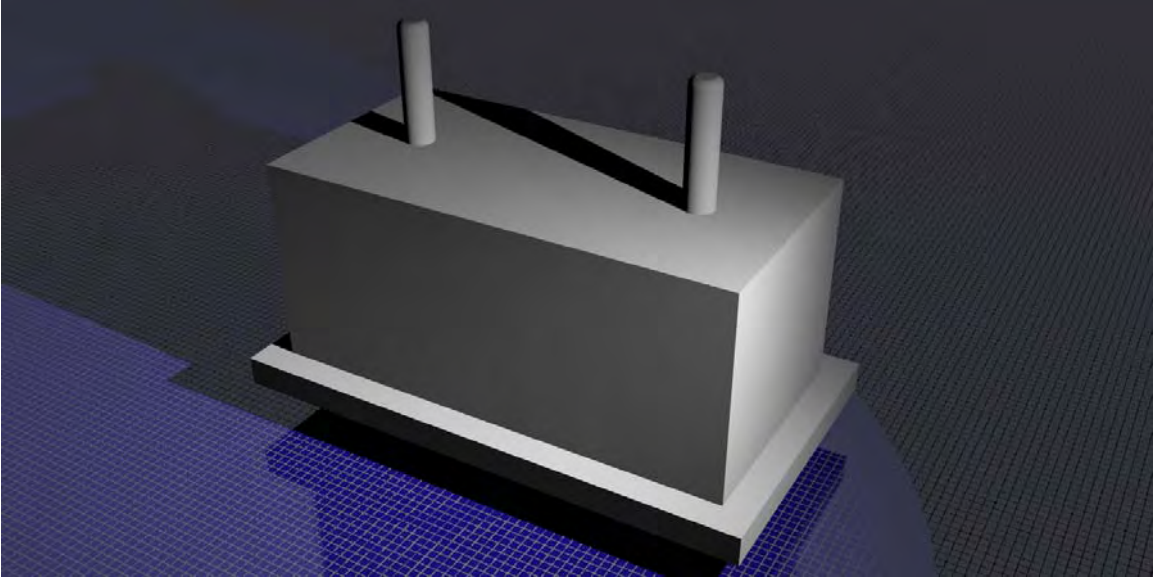


Figure 16. Aluminum Housing for Analog and Digital Circuitry.

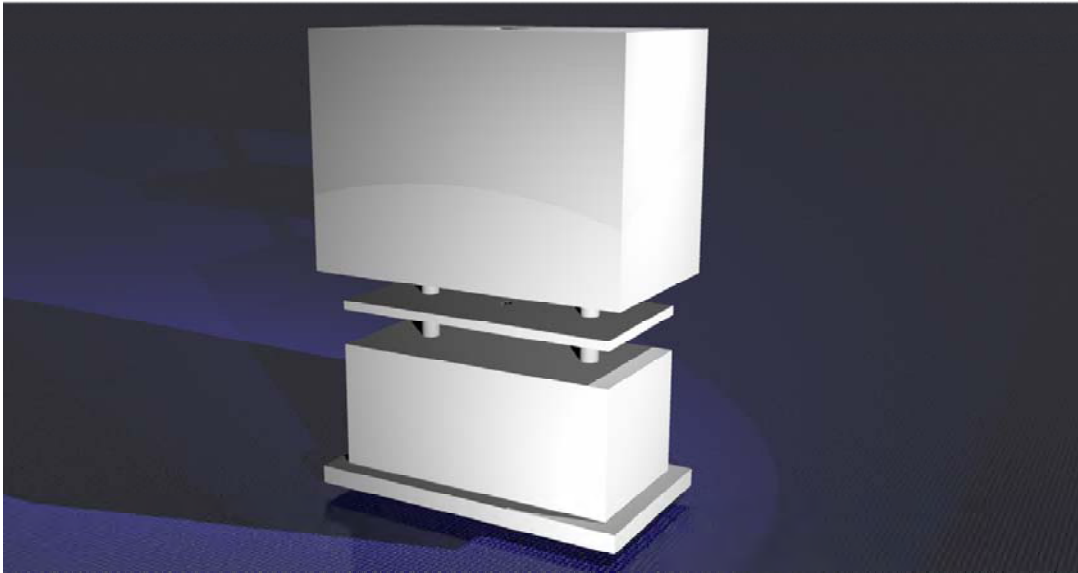


Figure 17. Kynar Board residing on Aluminum Box along with the sliding lid.

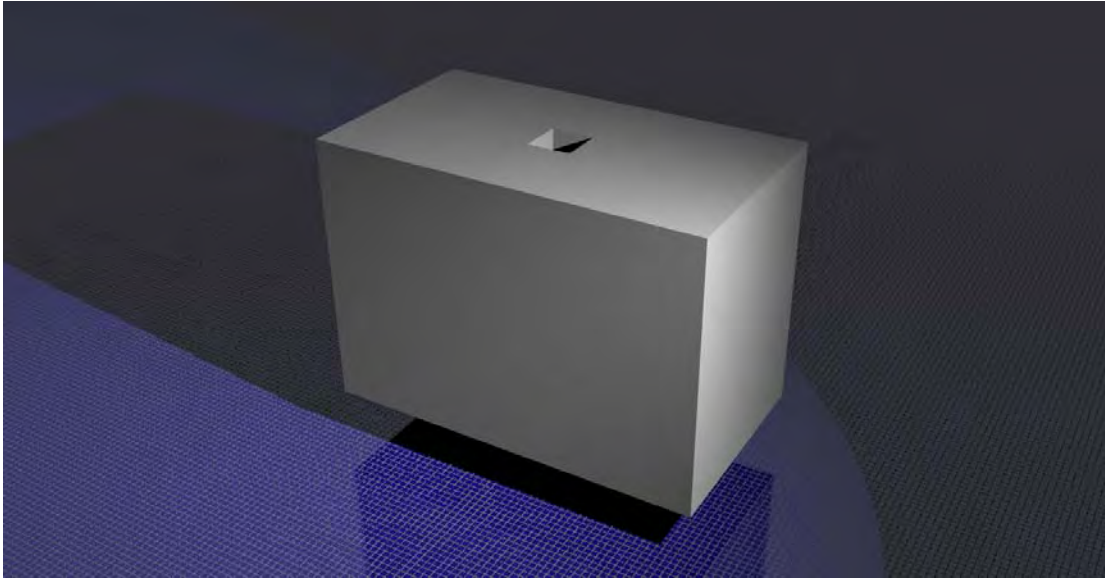


Figure 18. Aluminum Lid Covering the Base and providing Electromagnetic Shielding.

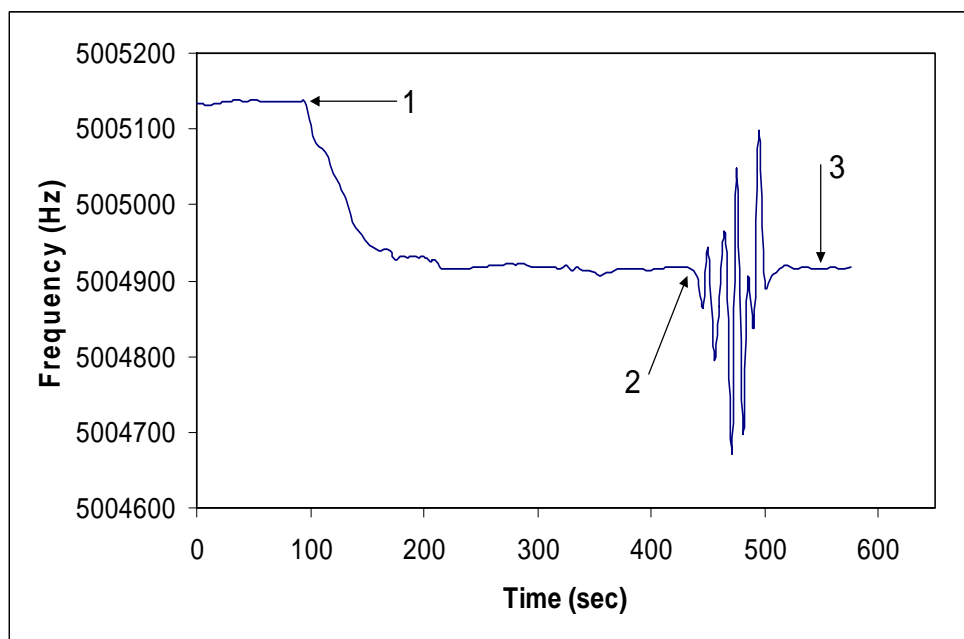


Figure 19. QCM frequency response for Protein A immobilization without polystyrene.

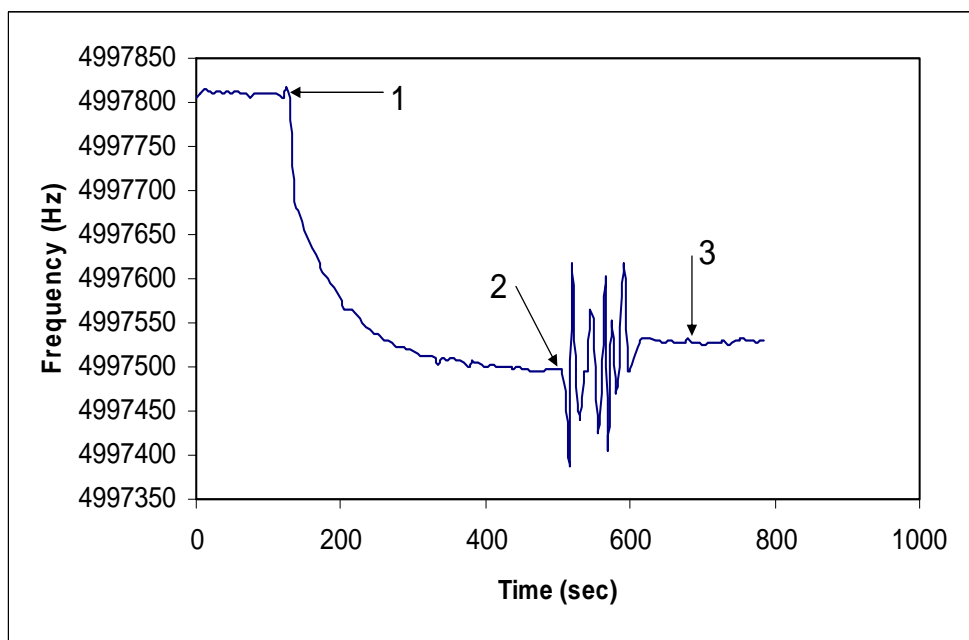


Figure 20. QCM frequency response for IgG immobilization without polystyrene.

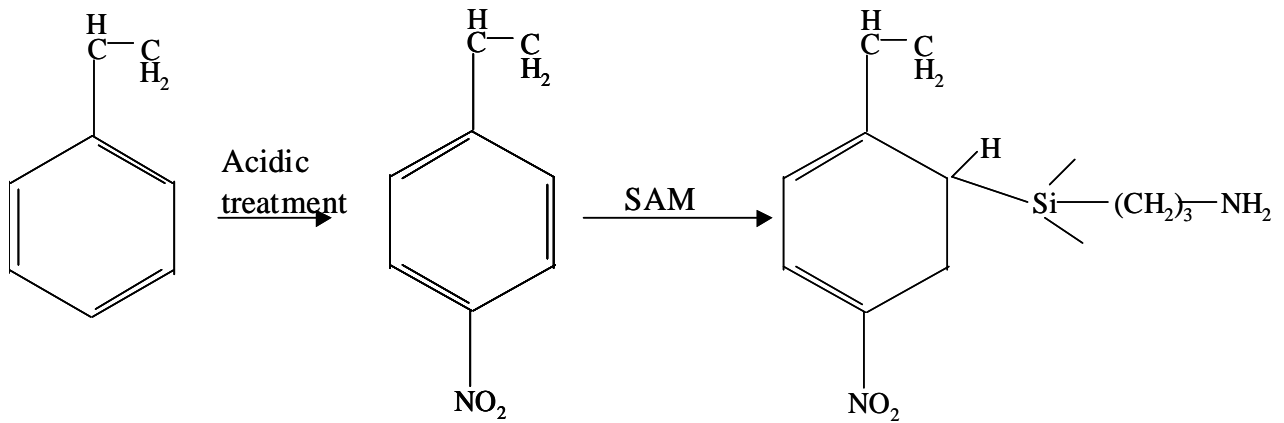


Figure 21. Polystyrene film when treated with acid and 3-APTES; (a) Polystyrene film (b) formation of the NO₂ groups by acidic treatment (c) formation of the amine groups by silanization.

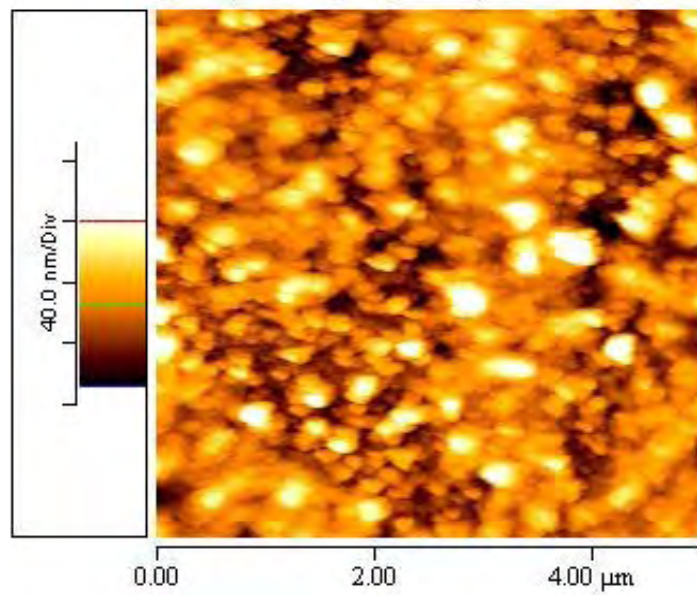


(a)

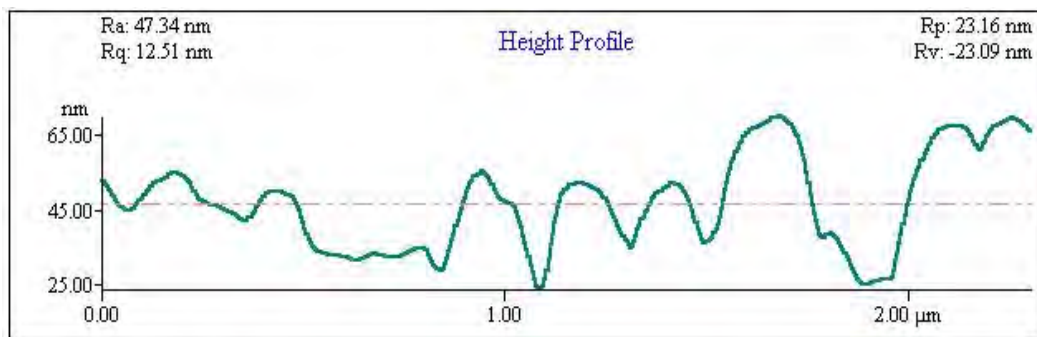


(b)

Figure 22. Image of water distribution on polystyrene (a) and APTES modified polystyrene (b) surfaces.



(a)



(b)

Figure 23. AFM image of IgG immobilized on polystyrene coated surface (b) height profile of the surface along a line.

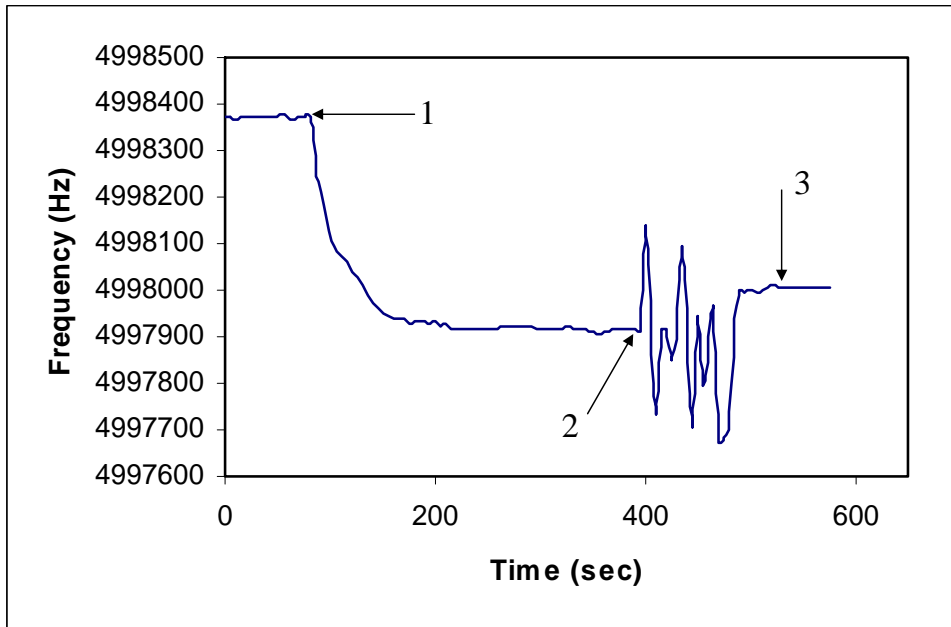


Figure 24. QCM frequency response for Protein A immobilization on polystyrene.

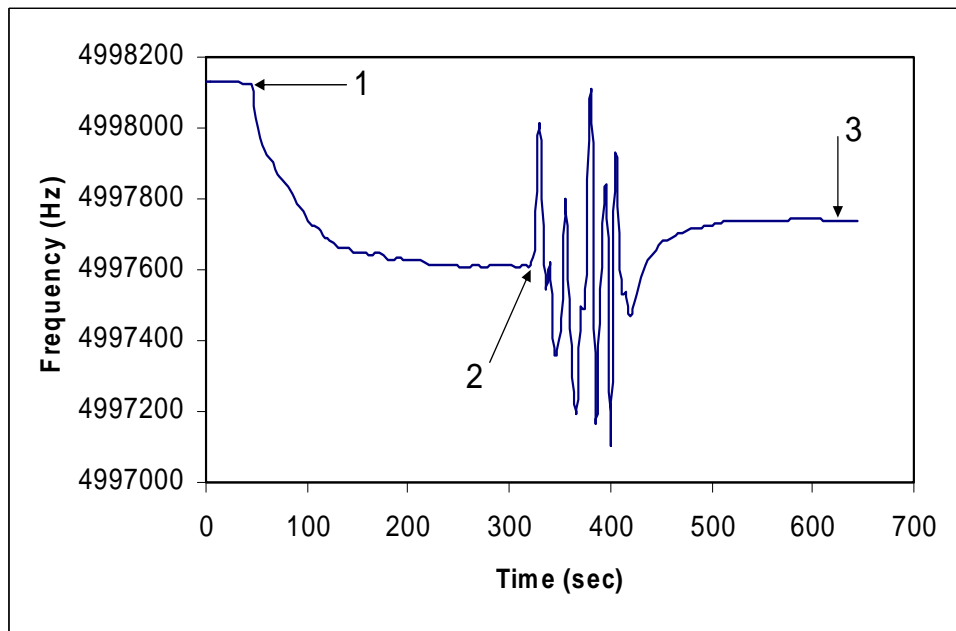
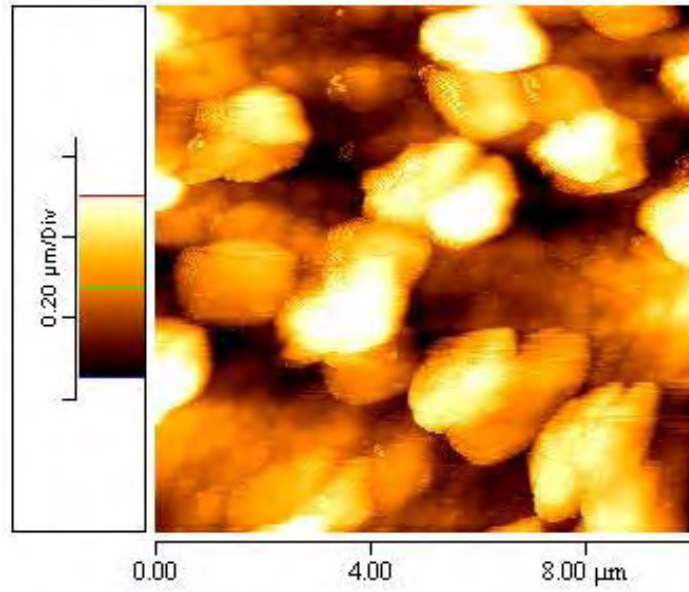
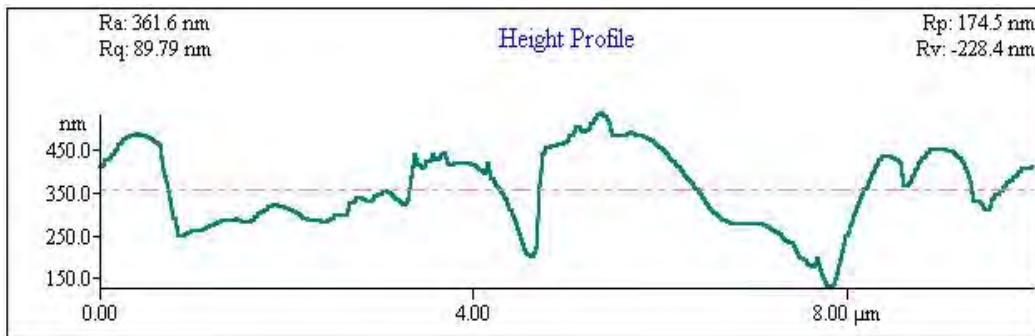


Figure 25. QCM frequency response for IgG immobilization on polystyrene.

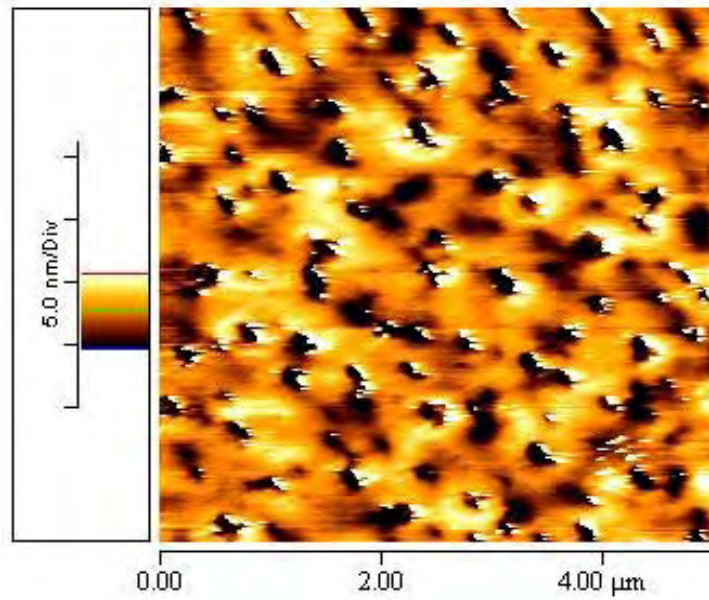


(a)

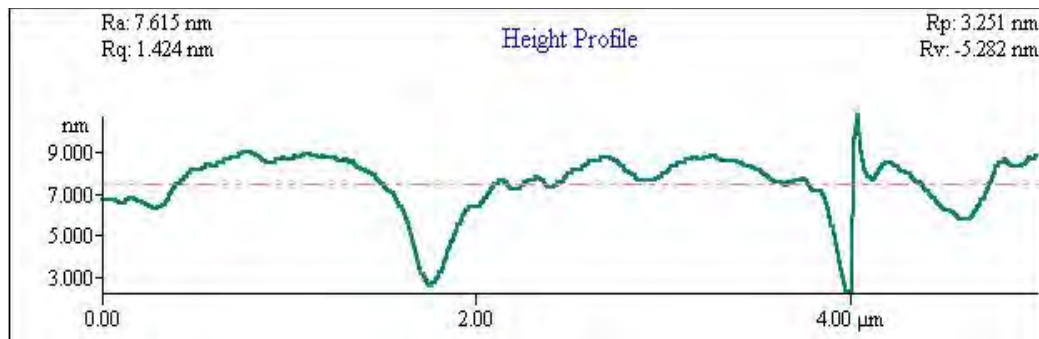


(b)

Figure 26. (a) AFM image of the gold surface of the QCM chip (b) height profile of the surface along a line.



(a)



(b)

Figure 27. AFM image of polystyrene coated gold surface and (b) the height profile of the polystyrene surface along a line.

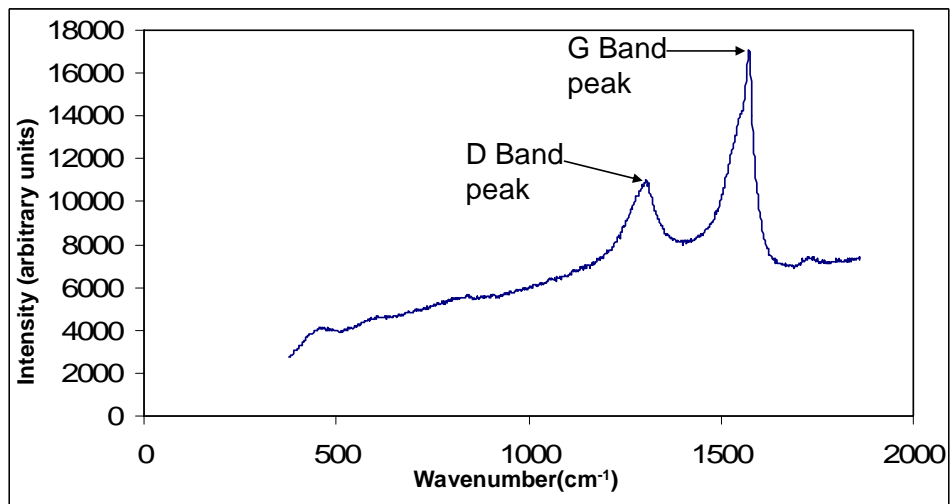


Figure 28. Raman spectrum of gold surface of QCM casted with SWNT.



Figure 29. Streptavidin molecules decorating the SWNT side walls.

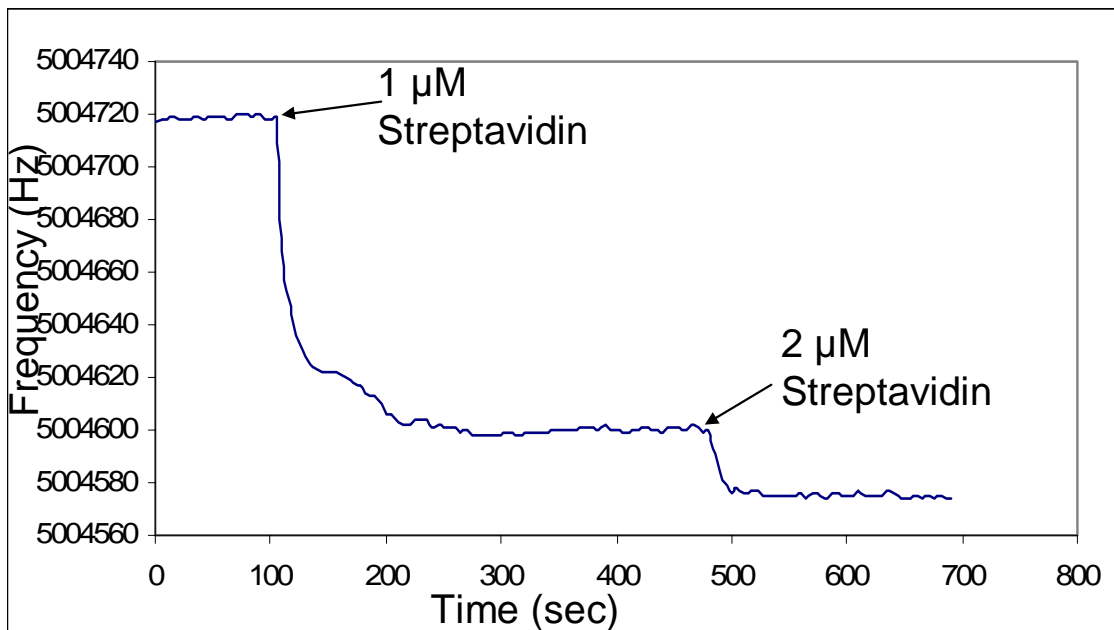


Figure 30. QCM response for various concentrations streptavidin.

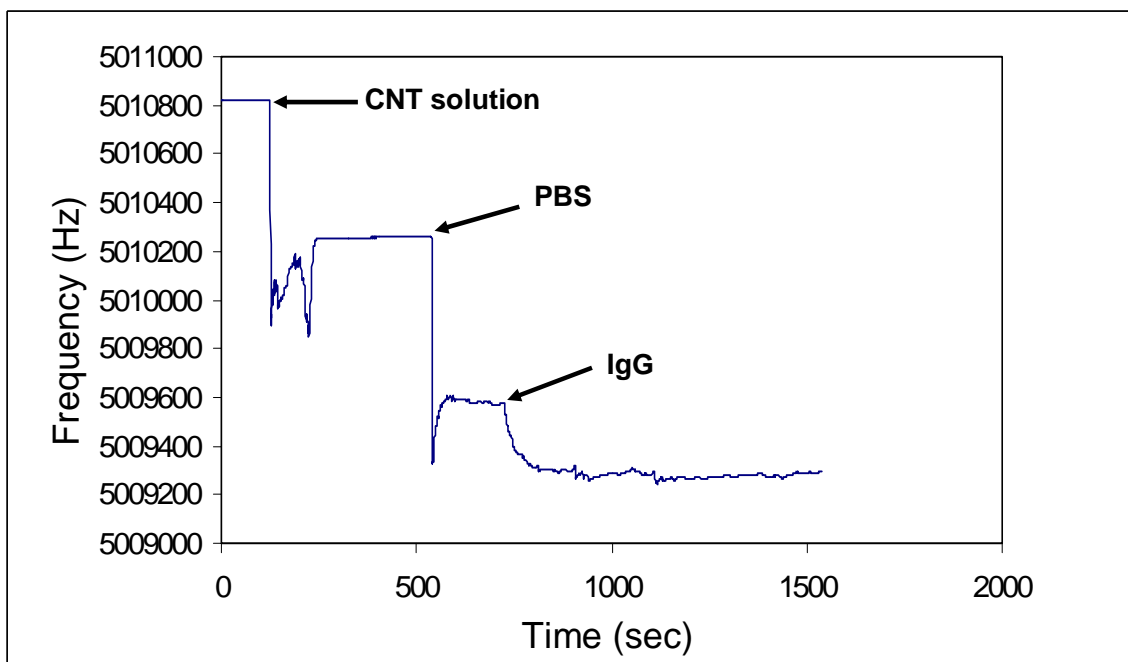


Figure 31. QCM response for various concentrations of IgG.

11-06-06 PSA test

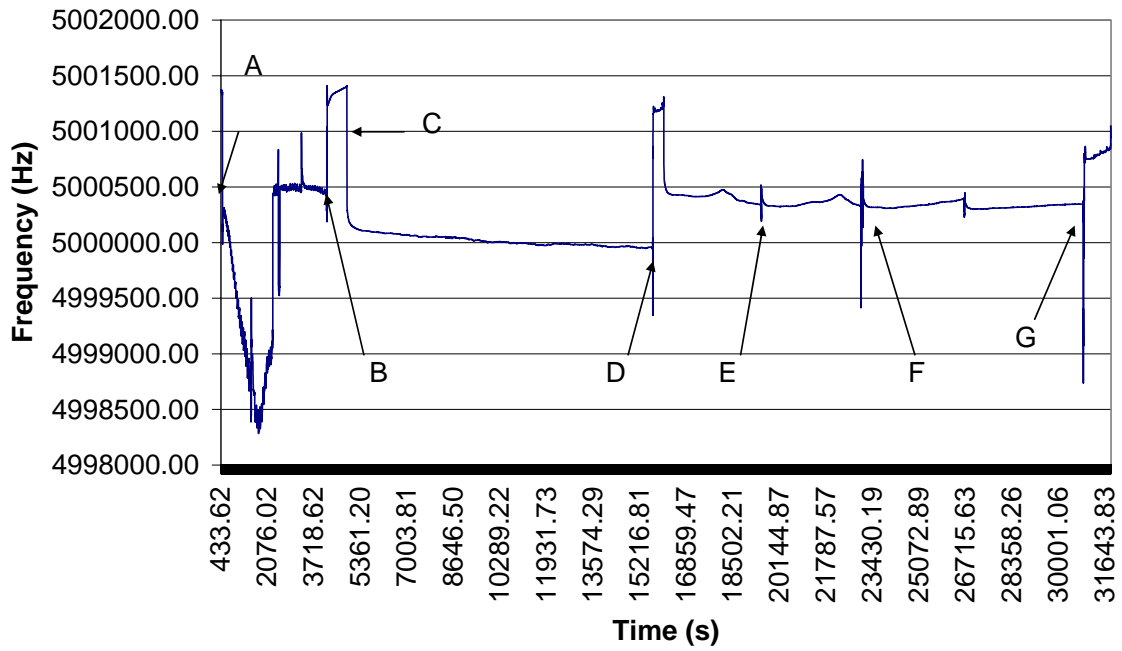


Figure 32. Frequency shift for PSA antibody (550ng/ml) immobilization.

11-07-06 PSA test

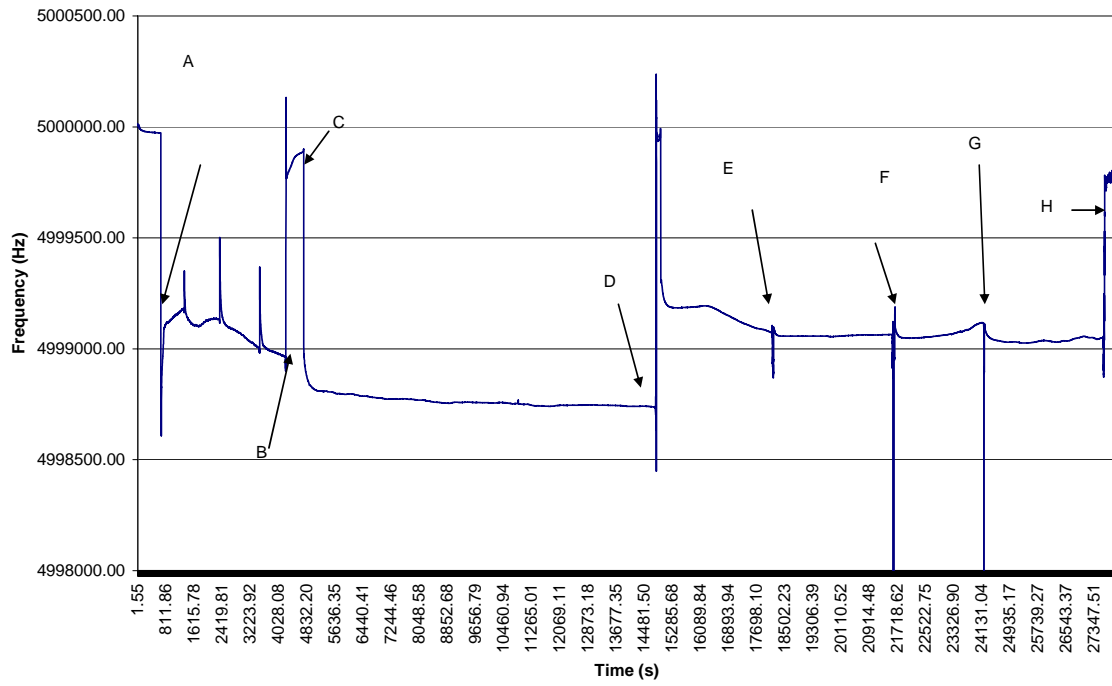


Figure 33. Frequency shift for PSA antibody (275ng/ml) immobilization.

11-13-06 PSA Test

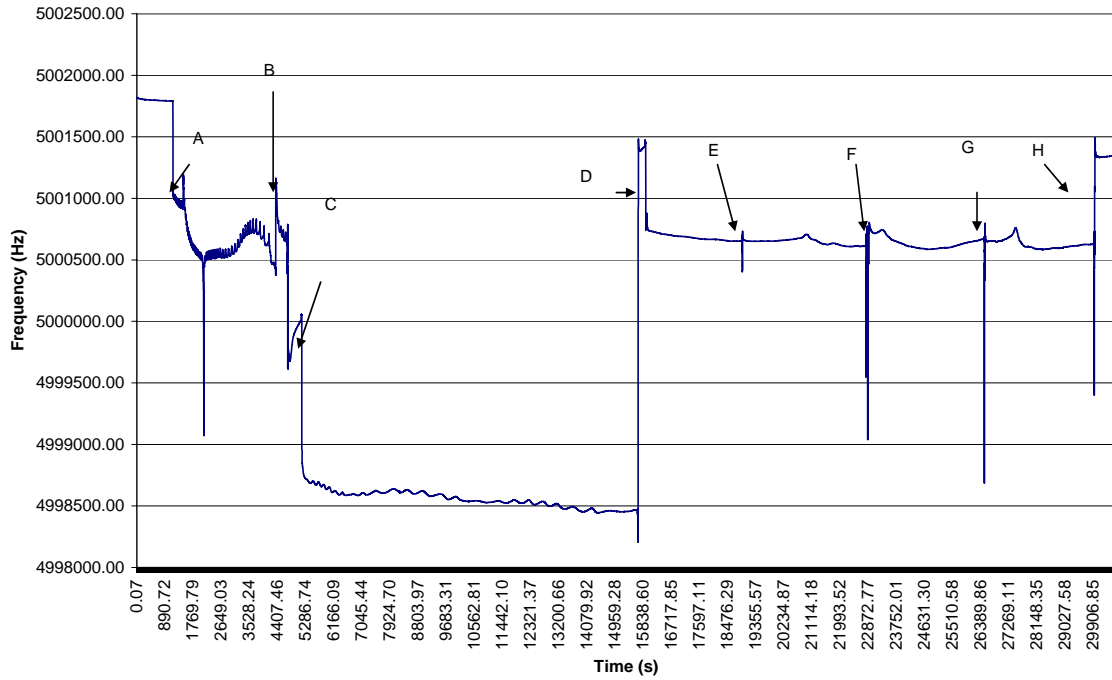


Figure 34. Frequency shift for PSA antibody (68.5ng/ml) immobilization.

Appendices

- 1) M.Z. Atashbar, B. Bejcek, A. Vijn, and S. Singamaneni “QCM Biosensor with ultra thin polymer film”, *Sensor and Actuators B*, Vol. 107, Issue 2: Jun 2005, pp. 945–951.
- 2) M.Z. Atashbar, B.E. Bejcek, S. Singamaneni “Carbon nanotube network-based biomolecule detection” *Sensors Journal*, IEEE, Volume 6, Issue 3, Jun 2006 pp. 524 – 528.
- 3) M.Z. Atashbar, B. Bejcek, and S. Singamaneni “SWNT Network for biomolecule detection” in *Functional Carbon Nanotubes*, edited by D.L. Carroll, B. Weisman, S. Roth, and A. Rubio (Mater. Res. Soc. Symp. Proc. 858E, Warrendale, PA , 2005), pp. HH14.8.1- HH14.8.6 (2005).
- 4) M.Z. Atashbar, B. Bejcek, S. Singamaneni “Carbon nanotube based biosensors”, *IEEE Sensor conference*, Vienna, Austria, Oct. 24th-27th, 2004, pp. 1048 - 1051 (2004).
- 5) M.Z. Atashbar, B. Bejcek, A. Vijn, S. Singamaneni “Sensitivity enhancement of QCM biosenor with polymer treatment”, *2004 IEEE International Ultrasonics, Ferroelectrics, and Frequency Control*, 23-27th August 2004 pp. 329-332, Monntreal, Canada (2004).
- 6) M.Z. Atashbar, B. Bejcek, A. Vijn, and S. Singamaneni “Piezoelectric biosensor for prostate cancer detection”, 4th Annual Symposium of Michigan Prostate Research Colloquium, Van Andel Research Institute, Grand Rapids, MI, May 1, (2004).

QCM biosensor with ultra thin polymer film

Massood Z. Atashbar^{a,*}, Bruce Bejcek^{b,1}, Aditya Vijn^a, Srikanth Singamaneni^a

^a *Electrical and Computer Engineering Department, Western Michigan University, MI 49008, USA*

^b *Department of Biological Sciences, Western Michigan University, MI 49008, USA*

Received 1 July 2004; received in revised form 24 November 2004; accepted 17 December 2004

Available online 21 January 2005

Abstract

Acoustic wave sensors have been widely used for detection of various chemical and biological species in liquid media. We report an improved binding of Protein A and IgG molecules on QCM biosensors by modifying the gold surface of the quartz crystal with a 35 nm polystyrene film followed by an acidic treatment. The frequency shifts due to the binding of the Protein A and IgG were 220 and 282 Hz, respectively for direct binding onto the chip. There was an appreciable increase in the frequency shift when the polystyrene film was used as an interfacial layer. The shift with the polystyrene film for Protein A was 364 Hz (an increase of 65%) and for the IgG it was 391 Hz (an increase of 40%). Complementary Atomic Force Microscopy (AFM) studies were carried out to understand the parameters responsible for such improved biomolecular binding. AFM studies revealed a significant decrease in the RMS roughness of the substrate from 98.4 to 1.75 nm when coated with polystyrene resulting in higher antibody coverage on the surface of the sensor. This increased surface smoothness resulted in higher biomolecular coverage on the surface of the sensor causing higher frequency shifts.

© 2004 Elsevier B.V. All rights reserved.

Keywords: Acoustic wave sensors; Quartz crystal microbalance; Ultra thin polystyrene film; Atomic force microscope

1. Introduction

Biosensors with rapid and highly sensitive detection capabilities of various biomolecules are of great demand in the field of life sciences. Existing immunoassay techniques such as enzyme linked immunoassay (ELISA), fluoroimmunoassay (FIA) and radioimmunoassay (RIA) are cumbersome, laborious, expensive, and hazardous and require specific labels for detection purposes thus making them more complex and time consuming [1–3]. Developing biosensors for detecting the concentration and activities of the various biological species therefore becomes very important. Recently acoustic wave sensors have been developed for the specific detection of various chemical and biological molecules in liquid media. The chemical interface selectively adsorbs materials in the solvent to the surface of the sensing

area. Changes in the physical parameters of an acoustic device may perturb the mechanical properties of the wave and/or its associated electrical field. For biological sensors, binding of a substance onto the resonating membrane surface causes a decrease in the acoustic wave velocity, which is related to the resonant frequency of the device. The changes in the acoustic and electromagnetic properties of the chip can be directly proportional to the changes in mass.

Quartz Crystal Microbalances (QCMs) are based on these principles wherein a shift in the resonant frequency of the QCM can be attributed to the mass bound on the sensor membrane as per the Sauerbrey equation [4]

$$\Delta f = \frac{-2f_0^2 \Delta m}{A\sqrt{\rho_q \mu_q}} \quad (1)$$

where f_0 is the fundamental resonant frequency, A the piezoelectrically active area defined by the two gold electrodes, ρ_q the density of quartz (2.648 g cm^{-3}) and μ_q the shear modulus ($2.947 \times 10^{11} \text{ dyn cm}^{-2}$). Eq. (1) is based on an assumption that the mass has been rigidly attached to the

* Corresponding author. Tel.: +1 269 276 3148; fax: +1 269 276 3151.

E-mail addresses: massood.atashbar@wmich.edu (M.Z. Atashbar), bruce.bejcek@wmich.edu (B. Bejcek).

¹ Tel.: +1 269 387 5634; fax: +1 269 387 5609.

crystal and has negligible thickness as compared to the crystal as a whole [4]. Under such conditions the thin film acts as an extension of the quartz thickness and experiences no shear force during the crystal oscillation [4].

Quartz Crystal Microbalances have been used extensively for protein sensing [5,6] and gravimetric immunoassays [1,2,7–9]. The simple relationship between the change in frequency (Δf) and the change in mass (Δm) enables QCM to be widely used in sensing applications. Modification of QCM surface with various polymers like polyurethane [10,11], polyethylene amine [12–14], and polystyrene [8,15,16] have been previously reported. Polystyrene (PS) is a very common polymer with a high processing ability due to its solubility in most of the organic solvents. The Young's modulus of PS is ~ 3 GPa as compared to ~ 3 MPa of polyurethane. Due to this high mechanical strength no significant viscoelastic coupling effects are observed between PS and the quartz crystal [17]. This particular property of PS makes it an ideal choice as an interfacial layer to improve the biomolecular binding. Previous reports on PS modified QCM surfaces involved immobilization of biomolecules directly onto the polymer surface [8,15,16]. In this work we report a silanization technique which improves the hydrophilicity of the PS surface by providing the terminal amine groups.

2. Experimental details

2.1. Protein and antibody

Protein A (Sigma–Aldrich) and mouse monoclonal IgG antibody (BioDesign International Inc.) were used throughout these studies. Protein A was resuspended in phosphate buffered saline (PBS; Sigma–Aldrich) at a concentration of 500 $\mu\text{g/ml}$ and the mouse monoclonal IgG was resuspended in PBS at a concentration of 160 $\mu\text{g/ml}$ and stored at -20°C in 50 μl aliquots before use.

2.2. Materials

Polystyrene, 3-aminopropyl triethoxysilane (3-APTES), glutaraldehyde, acetone, glycine and sodium chloride were purchased from Sigma–Aldrich Chemical Company. Polystyrene dissolved in chloroform (7%, w/v) was used to coat the QCM chips. Solutions of 5% 3-APTES in acetone, 5% glutaraldehyde in milli-Q water, PBS buffer with pH 7.0 in milli-Q water were prepared. 0.1 M Glycine solution in milli-Q water, 0.1 M glycine–HCl buffer with pH 2.4 and 0.5 M NaCl solution was prepared.

2.3. Experimental procedures

For promoting the immobilization of Protein A and to provide the necessary amine groups on the gold surface the protocol of Muramatsu et al. was followed [1]. To remove

any organic contamination from the surface of the crystal and improve the hydrophilic nature of the chip, it was cleaned with Piranha solution (three parts of H_2SO_4 in one part of 30% H_2O_2). Enough Piranha solution was employed to cover the gold surface of the chip and allowed to incubate at room temperature for two minutes before rinsing with milli-Q water. This procedure was repeated twice. Subsequently the chip was blown dried in a stream of nitrogen gas. A 5% solution of 3-APTES in acetone was added to create a self-assembled monolayer (SAM). After 1 h the sample was rinsed with milli-Q water after the APTES treatment to remove the physisorbed molecules. The chip was placed in a 5% glutaraldehyde solution for 3 h to allow for the cross linking between the chip and the Protein A. The crystal was then covered with 20 μl solution of Protein A (0.5 mg/ml). After 1 h the solution was removed and the crystal was subjected to several wash–dry cycles with milli-Q water until the QCM crystal reached its steady resonant frequency. The chip was then covered with 0.1 M glycine dissolved in PBS for 1 h to block any sites not bound to Protein A on the glutaraldehyde modified chip. The chip was then rinsed with 0.1 M glycine–HCl buffer (pH 2.4) to wash off any excess proteins or glycine before being thoroughly rinsed with milli-Q water. 20 μl of the mouse monoclonal IgG solution was then incubated on the chip for 1 h followed by rinsing with 0.5 M NaCl to remove any non-specifically adsorbed antibody. For the experiments in which binding was measured with the polymer film, polystyrene was spin coated onto the chip at a speed of 1000 rpm and then treated with 50% (v/v) HNO_3 in concentrated H_2SO_4 for 1 h [18]. The substrate was then modified with 3-APTES followed by glutaraldehyde as described above.

2.4. Characterization tools and methods

A Quartz Crystal Microbalance (Stanford Research Systems QCM100) with 5 MHz AT-cut quartz crystals (gold coated) was used to quantitatively study the ability to bind Protein A and mouse monoclonal IgG to the chip. The gold surface, which forms the active area for immobilization was 1.37 cm^2 and the mass sensitivity of the crystal was 0.057 Hz/ng/ cm^2 . Frequency was monitored using a Stanford Research System Universal Time Interval Counter (Model No. SR620).

Qualitative studies were made using AFM (Themomicroscopes Inc.; Autoprobe CP Research machine) in non-contact mode. For AFM studies silicon substrates were used with the same modification techniques as those described above for the QCM chips. The AFM tips used for imaging were silicon with an approximate radius of curvature of 20 nm. Biomolecular imaging was performed in non-contact mode. The AFM images were analyzed using image-processing software (IP 2.1) to calculate the RMS roughness value.

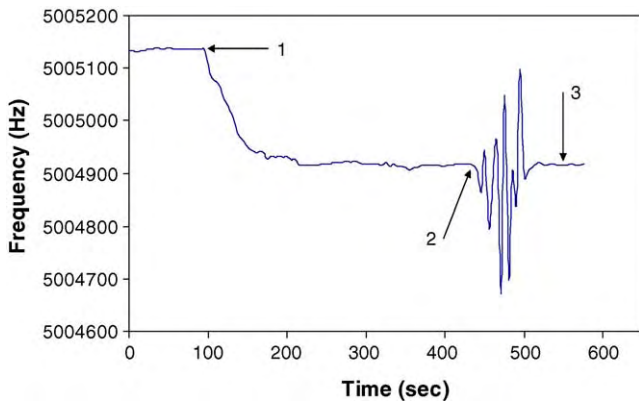


Fig. 1. QCM frequency response for Protein A immobilization without polystyrene.

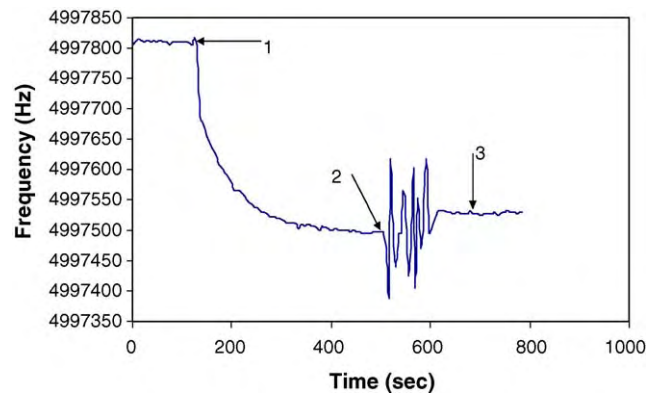


Fig. 2. QCM frequency response for IgG immobilization without polystyrene.

3. Results and discussions

Protein A, which has a particularly high affinity for the F_C fragment of IgG, was immobilized first on the chips to prevent the random immobilization of the antibodies, maximizing the ability of the chip immobilized with antibodies to bind to antigens [1,2]. Fig. 1 shows the QCM frequency response to Protein A immobilization without the polystyrene film. Point 1 refers to the point of addition of the Protein A containing solution to the chip. Point 2 indicates when the crystal was subjected to several wash–dry cycles and point 3 represents the frequency of crystal when Protein A was specifically bound on the surface. The frequency shift due to this direct binding was 220 Hz. From the Sauerbrey equation, this frequency shift corresponds to a $2.8 \mu\text{g}$ mass uptake.

To determine if antibodies could bind to the Protein A that had been immobilized, antibody-containing solutions were incubated with the chips. In Fig. 2 point 1 indicates the time at which the antibody-containing solution was added to the crystal. The binding of the antibody to the immobilized Protein A caused a decrease in the resonant frequency and stabilization occurred after 15 min. Point 2 represents the time when the crystal was rinsed with 0.5 M NaCl to remove any non-specifically adsorbed IgG and point 3 corresponds to the final resonant frequency after the NaCl rinsing. The frequency shift for IgG immobilization was found to be

282 Hz, which corresponds to a calculated mass change of $3.61 \mu\text{g}$.

To determine if coating the chips with a thin polymer film could also increase the efficiency of Protein A binding and hence improvement in antibody immobilization, we coated the surface of several chips with ultra thin film of polystyrene. However, polystyrene films are hydrophobic in nature causing the biomolecules to denature and hence loose their activity [19]. To avoid denaturation of the biomolecules, functional groups such as amino and hydroxyl groups can be chemically added to the polymer film. This helps the biomolecules retain their activity as immobilization now takes place through the hydrophilic arms of the polymer film [20,21]. To increase the hydrophilicity of the surface, which would increase the ability to add the functional groups, the chips were subjected to an acidic treatment followed by aqueous silanization [18]. Fig. 3 shows the schematic representation of the acidic treatment and the APTES modification of polystyrene. The acid treatment provides NO_2 groups and the APTES modification creates a polymer film with an amine group that can react with the glutaraldehyde used to covalently attach the biomolecules to the surface.

This improvement in the hydrophilicity was confirmed by monitoring the water distribution on polystyrene and APTES modified polystyrene surfaces. Fig. 4a and b shows the water distribution images (recorded using a Digital

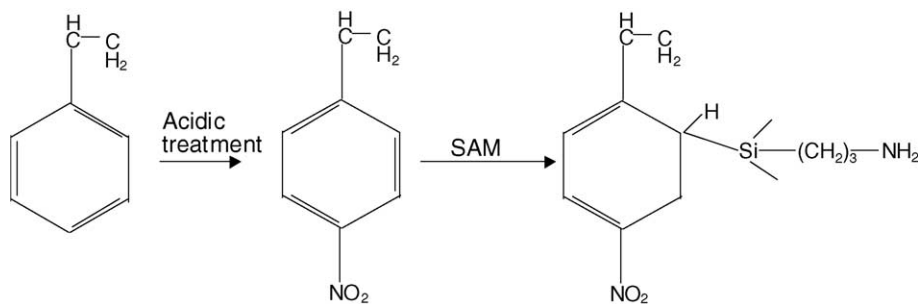


Fig. 3. Polystyrene film when treated with acid and 3-APTES: (a) polystyrene film; (b) formation of the NO_2 groups by acidic treatment; (c) formation of the amine groups by silanization.

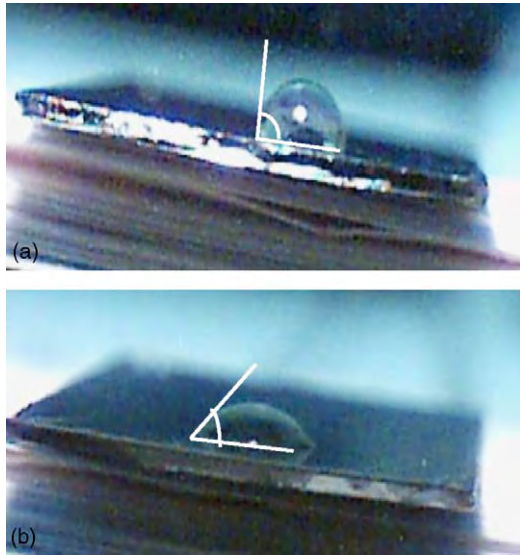


Fig. 4. Image of water distribution on polystyrene (a) and APTES modified polystyrene (b) surfaces.

Blue Computer microscope) on polystyrene and modified polystyrene surfaces. As is evident from the images there is a decrease in the contact angle of about 34° for APTES modified polystyrene surfaces compared to the unmodified surface indicating improvement in hydrophilicity.

Fig. 5 shows the AFM image of IgG immobilized on polystyrene coated surface. It can be seen that there is a uniform coverage of the antibody molecules of approximately

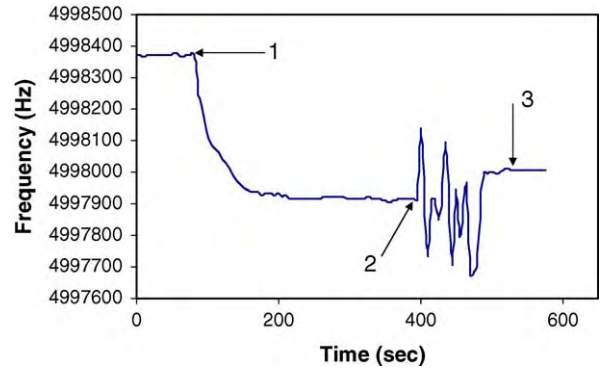


Fig. 6. QCM frequency response for Protein A immobilization on polystyrene.

10 nm in size on the substrate. The AFM imaging performed 2 h after the biomolecules immobilization revealed that the molecules still retain their characteristic “heart shape” proving that they still are not denatured.

The biomolecule immobilization on polystyrene coated surfaces was then quantitatively studied with QCM and compared to the immobilization performed without polystyrene. Fig. 6 shows the QCM response to Protein A immobilization. Point 1 indicates the time when Protein A was added and as can be seen the signal became stable only after 20 min. Point 2 represents when several wash–dry cycles were performed and point 3 is the time at which the frequency stabilized once all non-specifically adsorbed molecules were rinsed away. The

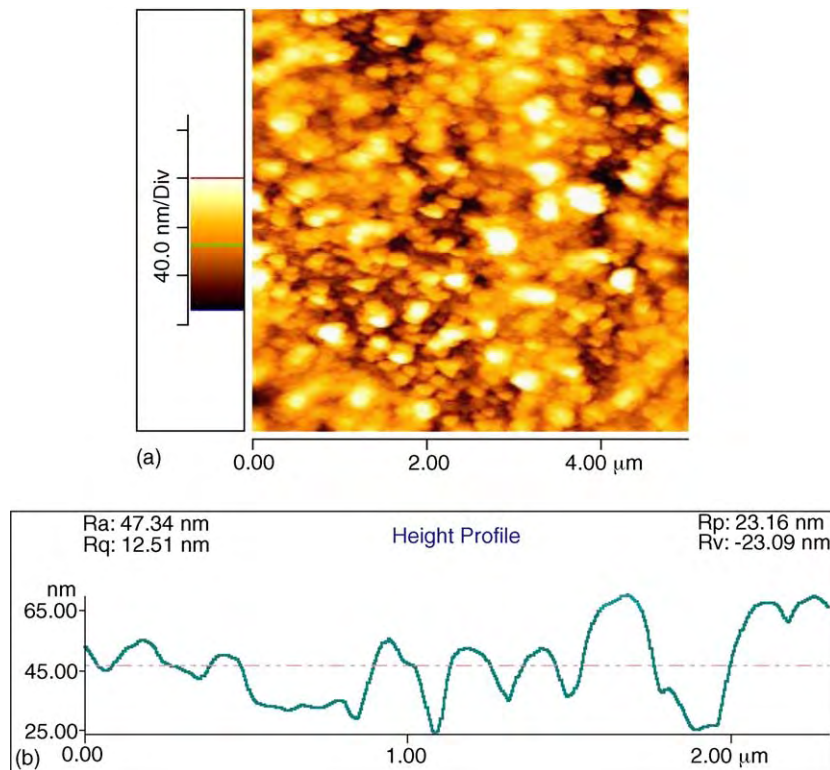


Fig. 5. AFM image of IgG immobilized on polystyrene coated surface and (b) the height profile of the surface along a line.

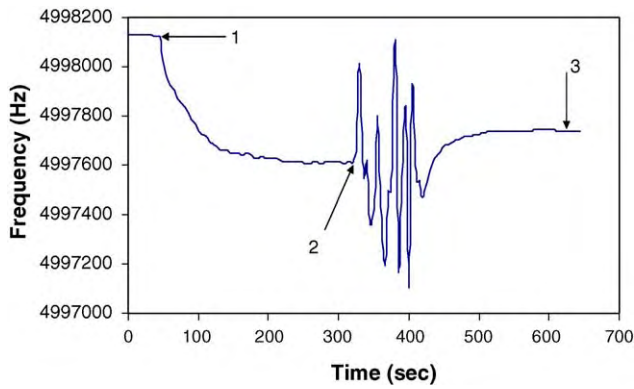


Fig. 7. QCM frequency response for IgG immobilization on polystyrene.

registered frequency shift was 364 Hz, which corresponds to a mass change of 4.66 μg . This represented a 65% increase when compared to the QCM chips that were not coated with the polymer film. Similar results were obtained for the binding of IgG. The QCM response (Fig. 7) for IgG immobilization on the polystyrene surface showed a frequency shift of 391 Hz corresponding to a mass uptake of 5.01 μg . This represented a 40% increase when compared to chips that had not been modified with polystyrene.

AFM images of the bare gold crystal and polystyrene coated crystal along with the height profile of the surface along a line are shown in Figs. 8 and 9, respectively. The AFM studies (as is evident from Fig. 8) revealed that the gold coated quartz crystals had a RMS surface roughness of 98.4 nm. An

appreciable decrease in the surface roughness to 1.75 nm was observed when the crystal was coated with an ultra thin layer of polystyrene. Gold and polystyrene are both hydrophobic in nature. APTES modification of the gold surface although improves the hydrophilicity of the surface, it doesn't result in much decrease in the roughness of the surface. On the other hand APTES modification of the polystyrene coated surface not only improves the hydrophilicity of the surface but there is a marked improvement in the surface roughness because of the polymer film. The improved biomolecular binding and hence the increased frequency shifts may be attributed to this improvement in the surface smoothness.

We speculate that with a gold surface roughness of 98.4 nm, the orientation of the protein A molecules is not uniform and hence there are chances that the active sites on one protein molecule would sterically hinder the active sites on the other resulting in a non uniform binding of biomolecules and hence loss of active sites. On the other hand a polymer coated surface although decreases the available surface area, provides the biomolecules with a much more plane and uniform surface resulting in less steric hindrance. Hence more active sites for antibody immobilization are available resulting in improved binding and hence higher sensitivity.

4. Conclusions

Owing to the increasing demands in consumer, medical and military field's development of the highly sensitive

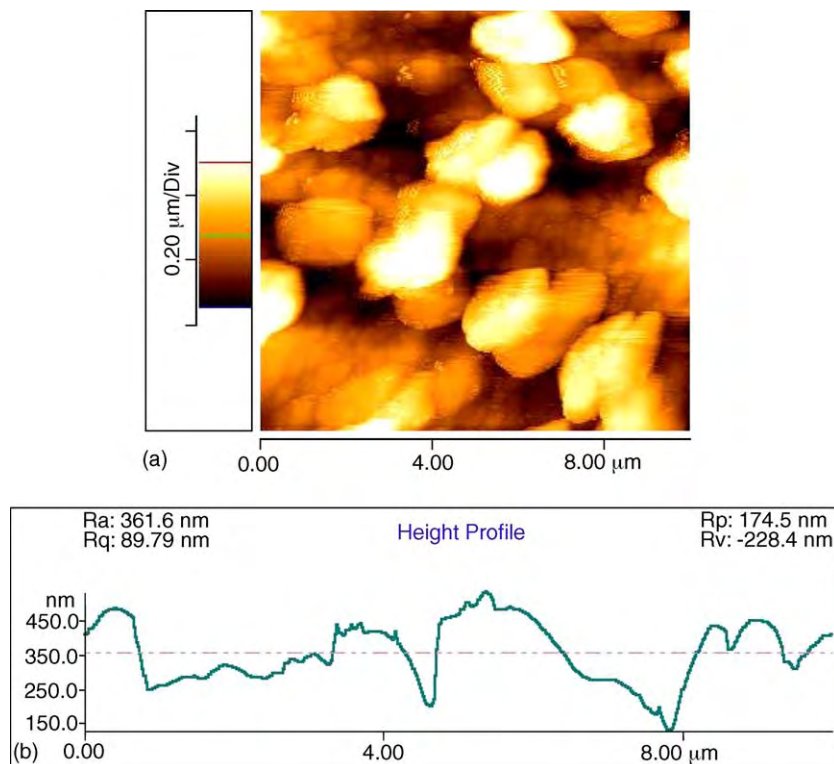


Fig. 8. (a) AFM image of the gold surface and (b) the height profile of the surface along a line.

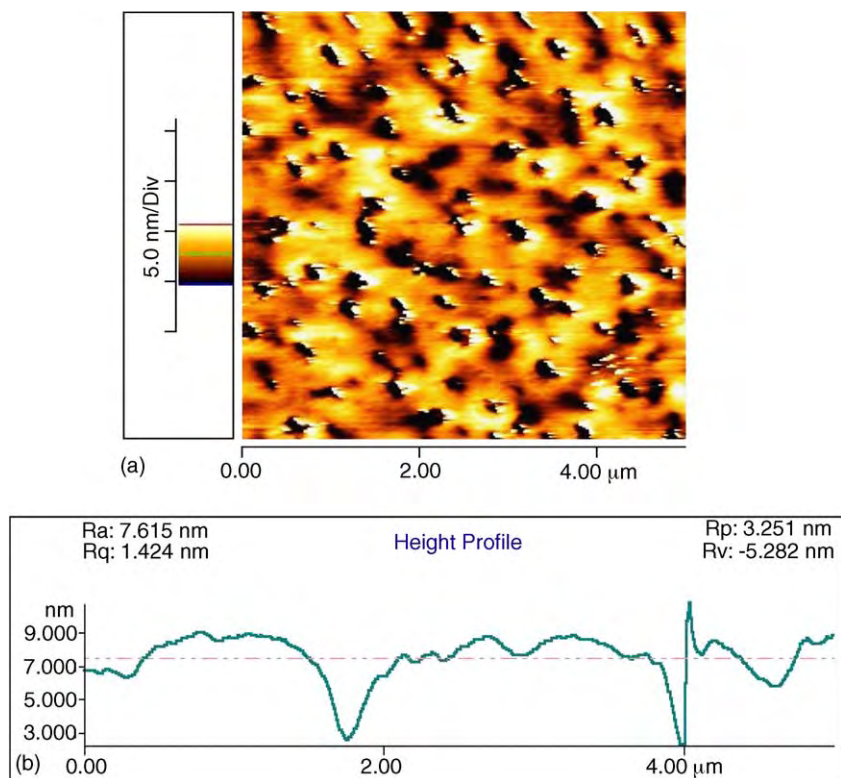


Fig. 9. (a) AFM image of polystyrene coated gold surface and (b) the height profile of the polystyrene surface along a line.

biosensors has gained utmost importance. It was demonstrated that the treatment of the QCM quartz chips with polystyrene exhibited a significant decrease in the RMS roughness of the gold crystal, resulting in a surface that was more uniform. The disadvantage of this technique, however, is that the hydrophobicity of the surface remains high. To counteract this undesirable trait, chips were treated by a simple aqueous silanization technique, which resulted in a significant improvement in the hydrophilicity of the surface. Chips that had an improved hydrophilicity were successfully utilized for biomolecular immobilization. Protein A resulted in a shift of 364 Hz on the polystyrene modified surface as opposed to the 220 Hz shift of frequency for direct immobilization. Subsequent IgG immobilizations also showed similar trend with the frequency shifts being 391 and 282 Hz for immobilizations with and without the polymer film, respectively. AFM imaging revealed uniform biomolecule coverage on polymer coated surfaces. This improved binding of biomolecules when coated with polystyrene is hypothesized to be due to the marked improvement in the roughness of the surface over which the biomolecules were immobilized.

Acknowledgements

The material presented here was supported by the US Department of Defence under contract number W81XWH-

04-10250. Authors would like to thank Dr. V. Bliznyuk for providing access to AFM.

References

- [1] H. Muramatsu, J.M. Dicks, E. Tamiya, I. Karube, Piezoelectric crystal biosensor modified with protein A for determination of immunoglobulins, *Anal. Chem.* 59 (1987) 2760–2763.
- [2] F. Caruso, E. Rodda, D.N. Furlong, Orientational aspects of antibody immobilization and immunological activity on quartz crystal microbalance electrodes, *J. Colloid Interf. Sci.* 178 (1996) 104–115.
- [3] Y.Y. Wong, S.P. Ng, M.H. Ng, S.H. Si, S.Z. Yao, Y.S. Fung, Immunosensor for the differentiation and detection of salmonella species based on a quartz crystal microbalance, *Biosens. Bioelectron.* 17 (2002) 676–684.
- [4] G. Sauerbrey, *Zeitschrift Fur Physik.* 155 (1959) 206–222.
- [5] C. Barnes, C. D'Silva, J.P. Jones, T.J. Lewis, Lectin coated piezoelectric crystal biosensors, *Sens. Actuat. B: Chem.* 7 (1992) 347–350.
- [6] S. Imai, H. Mizuno, M. Suzuki, T. Takeuchi, E. Tamiya, F. Mashige, A. Ohkubo, I. Karube, Total urinary protein sensor based on a piezoelectric quartz crystal, *Anal. Chim. Acta* 292 (1994) 65–70.
- [7] B. Guo, J. Anzai, T. Osa, Adsorption behavior of serum albumin on electrode surfaces and the effects of electrode potential, *Chem. Pharmaceut. Bull.* 44 (1996) 800–803.
- [8] S.P. Sakti, P. Hauptmann, B. Zimmermann, F. Buhling, S. Ansoerge, Disposable HSA QCM-immunosensor for practical measurement in liquid, *Sens. Actuat. B* 78 (2001) 257–262.
- [9] D.M. Gryte, M.D. Ward, W.S. Hu, Real-time measurement of anchorage-dependent cell adhesion using a quartz crystal microbalance, *Biotechnol. Prog.* 9 (1993) 105–108.

- [10] O. Hayden, R. Bindeus, F.L. Dickert, Combining atomic force microscope and quartz crystal microbalance studies for cell detection, *Meas. Sci. Technol.* 14 (2003) 1876–1881.
- [11] O. Hayden, F.L. Dickert, Selective microorganism detection with cell surface imprinted polymers, *Adv. Mater.* 13 (2001) 1480–1483.
- [12] B. König, M. Gratzel, Development of a piezoelectric immunosensor for the detection of human erythrocytes, *Anal. Chim. Acta* 276 (1993) 329–333.
- [13] B. König, M. Gratzel, Detection of human T-lymphocytes with a piezoelectric immunosensor, *Anal. Chim. Acta* 281 (1993) 13–18.
- [14] E.P. Sochaczewski, J.H.T. Luong, Development of a piezoelectric immunosensor for the detection of *Salmonella typhimurium*, *Enz. Microb. Technol.* 12 (1993) 173–177.
- [15] S.P. Sakti, S. Rosler, R. Lucklum, P. Hauptmann, F. Buhling, S. Ansoerge, Thick polystyrene-coated quartz crystal microbalance as a basis of a cost effective immunosensor, *Sens. Actuat. A* 76 (1999) 98–102.
- [16] C. Fredriksson, S. Khilman, B. Kasemo, D.M. Steel, In vitro real-time characterization of cell attachment and spreading, *J. Mater. Sci.: Mater. Med.* 9 (1998) 785–788.
- [17] R. Lucklum, C. Behling, P. Hauptmann, Gravimetric and non-gravimetric chemical quartz crystal resonators, *Sens. Actuat. B* 65 (2000) 277–283.
- [18] J. Kaur, K.V. Singh, M. Raje, G.C. Varshney, C.R. Suri, Strategies for direct attachment of hapten to a polystyrene support for applications in enzyme-linked immunosorbent assay (ELISA), *Anal. Chim. Acta* 506 (2004) 133–135.
- [19] J.E. Butler, L. Ni, W.R. Brown, K.S. Joshi, J. Chang, B. Rosenberg, E.W. Voss Jr., The immunochemistry of sandwich elisas—VI. Greater than 90% of monoclonal and 75% of polyclonal anti-fluorescyl capture antibodies (CAbs) are denatured by passive adsorption, *Mol. Immunol.* 30 (1993) 1165–1175.
- [20] J. Buijs, J.W.T. Lichtenbelt, W. Norde, J. Lyklema, Adsorption of monoclonal IgGs and their $F(ab')_2$ fragments onto polymeric surfaces, *Colloids Surf. B: Biointerf.* 5 (1995) 11–23.
- [21] N. Zammateo, C. Girardeaux, D. Delforge, J.J. Pireaux, J. Remacle, Amination of polystyrene microwells: application to the covalent grafting of DNA probes for hybridization assays, *Anal. Biochem.* 236 (1996) 85–94.

Biographies

Massood Z. Atashbar received the B.Sc. degree in electrical engineering from the Isfahan University of Technology, Isfahan, Iran, the M.Sc. degree in electrical engineering from the Sharif University of Technology, Tehran, and the Ph.D. degree from the Department of Communication and Electronic Engineering, RMIT University, Melbourne, Australia, in 1998. From 1998 to 1999, he was a Postdoctoral Fellow at the Center for Electronic Engineering and Acoustic Materials, The Pennsylvania State University, University Park. He is an Assistant Professor with the Electrical and Computer Engineering Department, Western Michigan University, Kalamazoo. His research interests include physical and chemical microsensors development, wireless sensors, and applications of nanotechnology in sensors, digital electronics, and advanced signal processing. He has published more than 75 articles in the area of physical and chemical sensors in refereed journals and refereed conference proceedings.

Bruce Bejcek received his BS degree in Microbiology from Michigan State University in East Lansing, MI and his Ph.D. from St. Louis University in St. Louis MO. After postdoctoral fellowships at the Jewish Hospital of St. Louis, St. Louis, MO and the University of Minnesota, Minneapolis, MN he joined the faculty at Western Michigan University in Kalamazoo, MI where he is currently an Associate Professor in the Biological Sciences Department. His research interests are primarily in the areas of cancer detection and cell biology.

Aditya Vijn was born in India in 1979 has pursued his Masters in Electrical Engineering from Western Michigan University. His current areas of interests are acoustic wave devices, novel MEMS and NEMS devices for biosensing applications.

Srikanth Singamaneni was born in India in 1981. He received the B.E. degree in Electronics engineering from Nagarjuna University, India in 2002. He pursued M.S. degree in Electrical Engineering from Western Michigan University, Kalamazoo. His current research interests include carbon nanotube based biosensors, self-assembly of carbon nanotubes and other nanostructured materials on patterned functional groups for device and sensing applications.

Carbon Nanotube Network-Based Biomolecule Detection

Massood Z. Atashbar, *Senior Member, IEEE*, Bruce E. Bejcek, and Srikanth Singamaneni, *Member, IEEE*

Abstract—In this paper, we describe a single-wall carbon nanotube (SWNT) based biological sensor for the detection of biomolecules like Streptavidin and IgG. SWNTs have been employed for two types of sensing mechanisms. First, the changes in the electrical conductance of the carbon nanotube (CNT) matrix on noncovalent binding of the biomolecules to the side walls of the CNT and, second, quantification of mass uptake of the matrix on biomolecule incubation are presented. Both sensing mechanisms exhibited consistent and highly sensitive responses. Biomolecular immobilization on the CNT surface was monitored by atomic force microscopy.

Index Terms—Atomic force microscopy (AFM), carbon nanotube (CNT), quartz crystal microbalance (QCM).

I. INTRODUCTION

SINGLE-WALL carbon nanotubes (SWNTs) can be realized as graphite sheets that have been rolled into seamless cylinders. Ever since carbon nanotubes (CNTs) discovery by Iijima [1] in 1991, they have been treated as the most promising nanostructured materials. CNTs exhibit both semi conducting and metallic behavior depending on their chirality [2], [3]. This special property of nanotubes makes them the ideal choice for interconnects and also as active devices of nanoelectronics. CNTs have been used as chemical sensors for the detection of hazardous gasses such as NH_3 and NO_2 [4]. The application of these quantum wires as biological sensors is a new facet which might find significant applications in the life sciences field [5]–[7], and it has been recently demonstrated that individual semiconducting SWNTs can be used for the detection of glucose oxidase [8], [9].

In this paper, we have fabricated a simple yet efficient carbon nanotube conductance-based sensor for the detection of streptavidin and mouse monoclonal immunoglobulin G (IgG) antibody. In addition, we employed quartz crystal microbalance (QCM) to quantify the mass of the biomolecules bound on the surface of the nanotubes. QCM is a thickness shear mode (TSM) acoustic wave device for detection of mass down to few nanograms.

Manuscript received February 24, 2005; revised October 21, 2005. This work was supported by the Department of Defense under Grant W81XWH-04-10250. The associate editor coordinating the review of this paper and approving it for publication was Dr. Alvin Crumbliss.

M. Z. Atashbar and S. Singamaneni are with the Electrical and Computer Engineering Department, Western Michigan University, Kalamazoo, MI 49008 USA (e-mail: massood.atashbar@wmich.edu; srikanth.singamaneni@wmich.edu).

B. E. Bejcek is with the Biological Sciences Department, Western Michigan University, Kalamazoo, MI 49008 USA (e-mail: bruce.bejcek@wmich.edu).

Digital Object Identifier 10.1109/JSEN.2006.874491

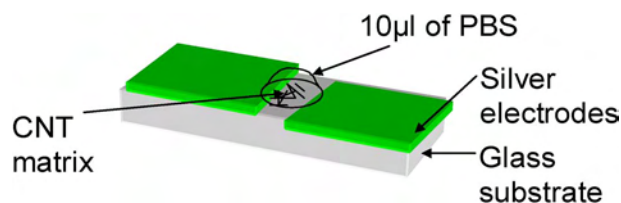


Fig. 1. Schematic representation of the sensor. (Color version available online at <http://ieeexplore.ieee.org>.)

II. EXPERIMENTAL DETAILS

Streptavidin from *Streptomyces avidinii* was purchased as a lyophilized powder from the Sigma-Aldrich Company. The protein was dissolved in phosphate buffered saline (PBS, Sigma-Aldrich) and stored as aliquots at -20°C . Mouse monoclonal IgG was purchased from Bio Design International, Inc. The antibody solution was resuspended in PBS and stored frozen at -20°C until use. SWNTs (70% pure with nickel and yttrium as catalyst residue) were purchased from Corborex, Inc. The SWNTs were dissolved in chloroform and then filtered through 0.02- μm pore size Anaport filters (Whatman). The filtered solution was then sonicated to derope the bundled CNTs. The CNTs were then cast on glass substrates using a micropipette. The glass substrates were cleaned before casting SWNT solution with isopropyl alcohol to remove any contamination on the surface. The thickness of the film was controlled by the amount of casting solution and its concentration. The matrix of the SWNT was studied using atomic force microscope (Thermomicroscopes Auto Probe CP Research machine) in noncontact mode. The thickness was measured using atomic force microscopy (AFM) by scanning along the edge of an artificially made scratch on the film. Microelectrode contacts across the matrix were formed by thermal evaporation of a 100-nm-thick silver film. The shadow masking technique was employed to form the gap between the electrodes. A tungsten wire (Sylvania) with a diameter of 60 μm was wrapped around the glass substrate to mask the area of the CNT. After silver evaporation, the tungsten wire was removed leaving the CNTs with the electrodes across them. An Agilent multimeter (Agilent-3458A) was employed to monitor the electrical changes of the CNT matrix which was interfaced with a computer. A constant voltage of 1 V was applied between the electrodes and the conductance changes for various concentrations of the protein and antibody were recorded. Protein solutions were added to 10 μl of PBS that had been placed on the sensor. PBS was employed as a buffer environment to distinguish changes in CNT matrix conductivity due to protein binding (see Fig. 1).

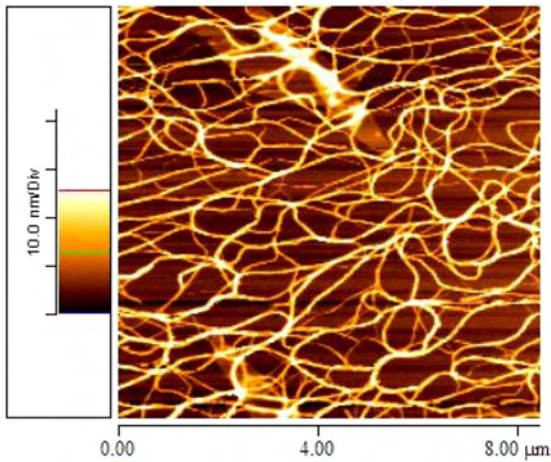


Fig. 2. AFM micrograph of CNT matrix on silicon substrate. (Color version available online at <http://ieeexplore.ieee.org>.)

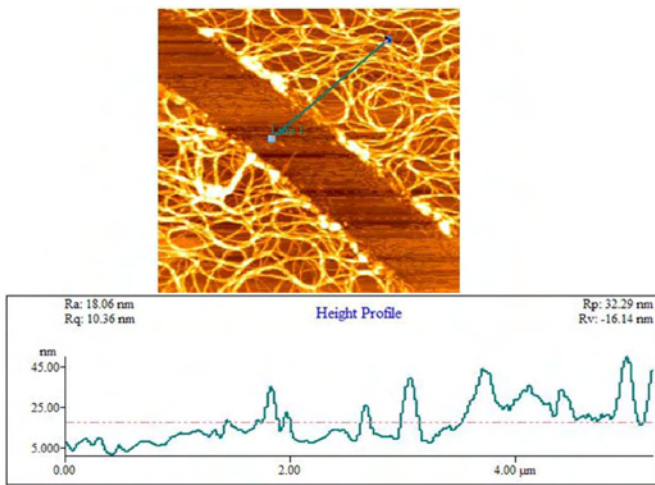


Fig. 3. AFM micrograph of CNT matrix showing scratch and height profile. (Color version available online at <http://ieeexplore.ieee.org>.)

III. RESULTS AND DISCUSSIONS

A. Purification of CNT

The CNTs were dissolved in chloroform (Sigma-Aldrich) and then casted on silicon substrates. However, AFM imaging of the samples revealed that there was a high content of catalyst residue. Filtration of the CNT solution using anatop filters resulted in a transparent solution. It is known that the CNTs have a tendency to form into parallel bundles resulting in a triangular lattice because of the intermolecular van der Waals forces between the nanotubes [10]. To overcome the intermolecular forces, the filtered CNT solution was sonicated for 1 h.

Fig. 2 shows uniformly distributed casted CNT matrix on the silicon substrate. It can be observed that most of the undesired catalyst residue has been filtered out leaving behind the nanotubes.

The thickness of the CNT film was controlled by the amount of solution casted and the concentration of the solution. Fig. 3 shows the micrograph of the CNT film and its height profile showing that the film thickness was approximately 20 nm.

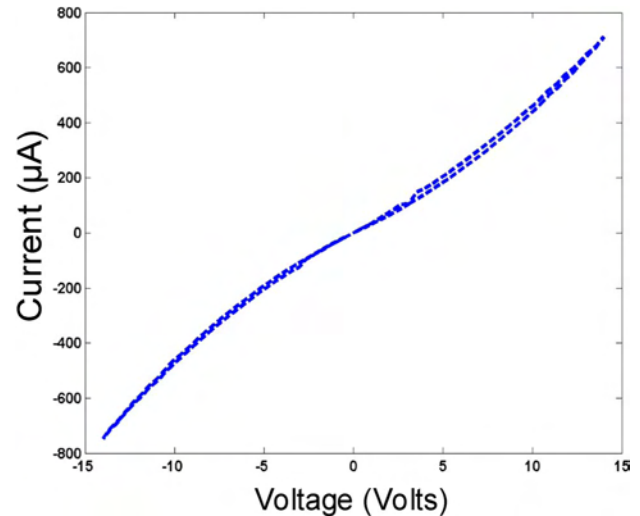


Fig. 4. I - V characteristics of CNT matrix. (Color version available online at <http://ieeexplore.ieee.org>.)

B. Electrical Characterization

Electrical characteristics of the sensor were studied using microelectrodes patterned by shadow masking technique as described above. Fig. 4 shows the electrical characteristics of the CNT matrix. The matrix demonstrated semiconducting behavior. This behavior is in agreement with the fact that a randomly selected CNT sample contains approximately 70% semiconducting nanotubes while the rest are metallic [2]. This makes the entire matrix semiconducting in nature.

C. Sensors Responses

Five microliters of a solution of Streptavidin with different concentrations was added to the 10 μ l of PBS to result in 10 nM, 1 μ M, and 2 μ M of protein. Fig. 5 shows the electrical response of the sensor to different protein concentrations. Point 1 indicates the instance at which 10 μ l of PBS was introduced between the electrodes and point 2 is the time at which 5 μ l of the streptavidin solution was added to the PBS making the final concentration of the protein to be 10 nM. It can be seen that there was no appreciable change in the current. It is worth mentioning that, although the PBS solution contained many ionizable salts, no change in the conductance was observed due to introducing PBS. This was due to the low voltage, 1 V, that was applied across the sensor which avoided ionization of the PBS. The ionization potential of potassium is 4.1 V, which is four times larger than applied voltage [11]. The protein concentration was increased to 1 μ M at Point 3 and a decrease in the conductance of the CNT matrix was observed. The current decreased from 97.7 to 60.3 μ A, which corresponds to approximately a 40% change in conductance. After the current stabilized, the protein concentration was further increased to 2 μ M, and a further decrease in current was recorded. The change in conductance was 17.5% (60.3 to 49.7 μ A), which is smaller compared to the initial change. The smaller change in the conductance can be attributed to fewer active sites available for the protein molecules to bind to CNT. Fig. 6 is an AFM micrograph of the CNT and protein molecules. The AFM imaging was performed after meticulously rinsing the sample using milli-Q water to

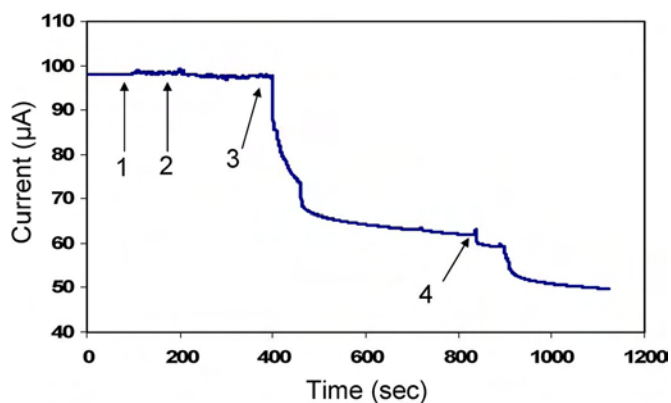


Fig. 5. CNT matrix sensor response for different concentrations of streptavidin. (Color version available online at <http://ieeexplore.ieee.org>.)

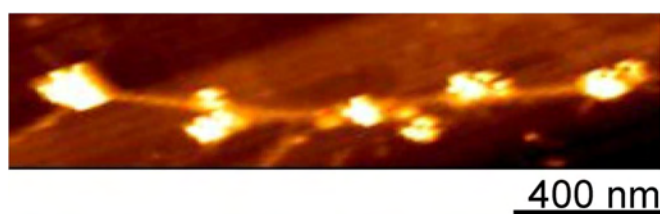


Fig. 6. AFM micrograph showing the protein molecules decorating a rope of CNT. (Color version available online at <http://ieeexplore.ieee.org>.)

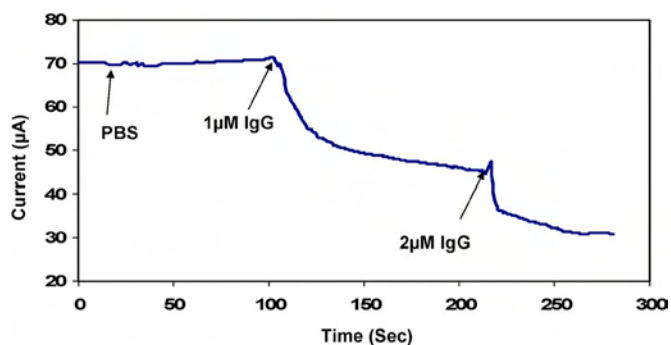


Fig. 7. Electrical response of sensor for various concentrations of IgG. (Color version available online at <http://ieeexplore.ieee.org>.)

wash away the salt deposits from PBS. From this figure, it can be seen that protein molecules were bound on the sidewalls of the tube and bundles of CNT were decorated with streptavidin molecules.

Fig. 7 shows the sensor response to the mouse mono-clonal IgG. Following introduction of PBS and 1 μM of IgG, the current decreased from 71.2 to 45.4 μA , which is nearly a 36% change in conductance. With an increase in concentration to 2 μM , the current further decreased to 30 μA , which is a 30% change. This is consistent with Streptavidin behavior which can be attributed to fewer active sites available for binding of IgG to CNT.

The concentration of the biomolecule forms the “control” for the fine modulation of current between the electrodes. The change in the conductance can be explained in a simple way. It is known from previous studies that streptavidin is electrically neutral at a pH between 6 and 7.2. However, the surface of the protein molecule still consists of strong residual bases. These

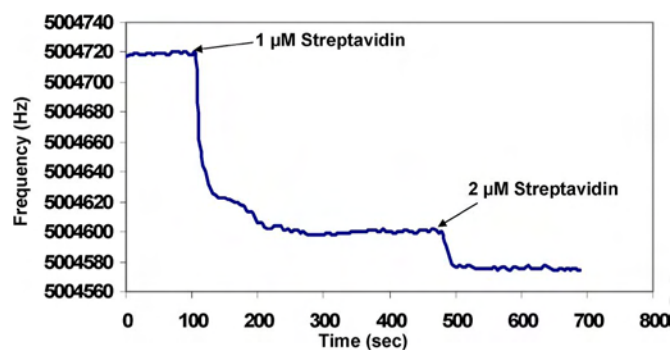


Fig. 8. QCM response to streptavidin incubation. (Color version available online at <http://ieeexplore.ieee.org>.)

bases are responsible for charge transfer with an average 160 electrons per biomolecule [12]. As a result, recombination will take effect, and, hence, the charge carrier population will decrease which leads to drop in current level.

The quantitative study of mass uptake of the CNT network due to biomolecules immobilization was performed using QCM. In QCM, a chemical interface on the surface of the sensor selectively adsorbs materials in the solvent to the surface of the sensing area. In our context, the chemical interface is the CNT matrix on the gold surface coated on the QCM crystal. The CNT matrix on the gold surface was characterized by Raman spectroscopy [13]. Characteristic “G” and “D” band peaks, which arise due to the in-plane Raman-active mode and disorder of the CNT, respectively, were observed in the Raman spectrum obtained from the sensor interface layer [13]–[15].

Measurements of CNT coated QCM crystals were performed by covering the chips with PBS before addition of the protein solutions. QCM are based on these principles wherein a shift in the resonant frequency of the QCM can be attributed to the mass bound on the sensor membrane as per the Sauerbrey equation [16] $\Delta f = -2f_0^2 \Delta m / A \sqrt{\rho_q \mu_q}$ where f_0 is the fundamental resonant frequency, A is the piezoelectrically active area defined by the two gold electrodes, ρ_q is the density of quartz (2.648 g cm^{-3}), and μ_q is the shear modulus ($2.947 \times 10^{11} \text{ dyn cm}^{-2}$). This equation is based on an assumption that the mass has been rigidly attached to the crystal and has negligible thickness, as compared to the crystal as a whole [16]. Under such conditions, the thin film acts as an extension of the quartz thickness and experiences no shear force during the crystal oscillation [16]. Fig. 8 depicts the QCM response using streptavidin. For a concentration of 1 μM of streptavidin, a change of 120 Hz in resonant frequency was recorded. From the Sauerbrey equation, the mass bound was calculated to be 1.538 μg ; when the concentration on the chip was increased to 2 μM , the change in the frequency was found to be 26 Hz. This corresponds to a mass uptake of 0.33 μg . The lower frequency shift can be attributed to fewer active sites available for the protein molecules as described in the conductance-based sensors.

Fig. 9 shows the detailed process flow of the QCM response to IgG incubation. CNT solution was placed on the gold surface at point 1, and a sudden change in the frequency was observed due to the change in the viscosity. Upon the evapora-

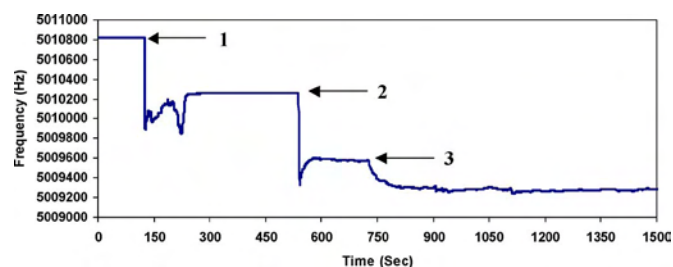


Fig. 9. QCM response to IgG incubation. (Color version available online at <http://ieeexplore.ieee.org>.)

TABLE I
SENSOR RESPONSES FOR VARIOUS CONCENTRATIONS OF BIOMOLECULES

	Streptavidin		Mouse monoclonal IgG	
	1 μ M	2 μ M	1 μ M	2 μ M
Electrical response	37.4 μ A	10.6 μ A	25.8 μ A	15.4 μ A
QCM response	120Hz (1.53 μ g)	26Hz (0.33 μ g)	192Hz (2.46 μ g)	56Hz (0.71 μ g)

tion of the solvent, a partial recovery of the frequency was observed. The frequency change due to the SWNT film was found to be 560 Hz. PBS buffer environment was established at point 2 and an abrupt change in the frequency due to the change in the viscosity was recorded. After the frequency stabilized, the biomolecule solution was added to the chip at point 3. The rate of changes due to the bimolecular binding in the frequency is quite smaller compared to that of viscosity effect due to binding dynamics of the biomolecule. Shift in the frequency due to the nonspecific binding of the biomolecule to the surface of the SWNT was found to be approximately 248 Hz, which accounts for a Δm of 3.17 μ g. Since the mass of each IgG molecule is 150 kDa (Dalton = 1.65×10^{-24} g), the average number of the biomolecules bound on each SWNT was calculated to be ~ 5 .

Table I summarizes the responses of the two types of sensors tested for various concentrations of the biomolecule. Both sensing approaches exhibited consistent pattern of bimolecular detection.

IV. CONCLUSION

We have demonstrated a simple and efficient method for purification of CNTs. The purified CNT network was employed in fabrication of conductometric and gravimetric biosensors. The conductance-based sensors exhibited a decrease in the current level due to the noncovalent binding of the biomolecules on

the sidewall of the SWNTs, which lead to a reduction in the charge carrier concentration. QCM experiments quantified the mass of the biomolecule bound on the CNT matrix with an average number of five biomolecules per CNT.

Further investigation is underway to better understand the sensing mechanism and to also improve the selectivity of the sensor by functionalizing CNTs toward biomolecules such as prostate specific antigen.

ACKNOWLEDGMENT

The authors would like to thank Dr. V. Bliznyuk of Western Michigan University for providing access to AFM, S. Hossein for technical support, and D. Smith for her useful discussions.

REFERENCES

- [1] S. Iijima, "Helical microtubules of graphitic carbon," *Nature*, vol. 354, pp. 56–58, Nov. 1991.
- [2] J. W. G. Wildoer, L. C. Venema, A. G. Rinzler, R. E. Smalley, and C. Dekker, "Electronic structure of atomically resolved carbon nanotubes," *Nature*, vol. 391, pp. 59–61, Jan. 1998.
- [3] R. Satio, G. Dresselhaus, and M. S. Dresselhaus, "Electronic structure of double-layer graphene double layers," *J. Appl. Phys.*, vol. 73, pp. 494–500, Oct. 1992.
- [4] J. Kong, N. R. Franklin, C. Zhou, M. G. Chapline, S. Peng, K. Cho, and H. Dai, "Nanotube molecular wires as chemical sensors," *Science*, vol. 287, pp. 622–625, January 2000.
- [5] R. J. Chen, H. C. Choi, S. Bangsaruntip, E. Yenilmez, X. Tang, Q. Wang, Y. Chang, and H. Dai, "An investigation of the mechanisms of electronic sensing of protein adsorption on carbon nanotube devices," *J. Amer. Chem. Soc.*, vol. 126, pp. 1563–1568, Jan. 2004.
- [6] P. Cherukuri, S. M. Bachilo, S. H. Litovsky, and R. B. Weisman, "Near-infrared fluorescence microscopy of single-walled carbon nanotubes in phagocytic cells," *J. Amer. Chem.*, vol. 126, pp. 15 638–15 639, Jun. 2004.
- [7] M. Z. Atashbar, B. Bejcek, and S. Singamaneni, "Carbon nanotube based biosensors," in *Proc. IEEE Sensor Conf.*, Vienna, Austria, Oct. 24–27, 2004, pp. 1048–1051.
- [8] K. Besteman, J. Lee, F. G. M. Wiertz, H. A. Heering, and C. Dekker, "Enzyme-coated carbon nanotubes as single-molecule biosensors," *Nanoletters*, vol. 3, pp. 727–730, Apr. 2003.
- [9] Y. Lin, F. Lu, Y. Tu, and Z. Ren, "Glucose biosensors based on carbon nanotube nanoelectrode ensembles," *Nanolett.*, vol. 4, pp. 191–195, Feb. 2004.
- [10] T. Hertel, R. E. Walkup, and P. Avouris, "Deformation of carbon nanotubes by surface van der Waals forces," *Phys. Rev. B*, vol. 58, pp. 13 870–13 873, Nov. 1998.
- [11] T. C. Hebb, "Ionization of mercury, sodium and potassium vapors and production of low voltage arcs in these vapors," *Phys. Rev. 12*, vol. 12, pp. 482–490, Dec. 1918.
- [12] K. Bradley, M. Briman, A. Star, and G. Gruner, "Charge transfer from adsorbed proteins," *Nanolett.*, vol. 4, no. 2, pp. 253–256, Feb. 2004.
- [13] A. G. S. Filho, A. Jorio, G. G. Samsonidze, G. Dresselhaus, R. Satio, and M. S. Dresselhaus, "Raman spectroscopy for probing chemically/physically induced phenomena in carbon nanotubes," *Nanotechnol.*, vol. 14, pp. 1130–1139, Sep. 2003.
- [14] N. R. Raravikar, P. Koblinski, A. M. Rao, M. S. Dresselhaus, L. S. Schadler, and P. M. Ajayan, "Temperature dependence of radial breathing mode Raman frequency of single-walled carbon nanotubes," *Phys. Rev. B*, vol. 66, pp. 235 424(1)–235 424(9), 2002.
- [15] M. Z. Atashbar and S. Singamaneni, "Comparative studies of temperature dependence of G-band peak in single walled carbon nanotube and highly oriented pyrolytic graphite," *Appl. Phys. Lett.*, vol. 86, pp. 123 112(1)–123 112(3), 2005.
- [16] G. Sauerbrey, *Zeitschrift Fur Phys.*, vol. 155, pp. 206–222, 1959.



Massood Z. Atashbar (S'93–M'97–SM'01) received the B.Sc. degree in electrical engineering from the Isfahan University of Technology, Tehran, Iran, the M.Sc degree in electrical engineering from the Sharif University of Technology, Tehran, and the Ph.D. degree from the Department of Communication and Electronic Engineering, RMIT University, Melbourne, Australia, in 1998.

From 1998 to 1999, he was a Postdoctoral Fellow at the Center for Electronic Engineering and Acoustic Materials, The Pennsylvania State University, University Park. He is an Assistant Professor with the Electrical and Computer Engineering Department, Western Michigan University, Kalamazoo. His research interests include physical and chemical microsensors development, wireless sensors, and applications of nanotechnology in sensors, digital electronics, and advanced signal processing. He has published more than 85 articles in the area of physical and chemical sensors in refereed journals and refereed conference proceedings.



Bruce E. Bejcek received the B.S. degree in microbiology from Michigan State University, East Lansing, and the Ph.D. degree from St. Louis University, St. Louis, MO.

After postdoctoral fellowships at the Jewish Hospital of St. Louis and the University of Minnesota, Minneapolis, he joined the faculty at Western Michigan University, Kalamazoo, where he is currently an Associate Professor in the Biological Sciences Department. His research interests are primarily in the areas of cancer detection and cell

biology.



Srikanth Singamaneni (M'03) was born in India in 1981. He received the B.E. degree in electronics engineering from Nagarjuna University, India, in 2002. He is currently pursuing the M.S. degree in electrical engineering at Western Michigan University, Kalamazoo.

His current research interests include carbon nanotube based biosensors, self-assembly of carbon nanotubes, and other nanostructured materials on patterned functional groups for device and sensing applications.

SWNT NETWORK for BIOMOLECULE DETECTION

Massood Z. Atashbar¹, Bruce Bejcek², and Srikanth Singamaneni¹

¹Electrical and Computer Engineering, ² Department of Biological Sciences
Western Michigan University, Kalamazoo, MI-49008, USA

ABSTRACT

In this paper we describe a single wall carbon nanotube (SWNT) based biological sensor for the detection of biomolecules using streptavidin and IgG. Two types of sensing mechanisms have been used to demonstrate the ability of carbon nanotubes to form nanoscale biosensors. The first sensing mechanism involves a CNT based conduction sensor in which the decrease in the current was observed when the specific biomolecule was bound. In the second mechanism Quartz Crystal Microbalance (QCM) was used to quantify the mass of the biomolecule bound on the sidewalls of the carbon nanotube. Both sensing mechanisms proved to be efficient and consistent. Immobilization of the biomolecules on the carbon nanotube surface was confirmed by Atomic Force Microscopy.

INTRODUCTION

Nanotechnology and Biotechnology are two emerging fields of science at the same size scale. Biological systems and structures such as found in DNA have served as new paradigms for the creation of many novel nanostructured materials. Carbon nanotube is an interesting material at the intersection of these two technologies. Although carbon nanotubes have many applications, one of the most important and promising applications which might find a significant place in the technologies related to these buckytubes is its biosensing ability [1]. The unique electronic properties of CNT in conjunction with the specific recognition properties of the incubated biomolecules would make CNTs as an ideal nanoscale biosensors. A close observation reveals that carbon nanotubes have a large surface area with all the carbon atoms on the surface. Hence, by a careful alteration of the surface chemistry of the carbon nanotube, they can be exploited for biosensing applications [2]. It has been recently demonstrated that individual semiconducting single wall carbon nanotubes can be used for the detection of glucose oxidase [3]. Controlled attachment of the glucose oxidase enzyme (GO_x) to the SWNT sidewall was achieved through a linking molecule which resulted in a clear change of the conductance of the sensing device. In the present work the electrical conductivity changes and the mass uptake of SWNT matrices on biomolecule incubation is reported.

EXPERIMENTAL DETAILS

Streptavidin from *Streptomyces avidinii* was purchased as a lyophilized powder from the Sigma-Aldrich Company. The Protein was dissolved in phosphate buffered saline (PBS, Sigma-Aldrich) and stored as aliquots at -20°C. Mouse monoclonal IgG was purchased from Bio Design International Inc. The antibody solution was diluted in PBS and stored frozen at -20°C until use.

Single wall carbon nanotubes (Corbolex Inc.) were synthesized with nickel and yttrium as catalyst with 70% purity. The SWNTs have been dissolved in chloroform and then filtered through a 0.02 µm pore size Anaport filters (Whatman). The filtered solution was then sonicated to derope the bundled CNTs. The CNTs were then casted on glass substrates. The glass substrates were cleaned before casting SWNT solution with isopropyl alcohol to remove any

contamination on the surface. The thickness of the film was controlled by the amount of casted solution and its concentration. The matrix of the SWNT was studied using Atomic Force Microscope (AFM; Thermomicroscopes Auto Probe CP Research machine) in non-contact mode. The thickness was measured using AFM by scanning along the edge of an artificially made scratch on the film.

Microelectrode contacts across the matrix were formed by silver thermal evaporation. The shadow masking technique was employed to form the gap between the electrodes. A tungsten wire (Sylvania) with a diameter of 60 μ m was wrapped around the glass substrate to mask the area of the CNT. After silver evaporation the tungsten wire was removed leaving the CNTs with the electrodes across them. A multimeter (Agilent-3458A) was employed to monitor the electrical changes of the CNT matrix which was interfaced with a computer. A constant voltage was applied between the electrodes and the conductance changes for various concentrations of the protein and antibody were recorded. Protein solutions were added to 10 μ l of PBS that had been placed on the sensor. PBS was employed as a buffer environment to distinguish changes in CNT matrix conductivity due to protein binding. Figure 1 shows a schematic representation of the SWNT based conduction sensor measurement set-up.

A Quartz Crystal Microbalance (Stanford Research Systems QCM100) with 5MHz AT-cut quartz crystals (gold coated) was used to quantitatively study the ability of the SWNTs to bind streptavidin and a mouse monoclonal IgG. SWNTs solutions were casted on the gold surface and then the crystal was baked at 50°C for two hours. The presence of SWNTs on the surface of the crystal was verified by Raman spectroscopy. The Raman spectrometer (Detection Limit Inc) was equipped with a laser source of 633nm wavelength and energy of 1.96eV.

RESULTS AND DISCUSSIONS

Figures 2 (a) and 2 (b) show the carbon nanotubes casted on silicon before and after filtration respectively. It is clearly evident that most of the undesired catalyst residue has been removed by filtration leaving the nanotubes. The thickness of the SWNT film was controlled by the concentration of the SWNT in the casting solution and the amount of solution used for casting.

Electrical characterization

Electrical characteristics of the sensor were studied using microelectrodes patterned by shadow masking technique as described above. Figure 3 shows the electrical characteristics of the SWNT matrix. The matrix demonstrated semiconducting behavior. This behavior is in agreement with the fact that a randomly selected SWNT sample contains approximately 70% semiconducting nanotubes while the rest are metallic [4]. Thus making the entire matrix semiconducting in nature.

Sensor responses

Five microliters of a solution of Streptavidin with different concentrations was added to the 10 μ l of PBS to result in final concentrations of 10nM, 1 μ M and 2 μ M of protein. Figure 4 shows the electrical response of the sensor to different protein concentrations. Point 1 indicates the instance at which 10 μ l of PBS was introduced between the electrodes and points 2, 3, and 4 indicate the

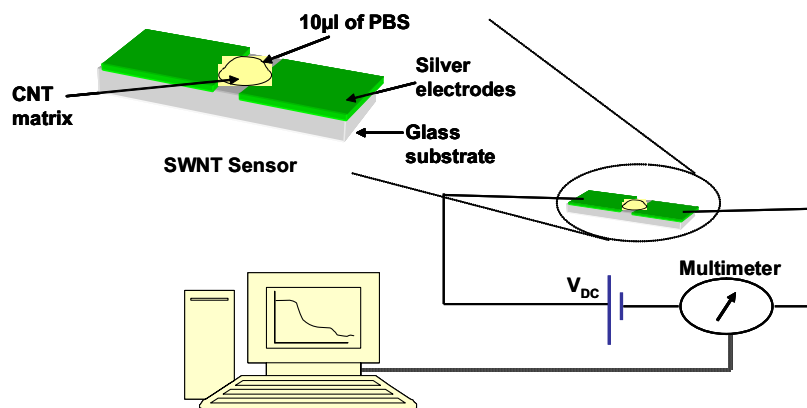


Figure 1. Schematic representation of the SWNT based conduction sensor measurement set-up.

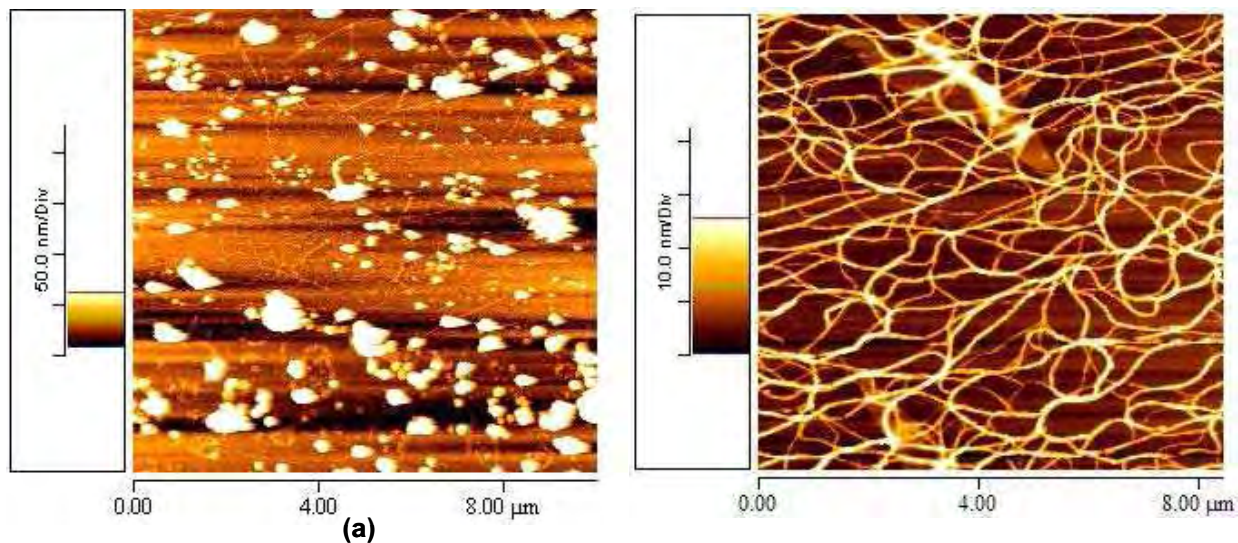


Figure 2. AFM images of SWNT before (a) and after filtration (b).

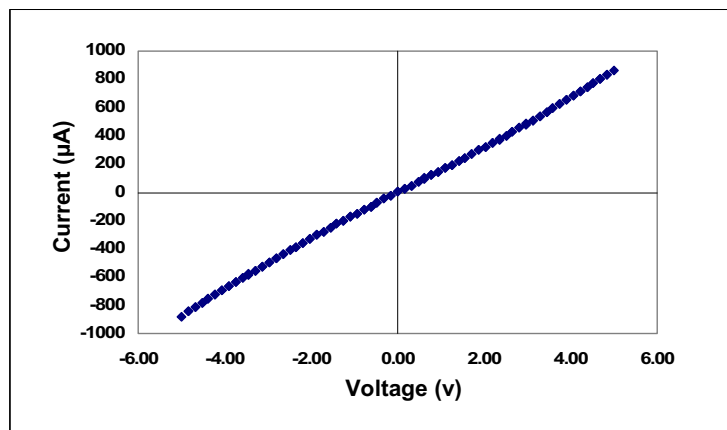


Figure 3. I-V characteristics of CNT matrix.

times when streptavidin solution was added to the PBS to form final concentration of the protein to be 10nM, 1 μ M, and 2 μ M respectively. It can be seen that there is no appreciable change in the current between the addition of PBS alone and the lowest concentration of streptavidin. Increasing the protein concentration to 1 μ M at Point 3 resulted in a decrease in the conductance of the SWNT matrix from 97.7 μ A to 60.3 μ A which corresponds to approximately 40% change in conductance. After the current stabilized the protein concentration was further increased to 2 μ M resulting in a further decrease in current. The change in conductance was 17.5% (60.3 μ A to 49.7 μ A) which is smaller compared to the initial change. These results indicate that most of the sites that are available for streptavidin to associate with the SWNT are already occupied for a concentration of 1 μ M.

Figure 5 (a) illustrates an AFM micrograph of the protein molecules bound on the surface of the substrate casted with SWNT and treated with 1 μ M of streptavidin and it can be seen that the streptavidin molecules mostly covered the SWNT network. Figure 5 (b) shows that SWNTs was decorated with streptavidin molecules when a concentration of 10nM the protein was used.

Figure 6 shows the sensor response to mouse monoclonal IgG. In this experiment following the introduction of PBS and 1 μ M of IgG the current decreased from 71.2 μ A to 45.4 μ A which is nearly a 36% change in conductance. With an increase in concentration of IgG to 2 μ M the current further decreased to 30 μ A which is a 30% change. This is consistent with Streptavidin behavior, which can be attributed to fewer active sites available for binding of IgG to CNT. The concentration of the biomolecule forms the “control” for the fine modulation of current between the electrodes. The spontaneous adsorption of both the biomolecules on the surface of carbon nanotube can be because of the hydrophobic interaction. The change in the conductance can be due to the charge transfer from biomolecule surface to the SWNT. SWNT is P-type semiconductor in nature and biomolecules are electron donors. Previous studies have shown that streptavidin is electrically neutral [5] at a pH between 6 and 7.2. However the surface of the protein molecule still consists of strong residual bases, which are responsible for charge transfer. Therefore electron transfer from biomolecule to the SWNT results in recombination of charge carriers which translates to conductivity reduction.

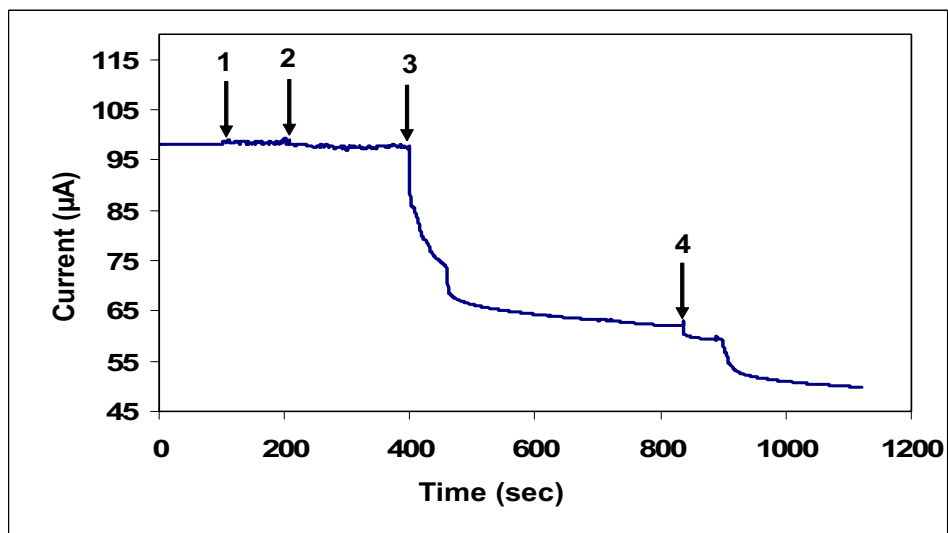


Figure 4. Electrical response of sensor for various concentrations of streptavidin.

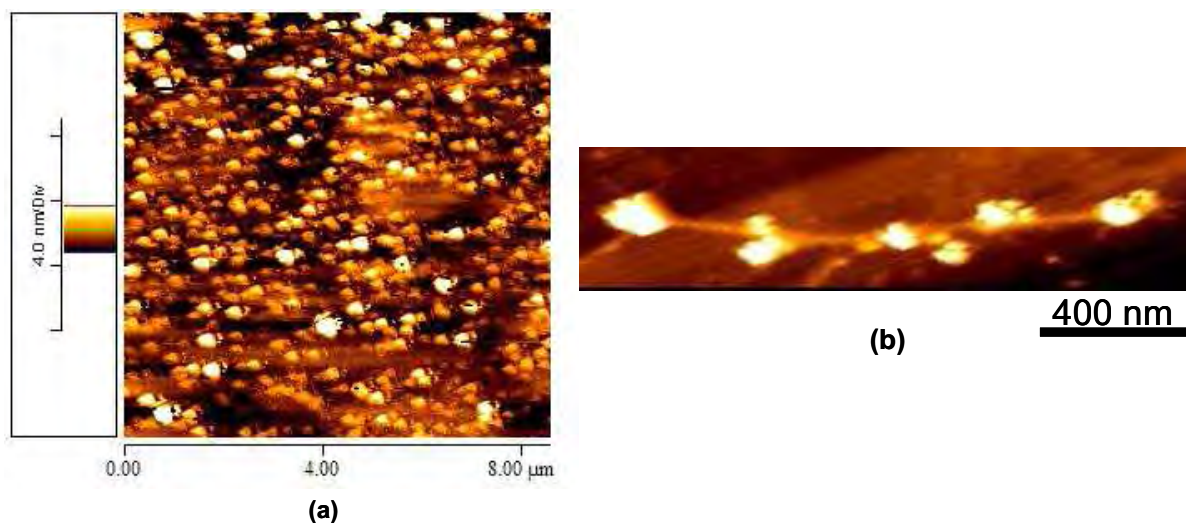


Figure 5. AFM micrograph completely covering SWNT matrix for a concentration of $1\mu\text{M}$ (a) and protein molecules decorating a rope of SWNT for a concentration of 10nM .

The quantitative study of mass uptake of SWNT network due to biomolecules immobilization was performed using QCM. In QCM a chemical interface on the surface of the sensor selectively adsorbs materials in the solvent to the surface of the sensing area. In our context the chemical interface is the SWNT matrix on the gold surface coated on quartz crystal.

Measurements of SWNT coated QCM crystals were performed by covering the chips with PBS before addition of the protein solutions. Figure 7 depicts the QCM response using streptavidin. For a concentration of $1\mu\text{M}$ of streptavidin a change of 120 Hz in resonant frequency was recorded. From the Sauerbrey equation the mass bound was calculated to be $1.538\mu\text{g}$. When the concentration on the chip was increased to $2\mu\text{M}$ the change in the frequency was found to be 26 Hz . This corresponds to a mass uptake of $0.33\mu\text{g}$. The lower frequency shift can be attributed to fewer active sites available for the protein molecules as described in the conductance based sensors. Similar results were observed for IgG with the frequency change being 248 Hz using a $2\mu\text{M}$ concentration.

CONCLUSIONS

This paper demonstrates two schemes of biomolecular detection using single wall carbon nanotubes network. The conductance based sensors exhibited a decrease in the current level due to the noncovalent binding of the biomolecules on the sidewall of the SWNTs. QCM experiments quantified the mass of the biomolecule bound on the SWNT matrix. Further investigation is underway to better understand the sensing mechanism and also improve the selectivity of the sensor through functionalization of carbon nanotubes.

ACKNOWLEDGEMENTS

The matter presented here is supported by Department of Defense under grant W81XWH-04-10250. The authors like to thank Dr. Valery Bliznyuk of Western Michigan University for providing access to AFM.

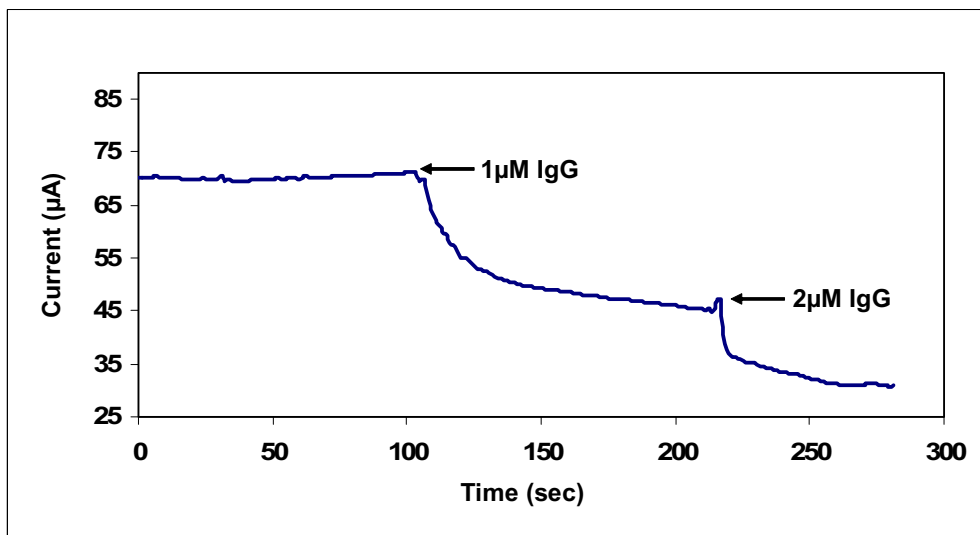


Figure 6. Electrical response of sensor for various concentrations of IgG.

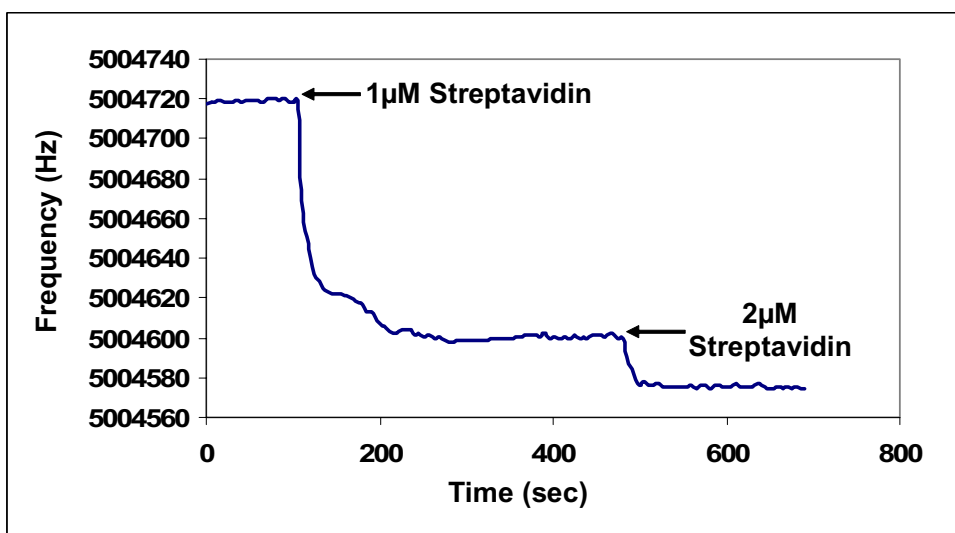


Figure 7. QCM response to streptavidin incubation.

REFERENCES

- [1] Y. Lin, F. Lu, Y. Tu, and Z. Ren, *Nanoletters*, **4**, 191, (2004).
- [2] R. J. Chen, H. C. Choi, S. Bangsaruntip, E. Yenilmez, X. Tang, Q. Wang, Y. L. Chang, and H. Dai, *J. Am. Chem. Soc.*, **126**, 1563, (2004).
- [3] K. Besteman, J. O. Lee, F. G. N. Wiertz, H. A. Heering, and C. Dekker, *Nanoletters*, **3**, 727, (2003).
- [4] J. W. G. Wildoer, L. C. Venema, A. G. Rinzler, R. E. Smalley, and C. Dekker, *Nature*, **391**, 59, (1998).
- [5] C.J. Van Oss, R.F. Giese, P.M. Bronson, A. Docoslis, P. Edwards, and W.T. Ruyechan, *Colloids Surf. B*, **30**, 25, (2003).

Carbon Nanotube Based Biosensors

Massood Z. Atashbar¹, Bruce Bejcek², Srikanth Singamaneni¹, and Sandro Santucci³

¹Electrical and Computer Engineering Department, Western Michigan University, Kalamazoo, MI-49008, USA

²Department of Biological sciences, Western Michigan University, Kalamazoo, MI-49008, USA

³Department of Physics, University of L'Aquila, Italy.

Abstract

In this paper we describe a single wall carbon nanotube (SWNT) based biological sensor for the detection of bio molecules like Streptavidin and IgG. SWNT have been employed for two types of sensing mechanisms. Firstly, the changes in the electrical conductance of the carbon nanotube matrix on non covalent binding of the biomolecules to the side walls of the carbon nanotube and secondly, quantification of mass uptake of the matrix on biomolecule incubation are presented. Both sensing mechanisms exhibited consistent and highly sensitive responses. Biomolecular immobilization on the carbon nanotube surface was monitored by Atomic Force Microscopy.

Keywords

Single walled Carbon nanotubes, Biomolecule, Atomic Force Microscopy.

INTRODUCTION

Single Wall Carbon nanotubes (SWNTs) can be realized as graphite sheets that have been rolled into seamless cylinders. Ever since Carbon nanotubes (CNTs) discovery by Iijima [1] in 1991, they have been treated as the most promising nanostructured materials. Carbon nanotubes exhibit both semi conducting and metallic behavior depending on their chirality [2]. This special property of nanotubes makes them the ideal choice for interconnects and also as active devices of nanoelectronics. CNTs have been used as chemical sensors for the detection of hazardous gasses such as NH₃, and NO₂ [3]. The application of these quantum wires as biological sensors is a new facet which might find significant applications in the life sciences field [4] and it has been recently demonstrated that individual semiconducting single wall carbon nanotubes can be used for the detection of glucose oxidase [5].

In this work we have fabricated a simple yet efficient carbon nanotube conductance based sensor for the detection streptavidin and mouse monoclonal immunoglobulin G (IgG) antibody. In addition we employed Quartz Crystal Microbalance (QCM) to quantify the mass of the biomolecules bound on the surface of the nanotubes. QCM is a Thickness Shear Mode (TSM) acoustic wave device for detection of mass down to few nanograms.

EXPERIMENTAL DETAILS

Streptavidin from *Streptomyces avidinii* was purchased as a lyophilized powder from the Sigma-Aldrich Company. The Protein was dissolved in phosphate buffered saline (PBS, Sigma-Aldrich) and stored as aliquots at -20°C. Mouse monoclonal IgG was purchased from Bio Design International Inc. The antibody solution was resuspended in PBS and stored frozen at -20°C until use.

Single wall Carbon nanotubes (70% pure with nickel and yttrium as catalyst residue) were purchased from Corborex Inc. The SWNTs have been dissolved in chloroform and then filtered through 0.02 μm pore size Anaport filters (Whatman). The filtered solution was then sonicated to derope the bundled CNTs. The CNTs were then casted on glass substrates using a micropipette. The glass substrates were cleaned before casting SWNT solution with isopropyl alcohol to remove any contamination on the surface. The thickness of the film was controlled by the amount of casted solution and its concentration. The matrix of the SWNT was studied using Atomic Force Microscope (Thermomicroscopes Auto Probe CP Research machine) in non-contact mode. The thickness was measured using AFM by scanning along the edge of an artificially made scratch on the film.

Microelectrode contacts across the matrix were formed by thermal evaporation of silver. The shadow masking technique was employed to form the gap between the electrodes. A tungsten wire (Sylvania) with a diameter of 60μm was wrapped around the glass substrate to mask the area of the CNT. After silver evaporation the tungsten wire was removed leaving the CNTs with the electrodes across them.

Agilent multimeter (Agilent-3458A) was employed to monitor the electrical changes of the CNT matrix which was interfaced with a computer. A constant voltage was applied between the electrodes and the conductance changes for various concentrations of the protein and antibody were recorded. Protein solutions were added to 10μl of PBS that had been placed on the sensor. PBS was employed as a buffer environment to distinguish changes in CNT matrix conductivity due to protein binding (see Figure 1).

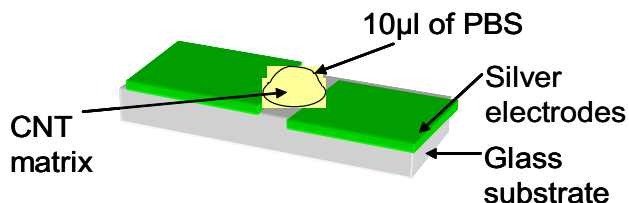


Figure 1. Schematic representation of the sensor.

Quartz Crystal Microbalance (Stanford Research Systems QCM100) with 5MHz AT-cut quartz crystals (gold coated) was used to quantitatively study the ability of the CNTs to bind streptavidin and mouse monoclonal IgG. CNT solution was casted on the gold surface and then the crystal was baked at 50°C for two hours. The CNT presence on the surface of the crystal was verified by Raman spectroscopy. The Raman spectrometer (Detection Limit Inc) was equipped with a laser source of 633nm wavelength and energy of 1.96eV.

RESULTS AND DISCUSSIONS

Purification of CNT

The CNTs were dissolved in chloroform (Sigma-Aldrich) and then casted on silicon substrates. However AFM imaging of the samples revealed that there was a high content of catalyst residue. Filtration of the CNT solution using antop filters resulted in transparent solution. Figure 2 shows the photograph of the CNT solution before and after filtration. It is known that the carbon nanotubes have a tendency to form into parallel bundles resulting to triangular lattice because of the inter-molecular van der Waals forces between the nanotubes [6]. To overcome the inter-molecular forces the filtered CNT solution was sonicated for 1 hour.

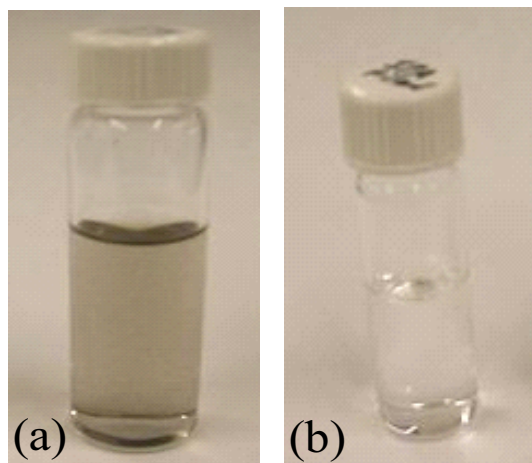


Figure 2: Photographs showing the solution of CNT (a) before and (b) after filtration

Figure 3 shows uniformly distributed casted CNT matrix on the silicon substrate. It can be observed that most of the undesired catalyst residue has been filtered out leaving behind the nanotubes.

The thickness of the CNT film was controlled by the amount of solution casted and the concentration of the solution. Figure 4 shows the micrograph of the CNT film and its height profile showing that the film thickness was approximately 20nm.

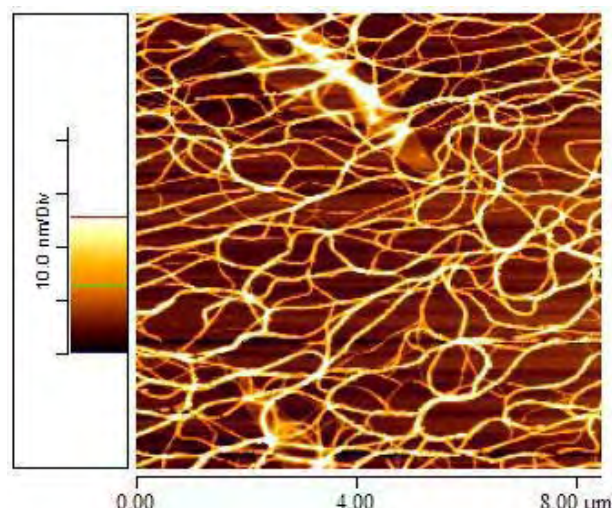


Figure 3. AFM micrograph of CNT matrix on silicon substrate.

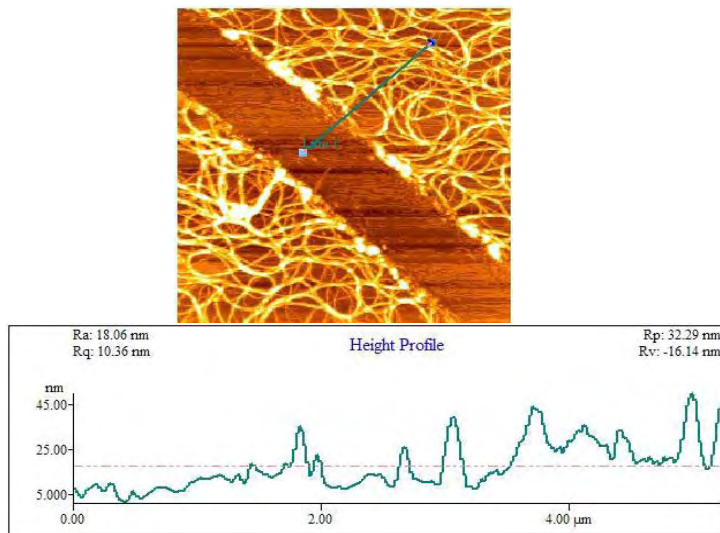


Figure 4. AFM micrograph of CNT matrix showing scratch and height profile.

Electrical characterization

Electrical characteristics of the sensor were studied using microelectrodes patterned by shadow masking technique as described above. Figure 5 shows the electrical characteris-

tics of the CNT matrix. The matrix demonstrated semiconducting behavior. This behavior is in agreement with the fact that a randomly selected CNT sample contains approximately 70% semiconducting nanotubes while the rest are metallic [2]. This makes the entire matrix to be semiconducting in nature.

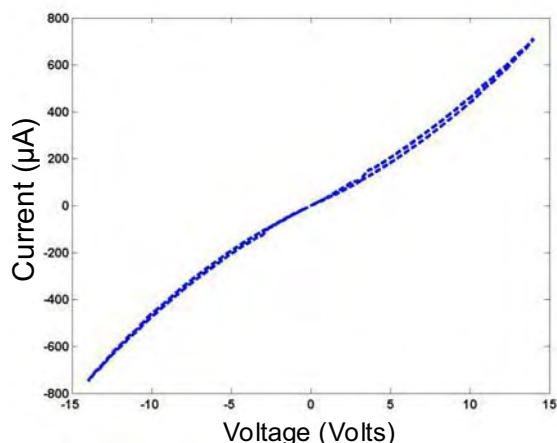


Figure 5. I-V characteristics of CNT matrix.

Sensor responses

Five microliters of a solution of Streptavidin with different concentrations was added to the 10µl of PBS to result in 10nM, 1µM and 2µM of protein. Figure 6 shows the electrical response of the sensor to different protein concentrations. Point 1 indicates the instance at which 10µl of PBS was introduced between the electrodes and point 2 is the time at which 5µl streptavidin solution was added to the PBS making the final concentration of the protein to be 10nM. It can be seen that there was no appreciable change in the current. The protein concentration was increased to 1µM at Point 3 and a decrease in the conductance of the CNT matrix was observed. The current decreased from 97.7µA to 60.3µA which corresponds to approximately a 40% change in conductance. After the current stabilized the protein concentration was further increased to 2µM and a further decrease in current was recorded. The change in conductance was 17.5% (60.3µA to 49.7 µA) which is smaller compared to the initial change.

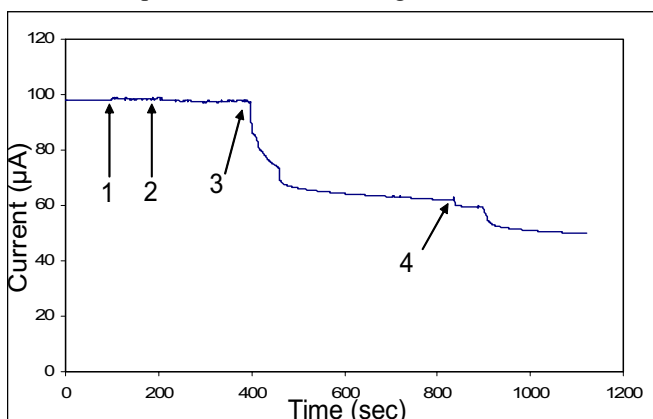


Figure 6. Electrical response of sensor for various concentrations of streptavidin.

The smaller change in the conductance can be attributed to less number of active sites available for the protein molecules to bind to CNT.

Figure 7 is an AFM micrograph of the CNT and protein molecules. From this Figure it can be seen that protein molecules were bound on the sidewalls of the tube and bundles of CNT were decorated with streptavidin molecules.



Figure 7. AFM micrograph showing the protein molecules decorating a rope of CNT.

Figure 8 shows the sensor response to the mouse monoclonal IgG. Following introduction of PBS and 1µM of IgG the current decreased from 71.2µA to 45.4µA which is nearly a 36% change in conductance. With increase of concentration to 2µM the current further decreased to 30µA which is a 30% change. This is consistent with Streptavidin behavior which can be attributed to less number of active sites available for binding of IgG to CNT.

The concentration of the biomolecule forms the “control” for the fine modulation of current between the electrodes. The change in the conductance can be explained in a simple way. It is known from previous studies that streptavidin is electrically neutral at a pH between 6 and 7.2. However the surface of the protein molecule still consists of strong residual bases. These bases are responsible for charge transfer.

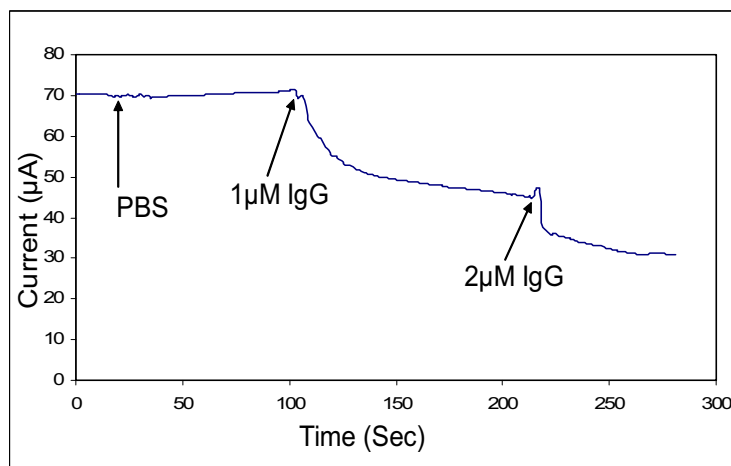


Figure 8. Electrical response of sensor for various concentrations of IgG.

The quantitative study of mass uptake of CNT network due to biomolecules immobilization was performed using QCM. In QCM a chemical interface on the surface of the sensor selectively adsorbs materials in the solvent to the surface of the sensing area. In our context the chemical

interface is the CNT matrix on the gold surface coated on the QCM crystal. The CNT matrix on the gold surface was characterized by Raman spectroscopy [7]. Figure 9 shows the Raman spectrum obtained from the CNT film on the gold surface of the quartz crystal. It can be seen that the Raman spectrum has characteristic 'G' band and 'D' band peaks which arise due to the in-plane Raman-active mode and disorder of the CNT respectively [7].

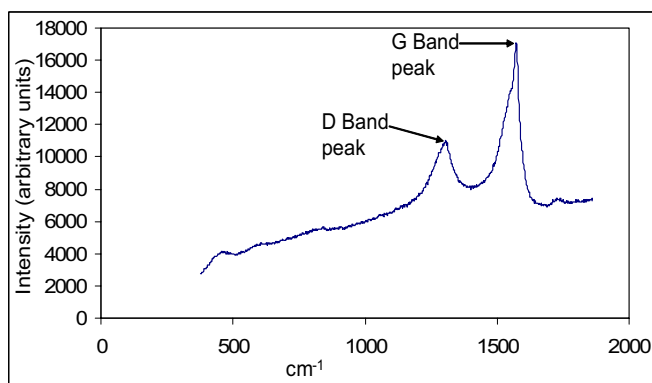


Figure 9. Raman spectrum of CNT on gold surface of QCM showing the characteristic 'G' band and 'D' band peaks.

Measurements of CNT coated QCM crystals were performed by covering the chips with PBS before addition of the protein solutions. Figure 10 depicts the QCM response using streptavidin. For a concentration of 1 μ M of streptavidin a change of 120 Hz in resonant frequency was recorded. From the Sauerbrey equation the mass bound was calculated to be 1.538 μ g. when the concentration on the chip was increased to 2 μ M the change in the frequency was found to be 26Hz. This corresponds to a mass uptake of 0.33 μ g. The lower frequency shift can be attributed to fewer active sites available for the protein molecules as described in the conductance based sensors. Similar results were observed for IgG with the frequency change being 248Hz using a 2 μ M concentration.

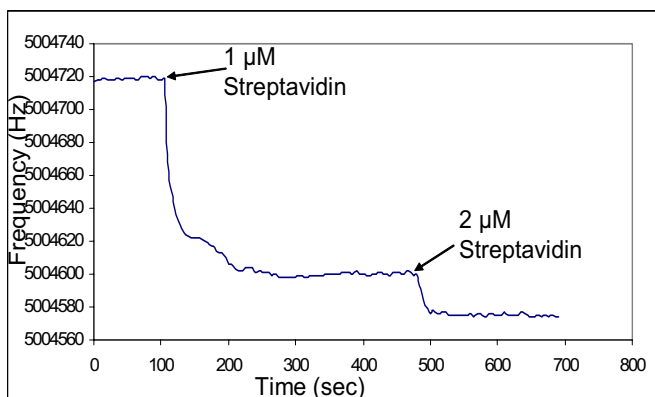


Figure10. QCM response to streptavidin incubation.

CONCLUSIONS

We have demonstrated a simple and efficient method for purification of carbon nanotubes for the fabrication of conductometric biosensor. Two schemes of biomolecular sensing using carbon nanotubes have been demonstrated. The conductance based sensors exhibited a decrease in the current level due to the noncovalent binding of the biomolecules on the sidewall of the CNTs. QCM experiments quantified the mass of the biomolecule bound on the CNT matrix. Further investigation is underway to better understand the sensing mechanism and also improve the selectivity of the sensor by functionalizing carbon nanotubes.

ACKNOWLEDGEMENTS

The matter presented here is supported by Department of Defense under grant W81XWH-04-10250. The authors like to thank Dr. Valery Bliznyuk of Western Michigan University for providing access to AFM.

REFERENCES

- [1] S. Iijima, "Helical microtubules of graphitic carbon", *Nature*, vol. 354, pp. 56-58, November 1991.
- [2] J.W.G. Wildoer, L.C. Venema, A.G. Rinzler, R.E. Smalley, and C. Dekker, "Electronically structure of atomically resolved carbon nanotubes", *Nature*, vol. 391, pp. 59-61, January 1998.
- [3] J. Kong, N.R. Franklin, C. Zhou, M.G. Chapline, S. Peng, K. Cho, and H. Dai, "Nanotube molecular wires as chemical sensors", *Science*, vol. 287, pp. 622-625, January 2000.
- [4] R.J. Chen, H.C. Choi, S. Bangsaruntip, E. Yenilmez, X. Tang, Q. Wang, Y. Chang, and H. Dai, "An investigation of the mechanisms of electronic sensing of protein adsorption on carbon nanotube devices", *Journal of American Chemical Society*, vol. 126, pp. 1563-1568, January 2004.
- [5] K. Besteman, J. Lee, F. G. M. Wiertz, H.A. Heering, and C. Dekker, "Enzyme-coated carbon nanotubes as single-molecule biosensors" *Nanoletters*, vol. 3, pp. 727-730, April 2003.
- [6] T. Hertel, R.E. Walkup, and P. Avouris, "Deformation of carbon nanotubes by surface van der Waals forces", *Physical Review B*, vol.58, pp. 13870-13873, November 1998.
- [7] A. G. S. Filho, A. Jorio, G. G. Samsonidze, G. Dresselhaus, R. Satio, and M.S. Dresselhaus, "Raman spectroscopy for probing chemically/ physically induced phenomena in carbon nanotubes", *Nanotechnology*, vol. 14, pp. 1130-1139, September 2003.

Sensitivity Enhancement of a QCM Biosensor using Polymer Treatment

¹M. Z. Atashbar, ²B. Bejcek, ¹A. Vijh and ¹S. Singamaneni

¹Department of Electrical and Computer Engineering, ²Department of Biological Sciences
Western Michigan University, Kalamazoo, MI-49008

Abstract--Quartz Crystal Microbalances (QCMs) have been widely used for detection of various chemical and biological species in liquid media. We report an improved binding of Protein A and IgG molecules on QCM biosensors by modifying the gold surface of the quartz crystal with a 35nm polystyrene film followed by an acidic treatment. An appreciable increase in the frequency shift was observed when the polystyrene film was used as an interfacial layer. Protein A and IgG immobilizations on quartz crystals with the polystyrene film represented a 65% increase and a 40% increase respectively when compared to immobilization done directly onto the crystals. Complementary Atomic Force Microscopy (AFM) studies revealed a significant decrease in the RMS roughness of the substrate from 98.4 nm to 1.75 nm when coated with polystyrene. This increased surface smoothness resulted in higher biomolecular coverage on the surface of the sensor causing higher frequency shifts.

I. INTRODUCTION

Existing immunoassay techniques for biomolecular detection such as fluoroimmunoassay (FIA), enzyme linked immunoassay (ELISA) and radioimmunoassay (RIA) are complex and time consuming as they require specific labels and reagents [1, 2]. Biosensors with rapid and highly sensitive detection capabilities for various biomolecules are therefore in great demand in the field of life sciences. Acoustic wave sensors have been widely used for the specific detection of various chemical and biological molecules in liquid media. The chemical interface on the surface of the sensor selectively adsorbs

materials in the solvent to the surface of the sensing area. Due to this adsorption, the physical and chemical properties of the surface change thus altering the phase and amplitude of the acoustic and electromagnetic fields on the surface. For biological sensors, binding of a substance onto the resonating membrane surface causes a decrease in the acoustic wave velocity, which is related to the resonant frequency of the device. The changes in the acoustic and electromagnetic properties of the chip can be directly proportional to the changes in mass.

Quartz Crystal Microbalances have been extensively used for gravimetric immunoassays of human serum albumin (HSA) [3], monoclonal mouse IgG [2], and human IgG [1]. The simple relationship relating the change in frequency (Δf) to the change in mass (Δm) enables QCM to be widely used in sensing applications. A shift in the resonant frequency of the QCM can be attributed to the mass bound on the sensor membrane as per the Sauerbrey equation

$$\Delta f = \frac{-2f_0^2 \Delta m}{A\sqrt{\rho_q \mu_q}} \quad (1)$$

where f_0 is the fundamental resonant frequency, A is the piezoelectrically active area defined by the two gold electrodes, ρ_q is the density of quartz (2.648 g cm^{-3}) and μ_q is the shear modulus ($2.947 \times 10^{11} \text{ dyn cm}^{-2}$). Equation (1) is based on an assumption that the mass has been rigidly attached to the crystal and has negligible thickness as compared to the crystal as a whole [1].

II. EXPERIMENTAL DETAILS

1. Materials

Polystyrene, 3-Aminopropyl triethoxysilane (3-APTES), glutaraldehyde, acetone, glycine and sodium chloride were purchased from Sigma-Aldrich Chemical Company. Protein A (Sigma-Aldrich) and mouse monoclonal IgG antibody (BioDesign International Inc) were used throughout these studies. Protein A was resuspended in phosphate buffered saline (PBS; Sigma-Aldrich) at a concentration of 500 μ g/ml.

2. Experimental Procedures

For promoting the immobilization of Protein A and to provide the necessary amine groups on the gold surface the protocol of Muramatsu et al. (1987) was followed [1]. The crystal was cleaned with Piranha solution (3 parts of H₂SO₄ in 1 part of 30 % H₂O₂) to remove any organic contamination from the surface of the crystal. Enough Piranha solution was employed to cover the gold surface of the chip and allowed to incubate at room temperature for two minutes before rinsing with milli-Q water. This procedure was repeated twice. The chip was subsequently blown dried in a stream of nitrogen gas. A self-assembled monolayer (SAM) was created using a 5% solution of 3-APTES in acetone. After 1 hour at room temperature the chip was placed in a 5% (v/v diluted in milli-Q water) glutaraldehyde solution for 3 hours to enhance the cross linking between the chip and the Protein A. The crystal was then covered with 20 μ l of a solution of Protein A (0.5 mg/ml diluted in PBS; pH7.4). After 1 hour the solution was removed and the crystal was subjected to several wash-dry cycles with milli-Q water until the QCM crystal reached its steady resonant frequency. The chip was then covered with 0.1 M glycine dissolved in PBS for 1 hour to block any sites not bound to Protein A on the glutaraldehyde modified chip. The chip was then rinsed with 0.1M glycine-HCl buffer (pH 2.4) to wash off any excess proteins or glycine before being thoroughly rinsed with milli-Q water. 20 μ l of the mouse monoclonal IgG solution was then incubated on the chip for 1 hour

followed by rinsing with 0.5M NaCl to remove any non-specifically adsorbed antibody. For the experiments in which binding was performed on a polymer film, polystyrene solution (7% w/v in chloroform) was spin coated onto the chip at a speed of 1000 rpm and then treated with 50 % (v/v) HNO₃ in concentrated H₂SO₄ for 1 hour [8]. The substrate was then modified with 3-APTES followed by glutaraldehyde as described above. The procedure was repeated for different concentrations of IgG on crystals with and without the polymer film and the frequency shifts were monitored.

3. Characterization tools and methods

A Quartz Crystal Microbalance (Stanford Research Systems QCM100) with 5MHz AT-cut quartz crystals (gold coated) was used to quantitatively study the ability to bind Protein A and mouse monoclonal IgG to the chip. The gold surface, which forms the active area for immobilization was 1.37cm² and the mass sensitivity of the crystal was 0.057 Hz/ng/cm². Frequency was monitored using a Stanford Research System Universal Time Interval Counter (Model No. SR620).

Qualitative studies were made using AFM (Autoprobe CP Research machine) in non-contact mode. For AFM studies silicon substrates were used with the same modification techniques as those described above for the QCM chips. The AFM tips used for imaging were silicon with an approximate radius of curvature of 20nm. Biomolecular imaging was performed in non-contact mode. The AFM images were analyzed using image-processing software (IP 2.1) to calculate the RMS roughness value.

III. RESULTS AND DISCUSSIONS

The AFM studies revealed that the commercially purchased quartz crystals had a RMS surface roughness of 98.4 nm. To determine if decreasing the RMS surface roughness would increase the efficiency of biomolecule binding and hence

improvement in antibody immobilization, the quartz crystals were coated with an ultra thin polymer film. Coating the surface with polystyrene resulted in a significant decrease in RMS surface roughness to 1.75 nm.

However, polystyrene films are hydrophobic in nature causing the biomolecules to denature and hence loose their activity. To avoid denaturation of the biomolecules, the polymer film functional groups such as amino and hydroxyl groups can be chemically added. This helps the biomolecules retain their activity as immobilization now takes place through the hydrophilic arms of the polymer film. To increase the hydrophilicity of the surface which would increase the ability to add the functional groups, the chips were subjected to an acidic treatment followed by aqueous silanization.

Figure 1 shows the schematic representation of the acidic treatment and the APTES modification of polystyrene. The acid treatment provides NO₂ groups and the APTES modification improves the

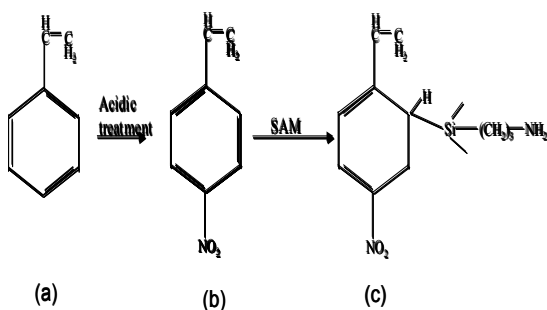


Figure1. Polystyrene film when treated with acid and 3-APTES; (a) Polystyrene film (b) formation of the NO₂ groups by acidic treatment (c) formation of the amine groups by silanization.

hydrophilicity of the surface by providing the required amine groups.

Figure 2 shows the AFM image of IgG immobilized on polystyrene coated surface. It can be seen that there is a uniform coverage of the antibody molecules of approximately 10 nm in size on the substrate. The AFM imaging performed two

hours after the biomolecules immobilization revealed that the molecules still retain their

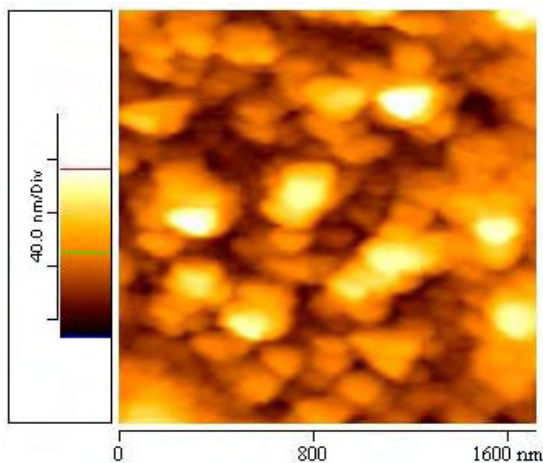


Figure2. IgG molecules immobilized on the polystyrene surface showing the characteristic heart shape indicating that they still are not denatured.

The biomolecule immobilization on gold and polystyrene coated gold surfaces was then quantitatively studied with QCM. Figure 3 shows the QCM frequency response to Protein A immobilization without the polystyrene film. Protein A, which has a particularly high affinity for the F_c portion of IgG, was immobilized first on the chips to prevent the random immobilization of the antibodies, and therefore maximizing the ability of the chip immobilized antibodies to bind to antigens [2].

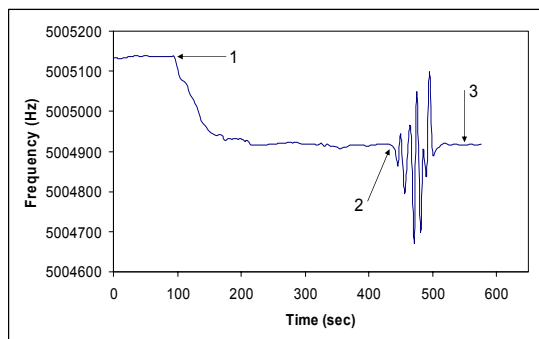


Figure3. QCM frequency response for Protein A immobilization on polystyrene.

In Figure 3 point 1 indicates the time of addition of the Protein A containing solution to the chip. Point 2 shows when the crystal was subjected to several wash-dry cycles and point 3 represents the new resonance frequency of the crystal when Protein A was specifically bound on the surface. The frequency shift due to this direct binding (the difference in frequency between point 1 and point 3) was 220 Hz. From the Sauerbrey equation, this frequency shift corresponds to a binding of 2.8 μg of protein. 160 $\mu\text{g/ml}$ solution of IgG was added to the Protein A modified chip. The chip was rinsed with 0.5M NaCl solution to remove the nonspecifically adsorbed IgG. The final frequency shift for the antibody immobilization was found to be 282 Hz which represents a mass of 3.61 μg .

Immobilization on polystyrene coated surfaces was compared to the immobilization performed without polystyrene. Figure 4 shows the QCM response to Protein A immobilization performed on polystyrene surface.

The registered frequency shift from point 1 to point 3 was 364 Hz which corresponds to a mass change of 4.66 μg . This represents a 65% increase when compared to the QCM chips that were not coated with the polymer film. Similar results were obtained for the binding of IgG. The QCM response for the immobilization of IgG (160 $\mu\text{g/ml}$) on the

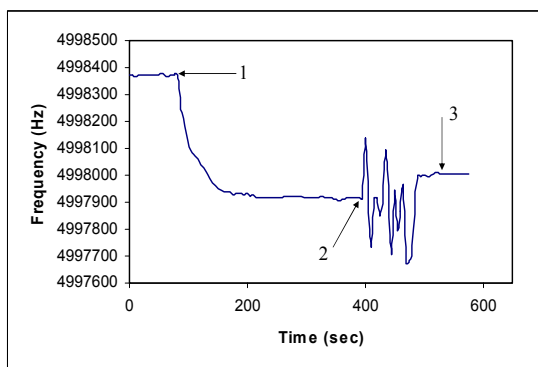


Figure 4. QCM frequency response for Protein A immobilization on polystyrene.

polystyrene surface showed a frequency shift of 391 Hz corresponding to a mass uptake of 5.01 μg . This represents a 40% increase when compared to chips that had not been modified with polystyrene.

IV. CONCLUSIONS

We have demonstrated a simple aqueous silanization technique to improve the ability of QCM gold chips to bind to protein A and subsequently IgG. Higher frequency shifts were observed for immobilizations carried on polymer-coated surfaces. Protein A resulted in a shift of 364 Hz on the polystyrene modified surface as opposed to the 220 Hz shift of frequency for direct immobilization. Subsequent IgG immobilizations also showed similar trend with the frequency shifts being 391 and 282 Hz for immobilizations with and without the polymer film respectively. AFM imaging also revealed uniform biomolecule coverage on polymer coated surfaces.

V. ACKNOWLEDGEMENTS

The material presented here was supported by the US Department of Defence under contract number W81XWH-04-10250. Authors would like to thank Dr. V. Bliznyuk for providing access to AFM and Mr. Shakil Hossein for technical support.

VI. REFERENCES

- [1] H. Muramatsu, J. M. Dicks, E. Tamiya, I. Karube, "Piezoelectric Crystal Biosensor Modified with Protein A for Determination of Immunoglobulins", *Analytical Chemistry*, Vol 59 (23), 2760-2763, 1987.
- [2] F. Caruso, E. Rodda, D. N. Furlong, "Orientational Aspects of Antibody Immobilization and Immunological Activity on Quartz Crystal Microbalance Electrodes", *Journal of Colloid and Interface Science*, Vol. 178 (1), 104-115, 1996.
- [3] B. Guo, J. Anzai, T. Osa, "Adsorption Behavior of Serum Albumin on Electrode Surfaces and the Effects of Electrode Potential", *Chemical & Pharmaceutical Bulletin*, Vol. 44 (4), 800-803, 1996.

Basic and Clinical Advances in Prostate Cancer Research

4th Annual Symposium of Michigan Prostate Research Colloquium
Van Andel Research Institute, Grand Rapids, MI

May 1, 2004

Abstract Deadline: April 10, 2004

PIEZOELECTRIC BIOSENSOR FOR PROSTATE CANCER DETECTION

Massood Z. Atashbar¹, Bruce Bejcek², Aditya Vijn¹, Srikanth Singamaneni¹

¹Department of Electrical and Computer Engineering,

²Department of Biological Sciences

Western Michigan University, Kalamazoo MI-49008, USA

Existing antibody detection techniques such as fluoroimmunoassay, radioimmunoassays and enzymeimmunoassays require specific labels and markers for detection, which makes them very complex and time consuming. To develop an assay for serum antigens that is simpler and less labor intensive we have used an acoustic wave biosensor for the detection of antibodies against free prostate specific antigen (fPSA). A Quartz Crystal Microbalance (QCM100) was used to measure the levels of immobilized antibody. It consisted of AT-cut Quartz crystal having a resonant frequency of 5 MHz and a mass sensitivity of 0.057 Hz/ng/cm². Any change in the mass on the membrane results in a change in the frequency of operation (Δf), which is related to the mass immobilized (Δm) as per the Sauerbrey equation

$$\Delta f = \frac{-2f_0^2 \Delta m}{A\sqrt{\rho_q \mu_q}}$$

To enhance the association of glutaraldehyde with the surface of the microbalance chip, a self-assembled monolayer (SAM) was formed by treating the substrate with aminopropyl triethoxysilane (3-APTES). To confirm the formation of the SAM Atomic Force Microscopy (AFM) studies were performed. AFM studies revealed a significant increase in the roughness of the surface of the chip from 0.44nm to 15.8nm confirming the formation of SAM. As antibodies added to these chips may bind in random orientations which could result in a high degree of variability in the ability of immobilized antibodies to bind to the appropriate ligand, we immobilized Protein A (500 μ g/ml) on the treated gold surface. AFM demonstrated a uniform coverage of the surface with molecules of approximately 10nm in size, which correlated well with previously published reports on the size of Protein A. Frequency shifts were approximately 220Hz, which indicated that 2.82 μ g of protein A had been immobilized. Any remaining active sites were blocked by glycine and different concentrations of antibody against fPSA were reacted with the chip. Frequency shifts were studied for different concentrations of antibody. QCM measurements for antibody concentration of 80 μ g/ml revealed a frequency shift of 90Hz corresponding to a mass of 1.153 μ g. At a concentration of 120 μ g/ml a frequency shift of 120 Hz was observed which corresponds to a mass of 1.538 μ g. These results indicate the feasibility of using quartz microbalances for the measurement of PSA.

Person to whom correspondence to be directed:

Name Aditya A. Vijn E-Mail adityavijn@rediffmail.com

Full Address 1903 W. Michigan Avenue, Department of Electrical and Computer Engineering, College of Engineering and Applied Sciences, Western Michigan University, Kalamazoo MI-49008

Phone Number (269) 599-5155 Fax Number (269) 276-3151

Name of the Person Presenting Abstract Aditya A. Vijn

P.S.: Please type abstracts single-spaced and within border. Title should be typed in uppercase letters. Include names of the author(s) and institution. Do not list academic degrees. **You may e-mail** (cindy.miranti@vai.org) or FAX (616-234-5359) your abstract(s). For further information contact: Dr. Cindy Miranti at (616) 234-5358.